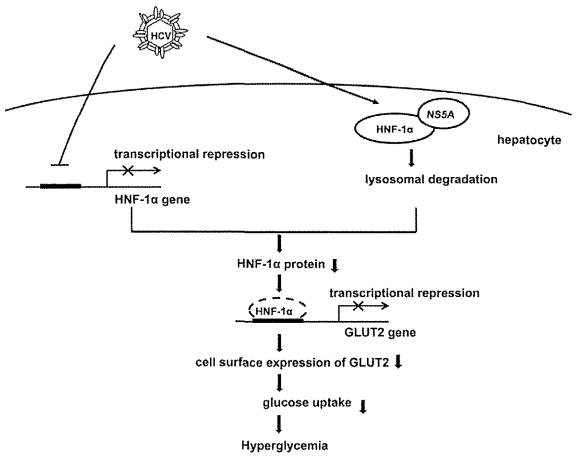

FIG 8 A proposed mechanism of the HCV-induced suppression of GLUT2 via downregulation of HNF-1α. HCV infection downregulates HNF-1α at transcriptional and posttranslational levels, resulting in suppression of GLUT2 gene transcription. HCV NS5A protein physically interacts with HNF-1α protein and enhances lysosomal degradation of HNF-1α protein.

Moreover, HNF-1α has been shown to regulate a large number of genes related to glucose, fatty acid, bile acid, cholesterol, and lipoprotein metabolisms as well as inflammation (1). Therefore, it is possible that HCV-induced downregulation of HNF-1α may play a crucial role in metabolic disorders as well as tumorigenesis.

To determine which HCV protein is involved in the suppression of the GLUT2 promoter, we examined the effects of transient expression of HCV proteins on GLUT2 promoter activity. Overexpression of NS5A suppressed GLUT2 promoter activity, whereas overexpression of p7 enhanced GLUT2 promoter activity (Fig. 5A). SGR cells express NS5A protein but lack p7 protein. FGR cells express both NS5A protein and p7 protein. However, GLUT2 promoter activity was suppressed in both SGR and FGR cells (Fig. 2B). This discrepancy between transient expression system and replicon cells may result from the differences in trafficking of p7 because it is a complex process potentially regulated by both the cleavage from its upstream signal peptides and targeting signals within the protein sequence (15).

We previously reported that HCV infection promotes hepatic gluconeogenesis in HCV J6/JFH1-infected Huh-7.5 cells (11). HCV infection transcriptionally upregulates the genes for phosphoenolpyruvate carboxykinase (PEPCK) and glucose 6-phosphatase (G6Pase), the rate-limiting enzymes for hepatic gluconeogenesis. We demonstrated that gene expression of PEPCK and G6Pase was regulated by the transcription factor forkhead box O1 (FoxO1) in HCV-infected cells. Phosphorylation of the FoxO1 at Ser319 was markedly diminished in HCV-infected cells, resulting in increased nuclear accumulation of FoxO1. HCV NS5A protein was directly linked with FoxO1-dependent increased gluconeogenesis. HCV-induced downregulation of GLUT2 expression and upregulation of gluconeogenesis may cooperatively contribute to development of type 2 diabetes in HCV-infected patients at least to some extent. HCV-induced downregulation of GLUT2 expression and upregulation of gluconeogenesis may result in high concentrations of glucose in HCV-infected hepatocytes. As suggested in a recent study, low glucose concentrations in the hepatocytes inhibit HCV replication (28). Therefore, high glucose levels in the hepatocytes may confer an advantage in efficient replication of HCV.

In conclusion, we provided evidence suggesting that HCV infection downregulates HNF-1α expression at both transcriptional and posttranslational levels. HCV-induced downregulation of HNF-1α may play a crucial role in glucose metabolic disorders caused by HCV infection. Strategies aimed at HCV-induced downregulation of HNF-1α protein may lead to the development of new therapeutic agents for HCV-induced diabetes.

ACKNOWLEDGMENTS

We are grateful to C. M. Rice (Rockefeller University, New York, NY) for providing Huh-7.5 cells and pFL-J6/JFH1, R. Bartenschlager (University of Heidelberg, Heidelberg, Germany) for providing an HCV subgenomic RNA replicon (pFK5B/2884Gly), and N. Kato (Okayama University, Okayama, Japan) for providing an HCV full-genome RNA replicon (pON/C-5B). We thank T. Adachi, M. Makimoto, K. Tsubaki, Y. Yasui, A. Asahi, M. Kohmoto, and Y.-H. Ide for their technical assistance. We also thank K. Hachida for secretarial work.

This work was supported in part by grants-in-aid for research on hepatitis from the Ministry of Health, Labor, and Welfare, Japan, and the Ministry of Education, Culture, Sports, Science, and Technology (MEXT), Japan. This work was also supported in part by the Japan Initiative for Global Research Network on Infectious Diseases program of MEXT, Japan. This study was also carried out as part of the Global Center of Excellence program of the Kobe University Graduate School of Medicine and the Science and Technology Research Partnership for Sustainable Development program of the Japan Science and Technology Agency and the Japan International Cooperation Agency.

We have no potential conflicts of interest to report.

REFERENCES

1. Armendariz AD, Krauss RM. 2009. Hepatic nuclear factor 1-alpha: inflammation, genetics, and atherosclerosis. Curr. Opin. Lipidol. 20:106–111.
2. Ban N, et al. 2002. Hepatocyte nuclear factor-1α recruits the transcriptional co-activator p300 on the GLUT2 gene promoter. Diabetes 51:1409–1418.
3. Blight KJ, Kolykhalov AA, Rice CM. 2000. Efficient initiation of HCV RNA replication in cell culture. Science 290:1972–1974.
4. Blight KJ, McKeating JA, Rice CM. 2002. Highly permissive cell lines for subgenomic and genomic hepatitis C virus RNA replication. J. Virol. 76:13001–13014.
5. Bluteau O, et al. 2002. Bi-allelic inactivation of TCF1 in hepatic adenomas. Nat. Genet. 32:312–315.
6. Bungyoku Y, et al. 2009. Efficient production of infectious hepatitis C virus with adaptive mutations in cultured hepatoma cells. J. Gen. Virol. 90:1681–1691.
7. Cha JY, Kim H, Kim KS, Hur MW, Ahn Y. 2000. Identification of transacting factors responsible for the tissue-specific expression of human glucose transporter type 2 isoform gene. Cooperative role of hepatocyte nuclear factors 1α and 3β. J. Biol. Chem. 275:18358–18365.
8. Denamur S, et al. 2011. Role of oxidative stress in lysosomal membrane permeabilization and apoptosis induced by gentamicin, an aminoglycoside antibiotic. Free Radic. Biol. Med. 51:1656–1665.
9. Deng L, et al. 2008. Hepatitis C virus infection induces apoptosis through a Bax-triggered, mitochondrion-mediated, caspase 3-dependent pathway. J. Virol. 82:10375–10385.
10. Deng L, et al. 2006. NS3 protein of Hepatitis C virus associates with the tumour suppressor p53 and inhibits its function in an NS3 sequence-dependent manner. J. Gen. Virol. 87:1703–1713.
11. Deng L, et al. 2011. Hepatitis C virus infection promotes hepatic gluconeogenesis through an NS5A-mediated, FoxO1-dependent pathway. J. Virol. 85:8556–8568.
12. Dice JF. 2007. Chaperone-mediated autophagy. Autophagy 3:295–299.
13. Dionisio N, et al. 2009. Hepatitis C virus NS5A and core proteins induce oxidative stress-mediated calcium signalling alterations in hepatocytes. J. Hepatol. 50:872–882.
14. Dreux M, Chisari FV. 2011. Impact of the autophagy machinery on hepatitis C virus infection. Viruses 3:1342–1357.
15. Griffin S, Clarke D, McCormick C, Rowlands D, Harris M. 2005. Signal peptide cleavage and internal targeting signals direct the hepatitis C virus p7 protein to distinct intracellular membranes. J. Virol. 79:15525–15536.
16. He Y, Staschke KA, Tan SL. 2006. HCV NS5A: a multifunctional regulator of cellular pathways and virus replication. *In* Tan SL (ed), Hepatitis C viruses: genomes and molecular biology. Horizon Bioscience, Norfolk, United Kingdom. http://www.ncbi.nlm.nih.gov/books/NBK1621/.
17. Ikeda M, et al. 2005. Efficient replication of a full-length hepatitis C virus genome, strain O, in cell culture, and development of a luciferase reporter system. Biochem. Biophys. Res. Commun. 329:1350–1359.
18. Inubushi S, et al. 2008. Hepatitis C virus NS5A protein interacts with and negatively regulates the non-receptor protein tyrosine kinase Syk. J. Gen. Virol. 89:1231–1242.
19. Kasai D, et al. 2009. HCV replication suppresses cellular glucose uptake through down-regulation of cell surface expression of glucose transporters. J. Hepatol. 50:883–894.
20. Lee YH, Sauer B, Gonzalez FJ. 1998. Laron dwarfism and non-insulin-dependent diabetes mellitus in the Hnf-1α knockout mouse. Mol. Cell Biol. 18:3059–3068.
21. Lemon SM, Walker C, Alter MJ, Yi M. 2007. Hepatitis C virus, p 1291–1304. *In* Knipe DM, et al (ed), Fields virology, 5th ed. Lippincott Williams & Wilkins, Philadelphia, PA.
22. Li ZY, Yang Y, Ming M, Liu B. 2011. Mitochondrial ROS generation for regulation of autophagic pathways in cancer. Biochem. Biophys. Res. Commun. 414:5–8.
23. Lindenbach BD, et al. 2005. Complete replication of hepatitis C virus in cell culture. Science 309:623–626.
24. Macheda ML, Rogers S, Best JD. 2005. Molecular and cellular regulation of glucose transporter (GLUT) proteins in cancer. J. Cell Physiol. 202:654–662.
25. Malecki MT, Mlynarski W. 2008. Monogenic diabetes: implications for therapy of rare types of disease. Diabetes Obes. Metab. 10:607–616.
26. Mason AL, et al. 1999. Association of diabetes mellitus and chronic hepatitis C virus infection. Hepatology 29:328–333.
27. Murakami K, et al. 2006. Production of infectious hepatitis C virus particles in three-dimensional cultures of the cell line carrying the genome-length dicistronic viral RNA of genotype 1b. Virology 351:381–392.
28. Nakashima K, Takeuchi K, Chihara K, Hotta H, Sada K. 2011. Inhibition of hepatitis C virus replication through adenosine monophosphate-activated protein kinase-dependent and -independent pathways. Microbiol. Immunol. 55:774–782.
29. Negro F. 2011. Mechanisms of hepatitis C virus-related insulin resistance. Clin. Res. Hepatol Gastroenterol. 35:358–363.
30. Negro F, Alaei M. 2009. Hepatitis C virus and type 2 diabetes. World J. Gastroenterol. 15:1537–1547.
31. Pontoglio M, et al. 1996. Hepatocyte nuclear factor 1 inactivation results in hepatic dysfunction, phenylketonuria, and renal Fanconi syndrome. Cell 84:575–585.
32. Qadri I, et al. 2004. Induced oxidative stress and activated expression of manganese superoxide dismutase during hepatitis C virus replication: role of JNK, p38 MAPK and AP-1. Biochem. J. 378:919–928.
33. Shirakura M, et al. 2007. E6AP ubiquitin ligase mediates ubiquitylation and degradation of hepatitis C virus core protein. J. Virol. 81:1174–1185.
34. Takeda J, Kayano T, Fukomoto H, Bell GI. 1993. Organization of the human GLUT2 (pancreatic beta-cell and hepatocyte) glucose transporter gene. Diabetes 42:773–777.
35. Tellinghuisen TL, Marcotrigiano J, Gorbalenya AE, Rice CM. 2004. The NS5A protein of hepatitis C virus is a zinc metalloprotein. J. Biol. Chem. 279:48576–48587.
36. Tellinghuisen TL, Marcotrigiano J, Rice CM. 2005. Structure of the zinc-binding domain of an essential component of the hepatitis C virus replicase. Nature 435:374–379.
37. Wakita T, et al. 2005. Production of infectious hepatitis C virus in tissue culture from a cloned viral genome. Nat. Med. 11:791–796.
38. Wang AG, et al. 2009. Non-structural 5A protein of hepatitis C virus induces a range of liver pathology in transgenic mice. J. Pathol. 219:253–262.
39. Wang H, Maechler P, Hagenfeldt KA, Wollheim CB. 1998. Dominant-negative suppression of HNF-1alpha function results in defective insulin gene transcription and impaired metabolism-secretion coupling in a pancreatic beta-cell line. EMBO J. 17:6701–6713.
40. Yamagata K, et al. 1996. Mutations in the hepatocyte nuclear factor-1α gene in maturity-onset diabetes of the young (MODY3). Nature 384:455–458.

J Gastroenterol (2012) 47:195–202
DOI 10.1007/s00535-011-0481-z

ORIGINAL ARTICLE—LIVER, PANCREAS, AND BILIARY TRACT

Geranylgeranylacetone has anti-hepatitis C virus activity via activation of mTOR in human hepatoma cells

Shigeyuki Takeshita · Tatsuki Ichikawa · Naota Taura · Hisamitsu Miyaaki · Toshihisa Matsuzaki · Masashi Otani · Toru Muraoka · Motohisa Akiyama · Satoshi Miuma · Eisuke Ozawa · Masanori Ikeda · Nobuyuki Kato · Hajime Isomoto · Fuminao Takeshima · Kazuhiko Nakao

Received: 27 July 2010 / Accepted: 29 August 2011 / Published online: 25 October 2011

Abstract
Background Geranylgeranylacetone (GGA), an isoprenoid compound which includes retinoids, has been used orally as an anti-ulcer drug in Japan. GGA acts as a potent inducer of anti-viral gene expression by stimulating ISGF3 formation in human hepatoma cells. This drug has few side effects and reinforces the effect of IFN when administered in combination with peg-IFN and ribavirin. This study verified the anti-HCV activity of GGA in a replicon system. In addition, mechanisms of anti-HCV activity were examined in the replicon cells.
Methods OR6 cells stably harboring the full-length genotype 1 replicon containing the *Renilla* luciferase gene, ORN/C-5B/KE, were used to examine the influence of the anti-HCV effect of GGA. After treatment, the cells were harvested with Renilla lysis reagent and then subjected to a luciferase assay according to the manufacturer's protocol.
Result The results showed that GGA had anti-HCV activity. GGA induced anti-HCV replicon activity in a time- and dose-dependent manner. GGA did not activate the tyrosine 701 and serine 727 on STAT-1, and did not induce HSP-70 in OR6 cells. The anti-HCV effect depended on the GGA induced mTOR activity, not STAT-1 activity and PKR. An additive effect was observed with a combination of IFN and GGA.
Conclusions GGA has mTOR dependent anti-HCV activity. There is a possibility that the GGA anti-HCV activity can be complimented by IFN. It will be necessary to examine the clinical effectiveness of the combination of GGA and IFN for HCV patients in the future.

Keywords mTOR · STAT-1 · Interferon · HCV · GGA

Abbreviations

IFN	Interferon
HCV	Hepatitis C virus
STAT	Signal transducers and activators of transcription
ISGF-3	IFN-stimulated gene factor 3
ISRE	IFN-stimulated regulatory element
PKR	Double-stranded RNA-dependent protein kinase
Rapa	Rapamycin
PI3-K	Phosphatidylinositol 3-kinase
mTOR	Mammalian target of rapamycin
GGA	Geranylgeranylacetone
siRNA	Small interfering RNA

S. Takeshita · T. Ichikawa (✉) · N. Taura · H. Miyaaki · T. Matsuzaki · M. Otani · T. Muraoka · M. Akiyama · S. Miuma · E. Ozawa · H. Isomoto · F. Takeshima · K. Nakao
Department of Gastroenterology and Hepatology, Graduate School of Biomedical Sciences, Nagasaki University, 1-7-1 Sakamoto, Nagasaki 852-8501, Japan
e-mail: ichikawa@net.nagasaki-u.ac.jp

M. Ikeda · N. Kato
Department of Molecular Biology, Graduate school of Medicine and Dentistry, Okayama University, Okayama, Japan

Introduction

Currently, chronic hepatitis C virus (HCV) infection is the major cause of hepatocellular carcinoma worldwide [1]. Therefore, an anti-HCV strategy is important for prevention of carcinogenesis. The treatment of HCV with a combination of pegylated interferon (IFN) and ribavirin is effective in 80% of HCV genotype 2 or 3 cases, but less than 50% of genotype 1 cases. New anti-HCV agents have been developed to inhibit the life cycle of HCV and are used in combination with IFN-α to ameliorate the salvage rate of HCV infection [2]. It is necessary to improve the salvage rate of HCV infection by clarifying the efficacy of IFN treatment since IFN-α is the most basic agent for HCV treatment. Any agents that can support IFN activity will improve the therapeutic effect for HCV infected patients.

Geranylgeranylacetone (GGA), an isoprenoid compound, which includes retinoids, has been used orally as an anti-ulcer drug developed in Japan [3]. GGA protects the gastric mucosa from various types of stress without affecting gastric acid secretion [4, 5]. Moreover, GGA suppresses cell growth and induces differentiation or apoptosis in several human leukemia cells [6, 7]. Another isoprenoid compound, 3,7,11,15-tetramethyl-2,4,6,-10,14-hexadecapentaenoic acid, which is designated as an acyclic retinoid because it has the ability to interact with nuclear retinoid receptors [8], causes apoptosis in certain human hepatoma cells [9]. GGA acts as a potent inducer of antiviral gene expression by stimulating the ISGF3 formation in human hepatoma cells [10]. GGA induces the expression of antiviral proteins such as 2′5′-oligoadenylate synthetase (2′5′-OAS) and double-stranded RNA-dependent protein kinase (PKR) in hepatoma cell lines. GGA stimulates 2′5′-OAS and PKR gene expression at the transcriptional level through the formation of interferon-stimulated gene factor 3 (ISGF-3), which regulates the transcription of both genes. GGA induces the expression of signal transducers and activators of transcription 1, 2 (STAT-1, STAT-2) and p48 proteins, components of ISGF3, together with the phosphorylation of STAT1 [10]. However, no anti-HCV activity was observed.

A cell culture HCV replicon system has been developed as a useful tool for the study of HCV replication and mass screening for anti-HCV reagents. OR6 cells stably harboring the full-length genotype 1 replicon containing the *Renilla* luciferase gene, ORN/C-5B/KE [11], were used to examine the influence of the anti-HCV effect of IFN. The luciferase activity in cell lysate of OR6 was correlated with the HCV-RNA concentration, and the IC50 of IFN-α was less than 10 IU/mL [11]. The OR6 system is a useful and sensitive cell culture replicon system.

This study verified the anti-HCV activity of GGA in the OR6 system. In addition, the mechanisms of anti-HCV activity were examined in OR6 cells.

Materials and methods

Reagents

GGA was a generous gift from Eisai Co. (Tokyo, Japan). Recombinant human IFN-α2a was purchased from Nippon Roche Co. (Tokyo, Japan). Wortmannin, LY294002, Akt inhibitor and rapamycin were purchased from Calbiochem (La Jolla, CA, USA).

HCV replicon system

OR6 cells stably harboring the full-length genotype 1 replicon, ORN/C-5B/KE, were used to examine the influence of the anti-HCV effect of GGA. The cells were cultured in Dulbecco's modified Eagle's medium (Gibco-BRL, Invitrogen) supplemented with 10% fatal bovine serum, penicillin and streptomycin and maintained in the presence of G418 (300 mg/L; Geneticin, Invitrogen). This replicon was derived from the 1B-2 strain (strain HCV-o, genotype 1b), in which the *Renilla* luciferase gene is introduced as a fusion protein with neomycin to facilitate the monitoring of HCV replication.

Reporter gene assay

The OR6 cells were grown in 24-well plates. One day later, the cells were incubated in the absence or presence of varying concentrations of chemical blockers and GGA. After treatment, the cells were harvested with Renilla lysis reagent (Promega, Madison, WI, USA) and luciferase activity in the cells was determined using a luciferase reporter assay system and a TD-20/20 luminometer. The data were expressed as the relative luciferase activity.

Western blotting and antibodies

Western blotting with anti-STAT-1, anti-PKR (Santa Cruz Biotechnology, Santa Cruz, CA, USA), anti-tyrosine-701 phosphorylated STAT-1, anti-serine-727 phosphorylated STAT-1, anti-serine-2448 phosphorylated mTOR, anti-mTOR, anti-threonine-389 phosphorylated p70S6K, anti-p70S6K (Cell Signaling, Beverly, MA, USA) and anti-HSP70 (Stressmarq Biosciences Inc, Victoria, Canada) was performed as described previously [10]. Briefly, OR6 cells were lysed by the addition of a lysis buffer (50 mmol/L Tris–HCl, pH 7.4, 1% Np40, 0.25% sodium deoxycholate, 0.02% sodium azide, 0.1% SDS, 150 mmol/L NaCl, 1 mmol/L EDTA, 1 mmol/L PMSF, 1 mg/mL each of aprotinin, leupeptin and pepstatin, 1 mmol/L sodium *o*-vanadate and 1 mmol/L NaF). The samples were separated by electrophoresis on 8–12% SDS polyacrylamide gels and electrotransferred to nitrocellulose membranes, and then blotted with each antibody. The membranes were incubated with horseradish peroxidase-conjugated anti-rabbit IgG or anti-mouse IgG, and the immunoreactive bands were visualized using the ECL chemiluminescence system (Amersham Life Science, Buckinghamshire, England).

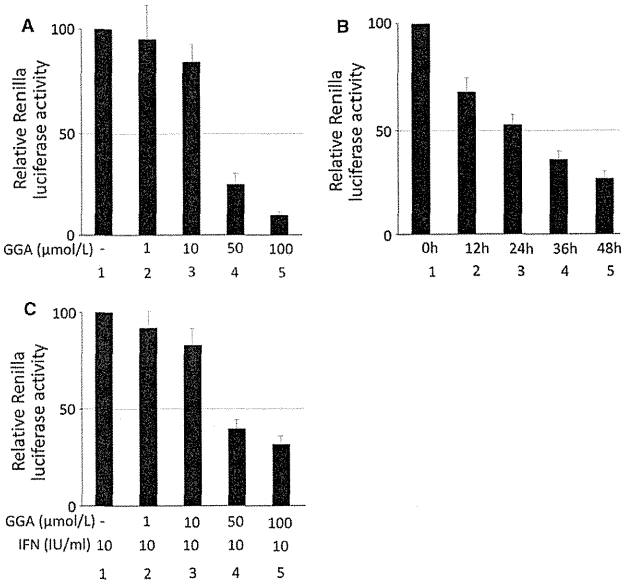

Fig. 1 The effect of GGA on the genome-length HCV RNA replication system. **a** Dose dependent effect of GGA. **b** Time course of GGA suppressed HCV replication. **c** The additive effect of GGA with IFN-α suppressed HCV replication. **a** The OR6 cells were treated with 1–100 μmol/L of GGA (*lanes 2–5*) and *lane 1* was not treated. One day later, *Renilla* luciferase activity was determined by luminometer ($n = 4$). The data are expressed as the mean ± SD and are representative of four similar experiments. The differences between *lane 3* versus *4*, *lane 3* versus *5* and *lane 3* versus *5* were statistically significant. **b** The OR6 cells were treated 50 μmol/L of GGA and at the indicated time, HCV replicon assay was done ($n = 4$). The differences between *lane 1* versus *3–5* and *lane 2* versus *4*, *5* were statistically significant. **c** The OR6 cells were treated with 10 IU/mL of IFN-α in the absence (*lane 1*) or presence of treatment with 1–100 μmol/L of GGA (*lanes 2–5*). Non-treatment OR6 cells has 100% of relative *Renilla* luciferase light unit. The differences between *lane 1* versus *4*, *5* were statistically significant. Statistical significance was accepted as a P value of <0.05. The data are expressed as the mean ± SD and are representative of four similar experiments

siRNA transfection assay

mTOR gene knockdown was performed using siRNA (Cell Signaling, Beverly, MA, USA). OR6 cells were transfected with100 nmol/L mTOR specific and non-targeted siRNA as a control in accordance with the appended manual. One day later, the cells were incubated in either the absence or presence of 50 μmol/L GGA.

mTOR kinase activity assay

The cells were washed two times with TBS and lysed by addition of lysis buffer [50 mM Tris HCl, pH 7.4, 100 mM NaCl, 50 mM β-glycerophosphate, 10% glycerol (w/v), 1% Tween-20 detergent (w/v), 1 mM EDTA, 20 nM microcystin-LR, 25 mM NaF, and a cocktail of protease inhibitors]. The insoluble materials were removed by centrifugation at 10,000 rpm for 15 min at 4°C, and the supernatants were collected and subjected to analysis of the mTOR kinase activity using a commercially available kit (Calbiochem, San Diego, USA) according to the manufacturer's instructions.

Results

GGA with or without IFN had anti-HCV activity

OR6 cells, the full-length HCV replication system, were used to examine the effect of GGA. The cells were treated with 1–100 μmol/L of GGA for 24 h and the amount of HCV replicon was measured by the *Renilla* luciferase assay (Fig. 1a). The relative *Renilla* luciferase activity decreased in a dose-dependent manner. Furthermore, GGA induced anti-HCV replicon activity was time dependent (Fig. 1b). GGA was combined with IFN-α to examine the additive effect (Fig. 1c). One or 10 μmol/L of GGA combined with IFN-α decreased the relative *Renilla* luciferase activity slightly (Fig. 1c). However, 50 or 100 μmol/L of GGA combined with IFN-α decreased the relative *Renilla* luciferase activity with statistical difference. GGA treatment did not have any statistically significant effect on cell viability from 1 to 100 μmol/L of GGA for 24 h (data not shown).

GGA did not activate the tyrosine-701 and serine-727 on STAT-1, and did not induce PKR and HSP-70 in OR6 cells

GGA mediated phosphorylation of STAT-1 at the tyrosine-701 and serine-727 residues was investigated using antibodies to phospho-specific STAT-1 on OR6 cells. No phosphorylation of tyrosine-701 and serine-727 on STAT-1 was detected in OR6 cells (Fig. 2a). IFN induce anti-viral protein, PKR, and STAT-1 has an interferon stimulating responsive element (ISRE) in the promoter region [12]. The expression levels of both proteins did not change throughout this study, as indicated by a Western blotting analysis (Fig. 2b, c). Next, the role of HSP in the mechanism of GGA activity was examined because GGA is an inducer of HSP. The HSP-70 expression was increased by pre-exposure to heat shock (Fig. 2d, lanes 2, 4), but it did not increase due to the effects of GGA (Fig. 2d, lanes 3, 4).

Rapamycin and mTOR specific siRNA, but not PI3-K inhibitor and Akt inhibitor, were able to cancel the GGA induced anti-HCV activity

The role of the PI3-K-Akt-mTOR pathway the anti-HCV activity of GGA was examined in OR6 cells. The cells were treated with GGA after 3 h in the presence or absence of rapamycin as an mTOR inhibitor, Akt inhibitor, or wortmannin as a PI3-K inhibitor (Fig. 3). Pretreatment with rapamycin attenuated the anti-HCV replication effect

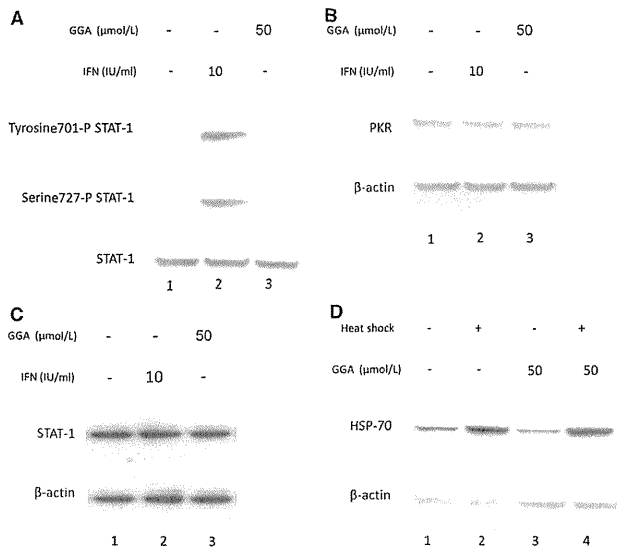

Fig. 2 Effect of GGA on STAT-1 (**a**), PKR (**b**) and HSP-70 (**c**). **a** The OR6 cells were either untreated (*lane 1*) or treated with 10 IU/mL of IFN-α (*lane 2*) for 30 min or treated with 50 μmol/L GGA (*lane 3*) and then were phosphorylated STAT-1 at tyrosine-701 residue (*upper panel*) and at serine-727 residue (*middle panel*), the expression STAT-1 (*lower panel*) was analyzed by Western blotting. **b** The OR6 cells were either untreated (*lane 1*) or treated with 10 IU/mL of IFN-α (*lane 2*) for 30 min or treated with 50 μmol/L GGA (*lane 3*), and then the expression of PKR (*upper panel*) was analyzed by a Western blotting analysis. The β-actin (*lower panel*) protein expression was used as an internal control. **c** The OR6 cells were either untreated (*lane 1*) or given heat shock (at 42°C 15 min, overnight recovery at 37°C) (*lanes 2, 4*) or treated with 50 μmol/L of GGA (*lanes 3, 4*) and then the expression HSP-70 (*upper panel*) was analyzed by Western blotting. β-Actin (*lower panel*) protein is the internal control

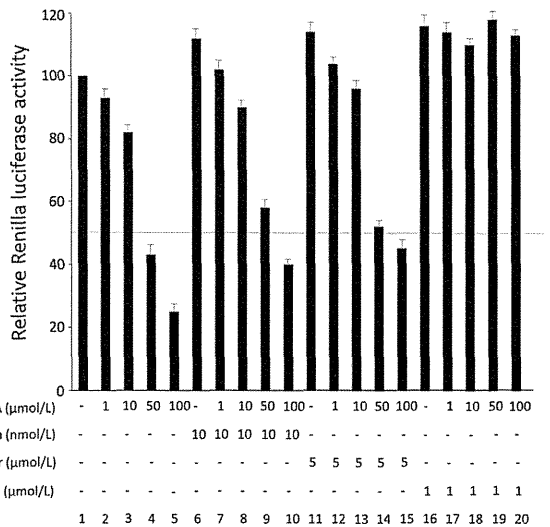

Fig. 3 Changes in GGA suppressed HCV replication by rapamycin, but not PI3-K inhibitor and Akt inhibitor. OR6 cells were treated with 1–100 μmol/L of GGA in the absence (*lanes 2–5*) or presence of pretreatment (*lanes 7–10, 12–15, 17–20*) for 3 h. *Lanes 1, 6, 11* and *16* were not treated with GGA. *Lanes 6, 11* and *16* were treated with wortmannin, an Akt inhibitor, and rapamycin, respectively. One day later, *Renilla* luciferase activity was determined by luminometer ($n = 4$). The data are expressed as the mean ± SD and are representative of four similar experiments

in comparison to GGA alone (Fig. 3, lanes 17–20), whereas pretreatment with wortmannin and Akt inhibitor did not increase the *Renilla* luciferase activity (Fig. 3, lanes 7–10, 12–15). siRNA transfection was used for mTOR knockdown to explore role of mTOR in the anti-HCV activity (Fig. 4). The transfection efficiency of the siRNA was confirmed by a Western blotting analysis. In this experiment, the detectable band intensities were quantified by the National Institutes of Health image software program. Although the transfection efficiency of siRNA was barely 46% (Fig. 4a), GGA-induced anti-HCV activity was clearly inhibited in mTOR-siRNA transfected cells (Fig. 4b, lane 4, 6) in comparison to the control cells (Fig. 4b, lanes 3, 5).

GGA induced mTOR activity, mTOR phosphorylation and p70S6K phosphorylation in OR6 cells

The phosphorylation of the serine-2448 residues of mTOR by 50 μmol/L of GGA was detected 30 min after GGA treatment. The band intensity of serine-2448 phosphorylated mTOR decreased by pretreatment with rapamycin but was almost same as with GGA alone following pretreatment with LY294002 (Fig. 5a). Furthermore, an mTOR activity assay was conducted to confirm the activity mechanism of GGA (Fig. 5b). The mTOR activity was increased by treatment with GGA alone (Fig. 5b, lane 4) and was inhibited by pretreatment with rapamycin (Fig. 5b, lane 6), whereas pretreatment with LY94002 did not suppress the mTOR activity (Fig. 5b, lane 5). Furthermore, to evaluate the mTOR activity, we investigated the level of phospholylated-p70S6K by a Western blotting analysis (Fig. 5c). The phosphorylation of the threonine-389 residue of p70S6K by 50 μmol/L of GGA was detected. Similar to mTOR, the band intensity of phospho-threonine-389 of p70S6K decreased after pretreatment with rapamycin, but the intensity was almost the same as that seen following treatment with GGA alone after pretreatment with LY294002 (Fig. 5c).

Discussion

GGA demonstrated the anti-HCV activity in this study. The anti-HCV effect depended on the GGA induced mTOR activity, not STAT-1 activity. An additive effect was observed with the combination of IFN and GGA.

GGA is a non-toxic heat shock protein (HSP) 70 inducer [13]. Various GGA activities outside of the stomach are also related to HSP induction [14–16]. GGA induced HSP-70 exerts an anti-ischemic stress activity in the heart and liver [16, 17], an anti-inflammatory activity in various cell types [18] and promotes liver regeneration [19]. GGA induces thioredoxin as well as HSP-70 in hepatocytes and other cells [20]. Thioredoxin anti-virus activity, is induced by AP-1 and NF-κB but not HSP-70 [21]. GGA has potent

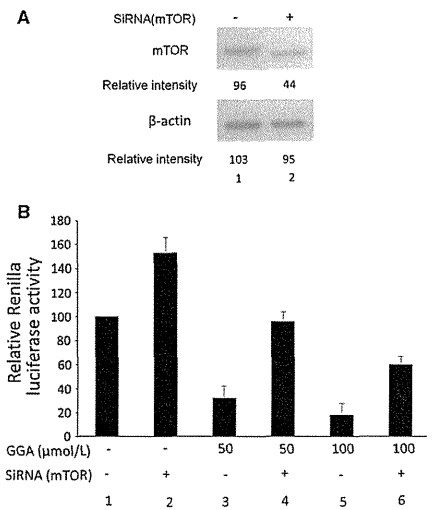

Fig. 4 Changes in GGA suppressed HCV replication by mTOR-siRNA. **a** OR6 cells were transfected with mTOR-siRNA (*lane 1*) or the non-targeted siRNA (*lane 2*). The expression of mTOR was evaluated by a Western blotting analysis. **b** The OR6 cells were transfected with mTOR-siRNA (*lanes 2, 4* and *6*) and the non-targeted siRNA (*lanes 1, 3* and *5*). One day later, the cells were treated with GGA (*lanes 3–6*). The HCV replicon assay is the same as Fig. 3. Non-treatment OR6 cells has 100% of relative *Renilla* luciferase light unit. The *Renilla* luciferase activity increased in the OR6 cells transfected with mTOR-siRNA (*lane 2*) in comparison to the non-targeted siRNA (*lane 1*). However, in OR6 cells treated with GGA, there was a greater elevation of *Renilla* luciferase activity in OR6 cells transfected with mTOR-siRNA (*lanes 4* and *6*) as compared to that with the non-targeted siRNA (*lanes 3* and *5*). The data are expressed as the mean ± SD and are representative example of four similar experiments

antiviral activity via the enhancement of antiviral factors and can clinically provide protection from influenza virus infection [22]. GGA significantly inhibits the synthesis of influenza virus-associated proteins and prominently enhances the expression of human myxovirus resistance 1 (MxA) followed by increased HSP-70 transcription [22]. Moreover, GGA augments the expression of an interferon-inducible double-strand RNA-activated protein kinase (PKR) gene and promotes PKR autophosphorylation and concomitantly alpha subunit of eukaryotic initiation factor 2 phosphorylation during influenza virus infection [22]. These anti-virus activities are related to GGA induced HSP-70. But, HSP-70 protein and PKR were not induced by GGA in OR6 cells in the current study. There is apparently no relationship between the GGA induced anti-HCV activity and HSP, PKR in OR6 cells. Therefore, we thought that HSP and PKR-independent anti-HCV activity induced by GGA was present in this hepatoma-derived cell line.

GGA induction of anti-viral protein is dependent upon STAT-1 tyrosine phosphorylation in HuH-7 and HepG2 [10]. However, GGA did not induce STAT-1 tyrosine phosphorylation and anti-virus protein, PKR, in OR6 cells in this study. Moreover, the GGA induced anti-HCV activity depended on mTOR activity, not STAT-1. OR6 cells are full length HCV replicon transfected HuH-7 cells [11]. HCV virus products inhibit the Jak-STAT pathway [23–25]. The mechanism of inhibition of the Jak-STAT pathway is multi-factorial including the suppressor of cytokine signaling 3 (SOCS-3) expression [26], protein phosphatase 2A (PP2A) induction [27], STAT-3 expression [28] and IL-8 expression [29]. GGA induced STAT-1 tyrosine phosphorylation and inducible PKR protein levels are also minor. Generally, the replicon transfection induces the intrinsic IFN [30], but STAT-1 tyrosine phosphorylation was not detected in combined OR6 cells. HCV replicon produced viral product might be inhibiting GGA-induced STAT-1 tyrosine phosphorylation.

mTOR is associated with the IFN induced anti-HCV signal [31]. The IFN activated mTOR pathway exhibits important regulatory effects in the generation of the IFN responses, including the anti-encephalomyocarditis virus effect [32]. IFN-induced mTOR is LY294002 sensitive and does not affect the IFN-stimulated regulatory element (ISRE) dependent promoter gene activity. A relationship has been observed between the replication of the hepatitis virus and mTOR activity. p21-activated kinase 1 is activated through the mTOR/p70 S6 kinase pathway and regulates the replication of HCV [33]. The IFN induced mTOR activity, independent of PI3K and Akt, is the critical factor for its anti-HCV activity and Jak independent TOR activity involves STAT-1 phosphorylation and nuclear localization, and then PKR is expressed in hepatocytes [31]. No relationship between GGA and mTOR has been reported. However, GGA induced anti-HCV activity depended on mTOR activity independent of PI3-K-Akt, as observed with IFN induced mTOR activity.

When 150 mg of GGA was administered orally, the serum concentration of GGA was approximately 7 μmol/L [34]. The concentration of GGA in the portal blood would be several-fold higher than the serum concentration of GGA; therefore, we speculated that the pharmacological action that would be obtained in clinical practice would be the same as that observed in this study.

GGA, a drug that can be safely administered orally, has mTOR dependent anti-HCV activity. The combination of IFN and GGA has an additive effect on anti-HCV activity. The current results suggest that combination therapy with

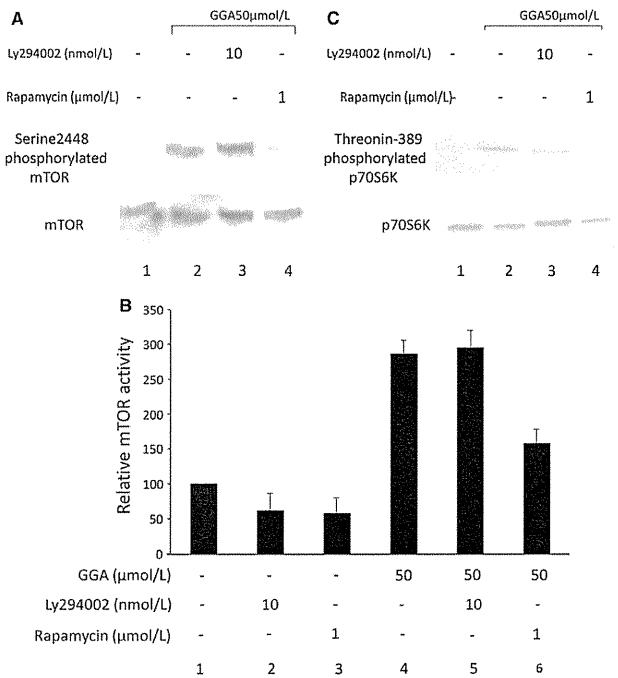

Fig. 5 Effect of GGA on mTOR and effect of LY294002 and rapamycin on GGA-induced serine phosphorylated mTOR and threonine phosphorylated p70S6K. **a** After pretreatment with 10 nmol/L LY294002 (*lane 3*) and 1 μmol/L rapamycin (*lane 4*) for 3 h, the OR6 cells were either untreated (*lane 1*) or treated with 50 μmol/L GGA (*lanes 2–4*) for 30 min and then were phosphorylated mTOR at serine-2448 residue (*upper panel*), the expression of mTOR (*lower panel*) was analyzed by Western blotting. **b** After pretreatment with 10 nmol/L LY294002 (*lanes 2* and *5*) and 1 μmol/L rapamycin (*lanes 3* and *6*) for 3 h, the OR6 cells were either untreated (*lanes 1–3*) or treated with 50 μmol/L GGA (*lanes 4–6*) for 30 min. The mTOR kinase activity was determined by ELISA-based mTOR kinase activity assay kit ($n = 4$). The differences between *lanes 1* and *4*, *lanes 4* and *6*, and *lanes 5* and *6* were statistically significant. The data are expressed as the mean ± SD and are representative of four similar experiments. **c** After pretreatment with 10 nmol/L LY294002 (*lane 3*) and 1 μmol/L, and with rapamycin (*lane 4*) for 3 h, the OR6 cells were either untreated (*lane 1*) or treated with 50 μmol/L GGA (*lanes 2–4*) for 30 min, and then were examined for phosphorylated p70S6K at the threonine-389 residue (*upper panel*), or the expression of p70S6K (*lower panel*) by a Western blotting analysis

GGA and IFN is, therefore, expected to improve the anti-HCV activity. It will, therefore, be necessary to examine the clinical effectiveness of the combination with GGA and IFN for HCV patients in the future.

References

1. Fattovich G, Stroffolini T, Zagni I, Donato F. Hepatocellular carcinoma in cirrhosis: incidence and risk factors. Gastroenterology. 2004;127:S35–50.
2. Pawlotsky JM, Chevaliez S, McHutchison JG. The hepatitis C virus life cycle as a target for new antiviral therapies. Gastroenterology. 2007;132:1979–98.
3. Murakami M, Oketani K, Fujisaki H, Wakabayashi T, Ohgo T. Antiulcer effect of geranylgeranylacetone, a new acyclic polyisoprenoid, on experimentally induced gastric and duodenal ulcers in rats. Arzneimittelforschung. 1981;31:799–804.
4. Murakami M, Oketani K, Fujisaki H, Wakabayashi T, Inai Y, Abe S, et al. Effect of synthetic acyclic polyisoprenoids on the cold-restraint stress induced gastric ulcer in rats. Jpn J Pharmacol. 1983;33:549–56.
5. Hirakawa T, Rokutan K, Nikawa T, Kishi K. Geranylgeranylacetone induces heat shock proteins in cultured guinea pig gastric mucosal cells and rat gastric mucosa. Gastroenterology. 1996;111:345–57.
6. Sakai I, Tanaka T, Osawa S, Hashimoto S, Nakaya K. Geranylgeranylacetone used as an antiulcer agent is a potent inducer of differentiation of various human myeloid leukemia cell lines. Biochem Biophys Res Commun. 1993;191:873–9.

7. Okada S, Yabuki M, Kanno T, Hamazaki K, Yoshioka T, Yasuda T, et al. Geranylgeranylacetone induces apoptosis in HL-60 cells. Cell Struct Funct. 1999;24:161–8.
8. Araki H, Shidoji Y, Yamada Y, Moriwaki H, Muto Y. Retinoid agonist activities of synthetic geranyl geranoic acid derivatives. Biochem Biophys Res Commun. 1995;209:66–72.
9. Kuhen KL, Vessey JW, Samuel CE. Mechanism of interferon action: identification of essential positions within the novel 15-base-pair KCS element required for transcriptional activation of the RNA-dependent protein kinase PKR gene. J Virol. 1998; 72:9934–9.
10. Ichikawa T, Nakao K, Nakata K, Hamasaki K, Takeda Y, Kajiya Y, et al. Geranylgeranylacetone induces antiviral gene expression in human hepatoma cells. Biochem Biophys Res Commun. 2001; 280:933–9.
11. Ikeda M, Abe K, Dansako H, Nakamura T, Naka K, Kato N. Efficient replication of a full-length hepatitis C virus genome, strain O, in cell culture, and development of a luciferase reporter system. Biochem Biophys Res Commun. 2005;329:1350–9.
12. Tanaka H, Samuel CE. Mechanism of interferon action. Structure of the mouse PKR gene encoding the interferon-inducible RNA-dependent protein kinase. Proc Natl Acad Sci USA. 1994;91: 7995–9.
13. Hirakawa T, Rokutan K, Nikawa T, Kishi K. Geranylgeranylacetone induces heat shock proteins in cultured guinea pig gastric mucosal cells and rat gastric mucosa. Gastroenterology. 1996; 111:345–57.
14. Uchida S, Fujiki M, Nagai Y, Abe T, Kobayashi H. Geranylgeranylacetone, a noninvasive heat shock protein inducer, induces protein kinase C and leads to neuroprotection against cerebral infarction in rats. Neurosci Lett. 2006;396:220–4.
15. Fujibayashi T, Hashimoto N, Jijiwa M, Hasegawa Y, Kojima T, Ishiguro N. Protective effect of geranylgeranylacetone, an inducer of heat shock protein 70, against drug-induced lung injury/fibrosis in an animal model. BMC Pulm Med. 2009;9:45.
16. Sakabe M, Shiroshita-Takeshita A, Maguy A, Brundel BJ, Fujiki A, Inoue H, et al. Effects of a heat shock protein inducer on the atrial fibrillation substrate caused by acute atrial ischaemia. Cardiovasc Res. 2008;78:63–70.
17. Fudaba Y, Ohdan H, Tashiro H, Ito H, Fukuda Y, Dohi K, et al. Geranylgeranylacetone, a heat shock protein inducer, prevents primary graft nonfunction in rat liver transplantation. Transplantation. 2001;72:184–9.
18. Mochida S, Matsura T, Yamashita A, Horie S, Ohata S, Kusumoto C, et al. Geranylgeranylacetone ameliorates inflammatory response to lipopolysaccharide (LPS) in murine macrophages: inhibition of LPS binding to the cell surface. J Clin Biochem Nutr. 2007;41:115–23.
19. Kanemura H, Kusumoto K, Miyake H, Tashiro S, Rokutan K, Shimada M. Geranylgeranylacetone prevents acute liver damage after massive hepatectomy in rats through suppression of a CXC chemokine GRO1 and induction of heat shock proteins. J Gastrointest Surg. 2009;13:66–73.
20. Hirota K, Nakamura H, Arai T, Ishii H, Bai J, Itoh T, et al. Geranylgeranylacetone enhances expression of thioredoxin and suppresses ethanol-induced cytotoxicity in cultured hepatocytes. Biochem Biophys Res Commun. 2000;275:825–30.
21. Schenk H, Klein M, Erdbrügger W, Dröge W, Schulze-Osthoff K. Distinct effects of thioredoxin and antioxidants on the activation of transcription factors NF-kappa B and AP-1. Proc Natl Acad Sci USA. 1994;91:1672–6.
22. Unoshima M, Iwasaka H, Eto J, Takita-Sonoda Y, Noguchi T, Nishizono A. Antiviral effects of geranylgeranylacetone: enhancement of MxA expression and phosphorylation of PKR during influenza virus infection. Antimicrob Agents Chemother. 2003;47:2914–21.
23. Lin W, Choe WH, Hiasa Y, Kamegaya Y, Blackard JT, Schmidt EV, et al. Hepatitis C virus expression suppresses interferon signaling by degrading STAT1. Gastroenterology. 2005;128:1034–41.
24. Lan KH, Lan KL, Lee WP, Sheu ML, Chen MY, Lee YL, et al. HCV NS5A inhibits interferon-alpha signaling through suppression of STAT1 phosphorylation in hepatocyte-derived cell lines. J Hepatol. 2007;46:759–67.
25. Luquin E, Larrea E, Civeira MP, Prieto J, Aldabe R. HCV structural proteins interfere with interferon-alpha Jak/STAT signalling pathway. Antiviral Res. 2007;76:194–7.
26. Huang Y, Feld JJ, Sapp RK, Nanda S, Lin JH, Blatt LM, et al. Defective hepatic response to interferon and activation of suppressor of cytokine signaling 3 in chronic hepatitis C. Gastroenterology. 2007;132:733–44.
27. Duong FH, Filipowicz M, Tripodi M, La Monica N, Heim MH. Hepatitis C virus inhibits interferon signaling through up-regulation of protein phosphatase 2A. Gastroenterology. 2004;126: 263–77.
28. Brender C, Lovato P, Sommer VH, Woetmann A, Mathiesen AM, Geisler C, et al. Constitutive SOCS-3 expression protects T-cell lymphoma against growth inhibition by IFNalpha. Leukemia. 2005;19:209–13.
29. Jia Y, Wei L, Jiang D, Wang J, Cong X, Fei R. Antiviral action of interferon-alpha against hepatitis C virus replicon and its modulation by interferon-gamma and interleukin-8. J Gastroenterol Hepatol. 2007;22:1278–85.
30. Fredericksen B, Akkaraju GR, Foy E, Wang C, Pflugheber J, Chen ZJ, et al. Activation of the interferon-beta promoter during hepatitis C virus RNA replication. Viral Immunol. 2002;15: 29–40.
31. Matsumoto A, Ichikawa T, Nakao K, Miyaaki H, Hirano K, Fujimito M, et al. Interferon-alpha-induced mTOR activation is an anti-hepatitis C virus signal via the phosphatidylinositol 3-kinase-Akt-independent pathway. J Gastroenterol. 2009;44: 856–63.
32. Kaur S, Lal L, Sassano A, Majchrzak-Kita B, Srikanth M, Baker DP, et al. Regulatory effects of mammalian target of rapamycin activated pathways in type I and II interferon signaling. J Biol Chem. 2007;282:1757–68.
33. Ishida H, Li K, Yi M, Lemon SM. p21-activated kinase 1 is activated through the mammalian target of rapamycin/p70 S6 kinase pathway and regulates the replication of hepatitis C virus in human hepatoma cells. J Biol Chem. 2007;282:11836–48.
34. Hasegawa J, Morishita N, Seki T, Hashida N, Kanazawa T, Sato A. Effect of meals in healthy adult administered Selbex. Syokakika. 1987;7:740–52.

Virus Genes (2012) 44:374–381
DOI 10.1007/s11262-012-0712-2

Development of a drug assay system with hepatitis C virus genome derived from a patient with acute hepatitis C

Kyoko Mori · Youki Ueda · Yasuo Ariumi · Hiromichi Dansako · Masanori Ikeda · Nobuyuki Kato

Received: 5 October 2011 / Accepted: 1 January 2012 / Published online: 18 January 2012

Abstract We developed a new cell culture drug assay system (AH1R), in which genome-length hepatitis C virus (HCV) RNA (AH1 strain of genotype 1b derived from a patient with acute hepatitis C) efficiently replicates. By comparing the AH1R system with the OR6 assay system that we developed previously (O strain of genotype 1b derived from an HCV-positive blood donor), we demonstrated that the anti-HCV profiles of reagents including interferon-γ and cyclosporine A significantly differed between these assay systems. Furthermore, we found unexpectedly that rolipram, an anti-inflammatory drug, showed anti-HCV activity in the AH1R assay but not in the OR6 assay, suggesting that the anti-HCV activity of rolipram differs depending on the HCV strain. Taken together, these results suggest that the AH1R assay system is useful for the objective evaluation of anti-HCV reagents and for the discovery of different classes of anti-HCV reagents.

Keywords HCV · Acute hepatitis C · Anti-HCV drug assay system · Anti-HCV activity of rolipram

Introduction

Hepatitis C virus (HCV) infection frequently causes chronic hepatitis, which progresses to liver cirrhosis and hepatocellular carcinoma. HCV is an enveloped virus with a positive single-stranded 9.6 kb RNA genome, which encodes a large polyprotein precursor of approximately 3,000 amino acid (aa) residues [1, 2]. This polyprotein is cleaved by a combination of the host and viral proteases into at least 10 proteins in the following order: Core, envelope 1 (E1), E2, p7, non-structural 2 (NS2), NS3, NS4A, NS4B, NS5A, and NS5B [1].

Human hepatoma HuH-7 cell culture-based HCV replicon systems derived from a number of HCV strains have been widely used for various studies on HCV RNA replication [3, 4] since the first replicon system (based on the Con1 strain of genotype 1b) was developed in 1999 [5]. Genome-length HCV RNA replication systems (see Fig. 2 for details) derived from a limited number of HCV strains (H77, N, Con1, O, and JFH-1) are also sometimes used for such studies, as they are more useful than the replicon systems lacking the structural region of HCV, although the production of infectious HCV from the genome-length HCV RNA has not been demonstrated to date [3, 4]. Furthermore, these RNA replication systems have been improved enough to be suitable for the screening of anti-HCV reagents by the introduction of reporter genes such as luciferase [3, 4, 6]. We also developed an HuH-7-derived cell culture assay system (OR6) in which genome-length HCV RNA (O strain of genotype 1b derived from an HCV-positive blood donor) encoding renilla luciferase (RL) efficiently replicates [7]. Such reporter assay systems could save time and facilitate the mass screening of anti-HCV reagents, since the values of luciferase correlated well with the level of HCV RNA after treatment with anti-HCV reagents. Furthermore, OR6 assay system became more useful as a drug assay system than the HCV subgenomic replicon-based reporter assay systems developed to date [3, 4], because the older systems lack the Core-NS2 regions containing structural proteins likely to be involved in the events that take place in the HCV-infected human liver.

K. Mori · Y. Ueda · Y. Ariumi · H. Dansako · M. Ikeda · N. Kato (✉)
Department of Tumor Virology, Okayama University Graduate School of Medicine, Dentistry, and Pharmaceutical Sciences, 2-5-1 Shikata-cho, Okayama 700-8558, Japan
e-mail: nkato@md.okayama-u.ac.jp

Indeed, by the screening of preexisting drugs using the OR6 assay system, we have identified mizoribine [8], statins [9], hydroxyurea [10], and teprenone [11] as new anti-HCV drug candidates, indicating that the OR6 assay system is useful for the discovery of anti-HCV reagents.

On the other hand, we previously established for the first time an HuH-7-derived cell line (AH1) that harbors genome-length HCV RNA (AH1 strain of genotype 1b) derived from a patient with acute hepatitis C [12]. In that study, we noticed different anti-HCV profiles of interferon (IFN)-γ or cyclosporine A (CsA) between AH1 and O cells supporting genome-length HCV RNA (O strain) replication [7]. From these results, we supposed that the diverse effects of IFN-γ or CsA were attributable to the difference in HCV strains [12].

To test this assumption in detail, we first developed an AH1 strain-derived assay system (AH1R) corresponding to the OR6 assay system, and then performed a comparative analysis using AH1R and OR6 assay systems. In this article, we report that the difference in HCV strains causes the diverse effects of anti-HCV reagents, and we found unexpectedly by AH1R assay that rolipram, an anti-inflammatory drug, is an anti-HCV drug candidate.

Materials and methods

Reagents

IFN-α, IFN-γ, and CsA were purchased from Sigma-Aldrich (St. Louis, MO). Rolipram was purchased from Wako Pure Chemical Industries (Osaka, Japan).

Plasmid construction

The plasmid pAH1RN/C-5B/PL,LS,TA,$(VA)_3$ was constructed from pAH1 N/C-5B/PL,LS,TA,$(VA)_3$ encoding genome-length HCV RNA clone 2 (See Fig. 2) obtained from AH1 cells [12], by introducing a fragment of the RL gene from pORN/C-5B into the *Asc*I site before the neomycin phosphotransferase (Neo^R) gene as previously described [7].

RNA synthesis

The plasmid pAH1RN/C-5B/PL,LS,TA,$(VA)_3$ DNA was linearized by *Xba*I, and used for RNA synthesis with T7 MEGAscript (Ambion, Austin TX) as previously described [7].

Cell cultures

AH1R and OR6 cells supporting genome-length HCV RNAs were cultured in Dulbecco's modified Eagle's medium (DMEM) supplemented with 10% fetal bovine serum (FBS) and 0.3 mg/mL of G418 (Geneticin; Invitrogen, Carlsbad, CA). AH1c-cured cells, which were created by eliminating HCV RNA from AH1 cells [12] by IFN-γ treatment, were also cultured in DMEM supplemented with 10% FBS.

RNA transfection and selection of G418-resistant cells

Genome-length HCV (AH1RN/C-5B/PL,LS,TA,$(VA)_3$) RNA synthesized in vitro was transfected into AH1c cells by electroporation, and the cells were selected in the presence of G418 (0.3 mg/mL) for 3 weeks as described previously [13].

RL assay for anti-HCV reagents

To monitor the effects of anti-HCV reagents, RL assay was performed as described previously [14]. Briefly, the cells were plated onto 24-well plates (2×10^4 cells per well) in triplicate and cultured with the medium in the absence of G418 for 24 h. The cells were then treated with each reagent at several concentrations for 72 h. After treatment, the cells were subjected to a luciferase assay using the RL assay system (Promega, Madison, WI). From the assay results, the 50% effective concentration (EC_{50}) of each reagent was determined.

Quantification of HCV RNA

Quantitative reverse transcription-polymerase chain reaction (RT-PCR) analysis for HCV RNA was performed using a real-time LightCycler PCR (Roche Applied Science, Indianapolis, IN, USA) as described previously [7]. The experiments were done in triplicate.

IFN-α treatment to evaluate the assay systems

To monitor the anti-HCV effect of IFN-α on AH1R cells, 2×10^4 cells and 5×10^5 cells were plated onto 24-well plates (for luciferase assay) and 10 cm plates (for quantitative RT-PCR assay) in triplicate, respectively, and cultured for 24 h. The cells were then treated with IFN-α at final concentrations of 0, 1, 10, and 100 IU/mL for 24 h, and subjected to luciferase and quantitative RT-PCR assays as described above.

Western blot analysis

The preparation of cell lysates, sodium dodecyl sulfate–polyacrylamide gel electrophoresis, and immunoblotting analysis with a PVDF membrane were performed as described previously [13]. The antibodies used in this study were those against HCV Core (CP11 monoclonal antibody;

Institute of Immunology, Tokyo), NS5B, and E2 (generous gifts from Dr. M. Kohara, Tokyo Metropolitan Institute of Medical Science, Japan). Anti-β-actin antibody (AC-15; Sigma, St. Louis, MO, USA) was used as a control for the amount of protein loaded per lane. Immunocomplexes were detected with the Renaissance enhanced chemiluminescence assay (Perkin-Elmer Life Sciences, Boston, MA).

WST-1 cell proliferation assay

The cells were plated onto 96-well plates (1×10^3 cells per well) in triplicate and then treated with rolipram at several concentrations for 72 h. After treatment, the cells were subjected to the WST-1 cell proliferation assay (Takara Bio, Otsu, Japan) according to the manufacturer's protocol. From the assay results, the 50% cytotoxic concentration (CC_{50}) of rolipram was estimated. The selective index (SI) value of rolipram was also estimated by dividing the CC_{50} value by the EC_{50} value.

RT-PCR and sequencing

To amplify the genome-length HCV RNA, RT-PCR was performed separately in two fragments as described previously [7, 15]. Briefly, one fragment covered from 5′-untranslated region to NS3, with a final product of approximately 6.2 kb, and the other fragment covered from NS2 to NS5B, with a final product of approximately 6.1 kb. These fragments overlapped at the NS2 and NS3 regions and were used for sequence analysis of the HCV open reading frame (ORF) after cloning into pBR322MC. PrimScript (Takara Bio) and KOD-plus DNA polymerase (Toyobo, Osaka, Japan) were used for RT and PCR, respectively. The nucleotide sequences of each of the three independent clones obtained were determined using the Big Dye terminator cycle sequencing kit on an ABI PRISM 310 genetic analyzer (Applied Biosystems, Foster City, CA, USA).

Statistical analysis

Differences between AH1R and OR6 cell lines were tested using Student's *t* test. *P* values <0.05 were considered statistically significant.

Results

Development of a luciferase reporter assay system that facilitates the quantitative monitoring of genome-length HCV-AH1 RNA replication

To develop an HCV AH1 strain-derived assay system corresponding to the OR6 assay system [7], a genome-length HCV RNA encoding RL (AH1RN/C-5B/PL,LS,TA,$(VA)_3$) was transfected into AH1c cells. Following 3 weeks of culturing in the presence of G418, more than 10 colonies were obtained, and then 8 colonies (#2, #3, #4, #5, #6, #8, #13, and #14) were successfully proliferated. We initially selected colonies #2, #3, and #14 because they had high levels of RL activity (>4×10^6 U/1.6×10^5 cells) (Fig. 1a). However, RT-PCR and the sequencing analyses revealed that the genome-length HCV-AH1 RNAs obtained from these colonies each had an approximately 1 kb deletion in the E2 region (data not shown). In this regard, we previously observed similar phenomenon and described the difficulty of the development of a luciferase reporter assay system using the genome-length HCV RNA of more than 12 kb [7], suggesting that the NS5B polymerase possesses the limited elongation ability (probably up to a total length of 12 kb). Indeed, in that study, we could overcome this obstacle by the selection of the colony harboring a complete genome-length HCV RNA among the obtained G418-resistant colonies [7]. Therefore, we next carried out the selection among the other colonies. Fortunately, we found that colony #4, showing a rather high level of RL activity (2×10^6 U/1.6×10^5 cells), possessed a complete genome-length HCV-AH1 RNA without any deleted forms, although most of the other colonies possessed some amounts of a deleted form in addition to a complete genome-length HCV-AH1 RNA (data not shown). We demonstrated that the HCV RNA sequence was not integrated into the genomic DNA in colony #4 (data not shown). From these results, we finally selected colony #4, and it was thereafter referred to as AH1R and used for the following studies.

We first demonstrated that AH1R cells expressed sufficient levels of HCV proteins (Core, E2, and NS5B) by Western blot analysis for the evaluation of anti-HCV reagents, and the expression levels were almost equivalent to those in OR6 cells (Fig. 1b). In this analysis, we confirmed that the size of the E2 protein in AH1R cells was 7 kDa larger than that in OR6 cells (Fig. 1b), as observed previously [12]. This result indicates that AH1R cells express AH1 strain-derived E2 protein possessing two extra N-glycosylation sites [12]. We next demonstrated good correlations between the levels of RL activity and HCV RNA in AH1R cells (Fig. 1c), as we previously demonstrated in OR6 cells treated with IFN-α for 24 h [7]. These correlations indicate that AH1R cells were as useful as OR6 cells as a luciferase assay system.

Aa substitutions detected in genome-length HCV RNA in AH1R cells

To examine whether or not genome-length HCV RNA in AH1R cells possesses additional conserved mutations such as adaptive mutations, we performed a sequence analysis of HCV RNA in AH1R cells. The results (Fig. 2) revealed that

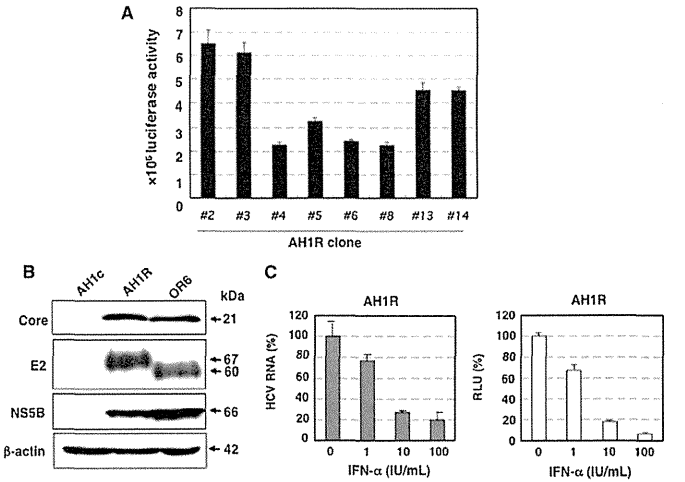

Fig. 1 Characterization of AH1R cells harboring genome-length HCV RNA. **a** Selection of G418-resistant cell clones. The levels of HCV RNA in G418-resistant cells were monitored by RL assay. **b** Western blot analysis. AH1c, AH1R, and OR6 cells were used for the comparison. *Core*, *E2*, and *NS5B* were detected by Western blot analysis. β-actin was used as a control for the amount of protein loaded per lane. **c** RL activity is correlated with HCV RNA level. The AH1R cells were treated with IFN-α (0, 1, 10, and 100 IU/mL) for 24 h, and then a luciferase reporter assay (*right panel*) and quantitative RT-PCR (*left panel*) were performed. The relative luciferase activity (RLU) (%) or HCV RNA (%) calculated at each point, when the level of luciferase activity or HCV RNA in non-treated cells was assigned to be 100%, is presented here

two additional mutations accompanying aa substitutions (W860R (NS2) and A1218E (NS3)) were detected commonly among the three independent clones sequenced, suggesting that these additional mutations are required for the efficient replication or stability of genome-length HCV RNA. The P1115L (NS3), L1262S (NS3), V1897A (NS4B), and V2360A (NS5A) mutations derived from the sAH1 replicon [12] were conserved in AH1R cell-derived clones. However, AH1-clone-2-specific mutations (T1338A and V1880A) were almost reverted to the consensus sequences of AH1 RNA [12] except for V1880A in AH1R clone 2 (Fig. 2). In addition, the Q63R (Core) mutation was observed in two of three clones (Fig. 2).

Comparison between the AH1R and OR6 assay systems regarding the sensitivities to IFN-α, IFN-γ, and CsA

Using quantitative RT-PCR analysis, we previously examined the anti-HCV activities of IFN-α, IFN-γ, and CsA in AH1 and O cells, and noticed different anti-HCV profiles of IFN-γ and CsA between AH1 and O cells [12]. In that study, AH1 cells seemed to be more sensitive than the O cells to CsA (significant difference was observed when 0.063, 0.12, or 0.25 μg/mL of CsA was used). Conversely, AH1 cells seemed to be less sensitive than the O cells to IFN-γ (significant difference was observed when 1 or 10 IU/mL of IFN-γ was used). However, we were not able to determine precisely the EC_{50} values of these reagents, because of the unevenness of the data obtained by RT-PCR.

After developing the AH1R assay system in this study, we determined the EC_{50} values of IFN-α, IFN-γ, and CsA using the AH1R assay and compared the values with those obtained by the OR6 assay. The results revealed that AH1R assay was more sensitive than OR6 assay to IFN-α (EC_{50}; 0.31 IU/mL for AH1R, 0.45 IU/mL for OR6) (Fig. 3a) and CsA (EC_{50}; 0.11 μg/mL for AH1R, 0.42 μg/mL for OR6) (Fig. 3b), and that the OR6 assay was more sensitive than the AH1R assay to IFN-γ (EC_{50}; 0.69 IU/mL for AH1R, 0.28 IU/mL for OR6) (Fig. 3c). Regarding these anti-HCV reagents, the anti-HCV activities observed between the AH1R and OR6 assays differed significantly in all of the concentrations examined (Fig. 3). In addition, regarding these anti-HCV reagents, cell growth was not suppressed within the concentrations used. Regarding IFN-γ and CsA, the present results clearly support those of our previous

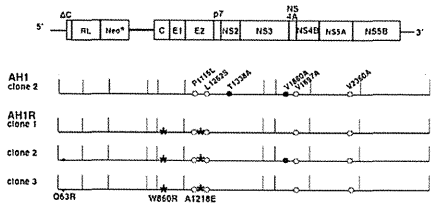

Fig. 2 Aa substitutions detected in intracellular AH1R genome-length HCV RNA. The *upper portion* shows schematic gene organization of genome-length HCV RNA encoding the *RL* gene developed in this study. Genome-length HCV RNA consists of 2 cistrons. In the first cistron, RL is translated as a fusion protein with Neo^R by HCV-IRES, and in the second cistron, all of HCV proteins (C-NS5B) are translated by encephalomyocarditis virus (EMCV)-IRES introduced in the region upstream of C-NS5B regions. Genome-length HCV RNA-replicating cells possess the G418-resistant phenotype because Neo^R is produced by the efficient replication of genome-length HCV RNA. Therefore, when genome-length HCV RNA is excluded from the cells or when its level is decreased, the cells are killed in the presence of G418. In this system, anti-HCV activity is able to evaluate the value of the reporter (RL activity) instead of the quantification of HCV RNA or HCV proteins. In addition, it has been known that the infectious HCV is not produced from this RNA replication system [3, 4, 6]. Core to NS5B regions of three independent clones (*AH1R clones 1–3*) sequenced are presented. W860R and A1218E conserved substitutions are indicated by *asterisks*. Q63R substitutions detected in two of three clones are each indicated by a *small dot*. Core to NS5B regions of *AH1 clone 2*, used to establish the AH1R cell line, are also presented. AH1-specific conserved substitutions and *AH1-clone-2*-specific substitutions are indicated by *open circles* and *black circles*, respectively

study [12]. Therefore, we suggest that the diverse effects of these anti-HCV reagents are due to the difference in HCV strains, although we are not able to completely exclude the possibility that AH1R cells are compromised cells causing the different responses against anti-HCV reagents. In summary, the previous and present findings suggest that the AH1R assay system is also useful for the evaluation of anti-HCV reagents as an independent assay system.

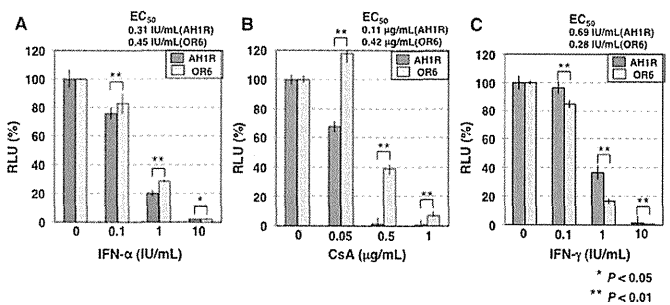

Fig. 3 The diverse effects of anti-HCV reagents on AH1R and OR6 assay systems. AH1R and OR6 cells were treated with anti-HCV reagents for 72 h, and then the RL assay was performed as described in Fig. 1c. **a** Effect of IFN-α. **b** Effect of CsA. **c** Effect of IFN-γ

Anti-HCV activity of rolipram was clearly observed in the AH1R assay, but not in the OR6 assay

From the above findings, we supposed that the anti-HCV reagents reported to date might show diverse effects between the drug assay systems derived from the different HCV strains. To test this assumption, we used the AH1R and OR6 assay systems to evaluate the anti-HCV activity of more than 10 pre-existing drugs (6-Azauridine, bisindoly maleimide I, carvedilol, cehalotaxine, clemizole, 2′-deoxy-5-fluorouridine, esomeprazole, guanazole, hemin, homoharringtonine, methotrexate, nitazoxanide, resveratrol, rolipram, silibinin A, Y27632, etc.), which other groups had evaluated using an assay system derived from the Con1 strain (genotype 1b) or JFH-1 strain (genotype 2a). The results revealed that most of these reagents in the AH1R assay showed similar levels of anti-HCV activities compared with those in the OR6 assay or those of the previous studies (data not shown). However, we found that only rolipram, a selective phosphodiesterase 4 (PDE4) inhibitor [16] that is used as an anti-inflammatory drug, showed moderate anti-HCV activity (EC_{50} 31 μM; $CC_{50} > 200$ μM; SI > 6) in the AH1R assay, but no such activity in the OR6 assay (upper panel in Fig. 4a). This remarkable difference was confirmed by Western blot analysis (lower panel in Fig. 4a). It is unlikely that rolipram's anti-HCV activity is due to the inhibition of exogenous RL, Neo^R or encephalomyocarditis virus internal ribosomal entry site (EMCV-IRES), all of which are encoded in the genome-length HCV RNA, because the AH1R and OR6 assay systems possess the same structure of genome-length HCV RNA except for HCV ORF. To demonstrate that rolipram's anti-HCV activity is not due to the clonal specificity of the cells or the specificity of genome-length HCV RNA, we examined the anti-HCV activity of rolipram using the monoclonal HCV replicon RNA-replicating cells (sAH1 cells for AH1 strain [12], and sO cells for O strain [13]). The results

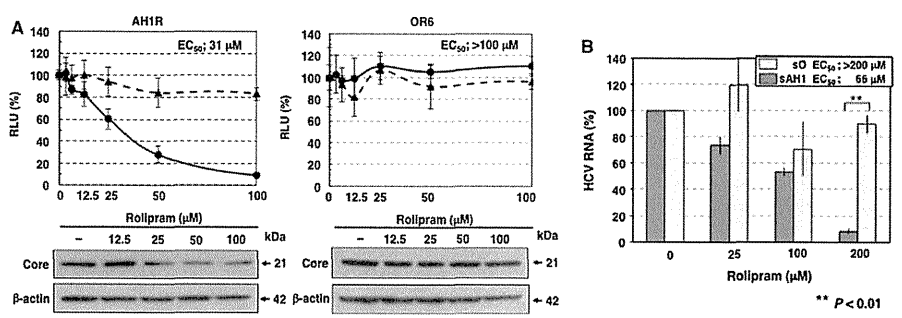

Fig. 4 Anti-HCV activity of rolipram. **a** Rolipram sensitivities on genome-length HCV RNA replication in AH1R and OR6 assay systems. AH1R and OR6 cells were treated with rolipram for 72 h, followed by RL assay (*black circle* with *linear line* in the *upper panels*) and WST-1 assay (*black triangle* with *broken line* in the *upper panels*). The relative value (%) calculated at each point, when the level in non-treated cells was assigned to 100%, is presented here. Western blot analysis of the treated cells for the HCV Core was also performed (*lower panels*). **b** Rolipram sensitivities on HCV replicon RNA replication in sAH1 and sO cells. sAH1 and sO cells were treated with rolipram for 72 h, and extracted total RNAs were subjected to quantitative RT-PCR for HCV 5′ untranslated region as described previously [7]. The HCV RNA (%) calculated at each point, when the level of HCV RNA in non-treated cells was assigned to be 100%, is presented here

revealed by quantitative RT-PCR that rolipram showed moderate anti-HCV activity (EC_{50} 66 μM) in sAH1 cells, but no such activity in sO cells (Fig. 4b). Anti-HCV activity of rolipram in sAH1 cells was a little weaker than that in AH1R cells (Fig. 4b). The similar phenomenon that the anti-HCV activity in genome-length HCV RNA-based reporter assay is stronger than that in HCV subgenomic replicon-based reporter assay was observed regarding other anti-HCV reagents in our previous studies [14, 17, 18]. This result suggests that the anti-HCV activity of rolipram is not either a clone-specific or genome-length HCV RNA-specific phenomenon. In our previous studies also [14, 18], we demonstrated that anti-HCV activities of several reagents including ribavirin and statins were not due to the clonal specificity of the cells. On the other hand, it was recently reported that rolipram did not show anti-HCV activity in the JFH-1 strain-derived assay [19]. Taken together, the previous and present results suggest that rolipram's anti-HCV activity differs depending on the HCV strain. In summary, rolipram was identified as a new anti-HCV candidate using the AH1R assay system.

Discussion

In the present study, we developed for the first time a drug assay system (AH1R), derived from the HCV-AH1 strain (from a patient with acute hepatitis C), in which HCV-AH1 RNA is efficiently replicated. Using this system, we found that rolipram, an anti-inflammatory drug, had potential anti-HCV activity. This potential had not been detected by preexisting assay systems such as OR6, in which HCV-O RNA was derived from an HCV-positive blood donor. Since an HCV replicon harboring the sAH1 cell line, the parent of the AH1R cell line, was obtained from OR6-cured cells [12], the divergence in rolipram's effects between AH1R and OR6 cells is probably attributable to the difference in HCV strains rather than to the difference in cell clones. Indeed, rolipram's anti-HCV activity was not observed in another ORL8 assay system (O strain), which was recently developed using a new hepatoma Li23 cell line (data not shown) [15]. Therefore, we propose that multiple assay systems derived from different HCV strains are required for the discovery of anti-HCV reagents such as rolipram or for the objective evaluation of anti-HCV activity.

Comparative evaluation analysis of anti-HCV activities of IFN-α, IFN-γ, and CsA using AH1-strain-derived AH1R and O-strain-derived OR6 assay systems demonstrated that each of these anti-HCV reagents showed significantly diverse antiviral effects between the two systems. Regarding IFN-γ and CsA, the present results obtained using a luciferase reporter assay fully supported our previous findings [12] using quantitative RT-PCR analysis. However, in the present analysis, we noticed that IFN-α also showed significantly diverse effects (especially at less than 1 IU/mL) between the AH1R and OR6 assays.

The differences in IFN-α sensitivity may be attributable to the difference in aa sequences in the IFN sensitivity-determining region (ISDR; aa 2209-2248 in the HCV-1b genotype), in which aa substitutions correlate well with IFN sensitivity in patients with chronic hepatitis C [20], because the AH1 strain possesses three aa substitutions (T2217A, H2218R, and A2224 V) in ISDR, whereas the O strain possesses no aa substitutions. However, no report has demonstrated the correlation between IFN sensitivity and the substitution numbers in ISDR using the cell culture-based HCV RNA replication system.

Alternatively, Akuta et al. [21] reported that aa substitutions at position 70 and/or position 91 in the HCV Core region of patients infected with the HCV-1b genotype are pretreatment predictors of null virological response (NVR) to pegylated IFN/ribavirin combination therapy. In particular, substitutions of arginine (R) by glutamine (Q) at position 70, and/or leucine (L) by methionine (M) at position 91, were common in NVR. The patients with position-70 substitutions often showed little or no decrease in HCV RNA levels during the early phase of IFN-α treatment [21]. Regarding this point, it is interesting that position 70 in the AH1 strain is R (wild type) and that in the O strain is Q (mutant type), whereas position 91 is L (wild type) in both strains. Therefore, wild-type R in position 70 of the AH1 strain may contribute to the high sensitivity to IFN-α in the AH1R assay. Regarding positions 70 and 91 of the HCV Core, it is noteworthy that, among all of the HCV strains used thus far to develop HCV replicon systems, only the AH1 strain possesses double wild-type aa (data not shown). Therefore, the AH1R assay system may be useful for further study of sensitivity to IFN/ribavirin treatment.

The anti-HCV activity of rolipram, which is currently used as an anti-inflammatory drug, is interesting, although its anti-HCV mechanism is unclear. As a selective PDE4 inhibitor [16], rolipram may attenuate fibroblast activities that can lead to fibrosis and may be particularly effective in the presence of transforming growth factor (TGF)-β1-induced fibroblast stimulation [22]. On the other hand, HCV enhances hepatic fibrosis progression through the generation of reactive oxygen species and the induction of TGF-β1 [23]. Taken together, the previous and present results suggest that rolipram may inhibit both HCV RNA replication and HCV-enhanced hepatic fibrosis. However, it is unclear that rolipram shows anti-HCV activity against the majority of HCV strains, because rolipram has been effective for AH1 strain, but not for O strain. Although rolipram's anti-HCV activity would be HCV-strain-specific, it is not clear which HCV strain is the major type regarding the sensitivity to rolipram. Since developed assay systems using genome-length HCV RNA-replicating cells are limited to several HCV strains including O and AH1 strains to date, further analysis using the assay systems of other HCV strains will be needed to clarify this point.

In this study, we demonstrated that the AH1R assay system, which was for the first time developed using an HCV strain derived from a patient with acute hepatitis C, showed different sensitivities against anti-HCV reagents in comparison with assay systems in current use, such as OR6 assay. Therefore, AH1R assay system would be useful for various HCV studies including the evaluation of anti-HCV reagents and the identification of antiviral targets.

Acknowledgment This study was supported by grants-in-aid for research on hepatitis from the Ministry of Health, Labor, and Welfare of Japan. K. M. was supported by a Research Fellowship for Young Scientists from the Japan Society for the Promotion of Science.

References

1. N. Kato, Acta Med. Okayama **55**, 133–159 (2001)
2. N. Kato, M. Hijikata, Y. Ootsuyama, M. Nakagawa, S. Ohkoshi, T. Sugimura, K. Shimotohno, Proc. Natl. Acad. Sci. USA **87**, 9524–9528 (1990)
3. R. Bartenschlager, S. Sparacio, Virus Res. **127**, 195–207 (2007)
4. D. Moradpour, F. Penin, C.M. Rice, Nat. Rev. Microbiol. **5**, 453–463 (2007)
5. V. Lohmann, F. Korner, J. Koch, U. Herian, L. Theilmann, R. Bartenschlager, Science **285**, 110–113 (1999)
6. M. Ikeda, N. Kato, Adv. Drug Deliv. Rev. **59**, 1277–1289 (2007)
7. M. Ikeda, K. Abe, H. Dansako, T. Nakamura, K. Naka, N. Kato, Biochem. Biophys. Res. Commun. **329**, 1350–1359 (2005)
8. K. Naka, M. Ikeda, K. Abe, H. Dansako, N. Kato, Biochem. Biophys. Res. Commun. **330**, 871–879 (2005)
9. M. Ikeda, K. Abe, M. Yamada, H. Dansako, K. Naka, N. Kato, Hepatology **44**, 117–125 (2006)
10. A. Nozaki, M. Morimoto, M. Kondo, T. Oshima, K. Numata, S. Fujisawa, T. Kaneko, E. Miyajima, S. Morita, K. Mori, M. Ikeda, N. Kato, K. Tanaka, Arch. Virol. **155**, 601–605 (2010)
11. M. Ikeda, Y. Kawai, K. Mori, M. Yano, K. Abe, G. Nishimura, H. Dansako, Y. Ariumi, T. Wakita, K. Yamamoto, N. Kato, Liver Int. **31**, 871–880 (2011)
12. K. Mori, K. Abe, H. Dansako, Y. Ariumi, M. Ikeda, N. Kato, Biochem. Biophys. Res. Commun. **371**, 104–109 (2008)
13. N. Kato, K. Sugiyama, K. Namba, H. Dansako, T. Nakamura, M. Takami, K. Naka, A. Nozaki, K. Shimotohno, Biochem. Biophys. Res. Commun. **306**, 756–766 (2003)
14. K. Mori, M. Ikeda, Y. Ariumi, H. Dansako, T. Wakita, N. Kato, Virus Res. **157**, 61–70 (2011)
15. N. Kato, K. Mori, K. Abe, H. Dansako, M. Kuroki, Y. Ariumi, T. Wakita, M. Ikeda, Virus Res. **146**, 41–50 (2009)
16. S.J. MacKenzie, M.D. Houslay, Biochem. J. **347**, 571–578 (2000)
17. M. Yano, M. Ikeda, K. Abe, H. Dansako, S. Ohkoshi, Y. Aoyagi, N. Kato, Antimicrob. Agents Chemother. **51**, 2016–2027 (2007)
18. G. Nishimura, M. Ikeda, K. Mori, T. Nakazawa, Y. Ariumi, H. Dansako, N. Kato, Antiviral Res. **82**, 42–50 (2009)
19. P. Gastaminza, C. Whitten-Baue, F.V. Chisari, Proc. Natl. Acad. Sci. USA **107**, 291–296 (2010)
20. N. Enomoto, I. Sakuma, Y. Asahina, M. Kurosaki, T. Murakami, C. Yamamoto, Y. Ogura, N. Izumi, F. Marumo, C. Sato, N. Engl. J. Med. **334**, 77–81 (1996)

21. N. Akuta, F. Suzuki, Y. Kawamura, H. Yatsuji, H. Sezaki, Y. Suzuki, T. Hosaka, M. Kobayashi, M. Kobayashi, Y. Arase, K. Ikeda, H. Kumada, J. Med. Virol. **79**, 1686–1695 (2007)
22. S. Togo, X. Liu, X. Wang, Am. J. Physiol. Lung Cell. Mol. Physiol. **296**, L959–L969 (2009)
23. W. Lin, W.L. Tsai, R.X. Shao, G. Wu, L.F. Peng, L.L. Barlow, W.J. Chung, L. Zhang, H. Zhao, J.Y. Jang, R.T. Chung, Gastroenterology **138**, 2509–2518 (2010)

FEBS Open Bio 2 (2012) 279–283

ELSEVIER

FEBS openbio

journal homepage: www.elsevier.com/locate/febsopenbio

Raloxifene inhibits hepatitis C virus infection and replication

Midori Takeda[a,1], Masanori Ikeda[a,*,1], Kyoko Mori[a], Masahiko Yano[a], Yasuo Ariumi[a,2], Hiromichi Dansako[a], Takaji Wakita[b], Nobuyuki Kato[a]

[a] Department of Tumor Virology, Okayama University Graduate School of Medicine, Dentistry, and Pharmaceutical Sciences, Okayama 700-8558, Japan
[b] Department of Virology II, National Institute of Infectious Disease, Tokyo 162-8640, Japan

ARTICLE INFO

Article history:
Received 21 May 2012
Received in revised form 27 July 2012
Accepted 8 August 2012

Keywords:
Hepatitis C virus
Raloxifene
Estrogen
Osteoporosis
Statin

ABSTRACT

Postmenopausal women with chronic hepatitis C exhibited a poor response to interferon (IFN) therapy compared to premenopausal women. Osteoporosis is the typical complication that occurs in postmenopausal women. Recently, it was reported that an osteoporotic reagent, vitamin D3, exhibited anti-hepatitis C virus (HCV) activity. Therefore, we investigated whether or not another osteoporotic reagent, raloxifene, would exhibit anti-HCV activity in cell culture systems. Here, we demonstrated that raloxifene inhibited HCV RNA replication in genotype 1b and infection in genotype 2a. Raloxifene enhanced the anti-HCV activity of IFN-α. These results suggest a link between the molecular biology of osteoporosis and the HCV life cycle.

1. Introduction

Hepatitis C virus (HCV) belongs to the *Flaviviridae* family and contains a positive single-stranded RNA genome of 9.6 kb. The HCV genome encodes a single polyprotein precursor of approximately 3000 amino acid residues, which is cleaved by the host and viral proteases into at least 10 proteins in the following order: Core, envelope 1 (E1), E2, p7, nonstructural 2 (NS2), NS3, NS4A, NS4B, NS5A, and NS5B [1–3].

The virological study and screening of antiviral reagents for HCV was difficult until the replicon system was developed [4–7]. In 2005, an infectious HCV production system was developed using genotype 2a HCV JFH-1 and hepatoma-derived HuH-7 cells, and the HCV life cycle was reproduced in a cell culture system [8]. We previously developed genome-length HCV reporter assay systems using HuH-7-derived OR6 cells [4]. In OR6 cells, the genotype 1b HCV-O with renilla luciferase (*RL*) replicates robustly. We also developed an HCV JFH-1 reporter infection assay system [9].

HCV infection frequently causes chronic hepatitis (CH) and leads to serious liver cirrhosis and hepatocellular carcinoma. Therefore, HCV infection is a major health problem worldwide. The elimination of HCV by antiviral reagents seems to be the most efficient therapy for preventing the fatal state of the disease. Pegylated-interferon (PEG-IFN) with ribavirin (RBV) is the current standard therapy for CH–C, but its sustained virological response (SVR) rate has remained 40–50%. Recently, a protease inhibitor, telaprevir, improved the SVR rate by up to 60–70% in combination with PEG-IFN/RBV [10]. The response to PEG-IFN/RBV therapy depends on host factors as well as viral factors. Among the host factors, age and gender are known to be associated with the outcome of IFN/RBV therapy [11,12]. Postmenopausal women with CH–C exhibited a poor response to IFN therapy compared to premenopausal women [11]. The decrease in estrogen may affect the response to IFN therapy. Dyslipidemia and osteoporosis are the typical complications in postmenopausal women. We and other groups reported that statins, which are dyslipidemia reagents, inhibited HCV proliferation in vitro and in vivo [13–17]. Recently it was reported that vitamin D3, an osteoporotic reagent, exhibited anti-HCV activity in vitro and in vivo [18–21]. It was also reported that 17β-estradiol inhibited the production of infectious HCV [22]. Taken together, these reports suggest an association between hepatitis C and complications due to the decrease of estrogen.

Raloxifene and tamoxifen are synthetic selective estrogen receptor modulators (SERMs) and are used for breast cancer and osteoporosis, respectively, in clinical settings. The responses of SERMs are mediated by estrogen receptors (ERs), either ERα or ERβ. SERMs exhibit agonistic actions in some tissues but antagonistic actions in others. Both raloxifene and tamoxifen are antagonists in breast and agonists in bone. However, only tamoxifen, and not raloxifene, exhibited agonistic activity in the uterus. It was reported that tamoxifen inhibited HCV RNA replication [23]. However, tamoxifen's agonist action leads to uterine cancer. Raloxifene belongs to an antiosteoporotic reagent and offers the advantage of safety without uterine cancer. Therefore, we decided to investigate whether or not raloxifene would exhibit anti-HCV activity in our developed cell culture systems.

[1] These authors contributed equally to this work.
[2] Current address: Center for AIDS Research, Kumamoto University, Kumamoto 860-0811, Japan.
* Corresponding author. Fax: +81 86 235 7392.
E-mail address: maikeda@md.okayama-u.ac.jp (M. Ikeda).

2211-5463/$36.00 © 2012 Federation of European Biochemical Societies. Published by Elsevier B.V. All rights reserved.
http://dx.doi.org/10.1016/j.fob.2012.08.003

2. Materials and methods

2.1. Reagents and antibodies

Raloxifene was purchased from LKT Laboratories, Inc. (St. Paul, MN). IFN-α and tamoxifen were purchased from Sigma–Aldrich (St. Louis, MO). Pitavastatin (PTV) was purchased from Kowa Company (Nagoya, Japan). The antibodies used in this study were those specific to HCV Core (CP11, Institute of Immunology, Tokyo, Japan), NS3 (Novocastra Laboratories, Newcastle, UK), and β-actin (Sigma).

2.2. Cell culture and HCV RNAs

HuH-7 cells were cultured in Dulbecco's modified Eagle's medium (Gibco-BRL, Invitrogen Life Technology, Carlsbad, CA) supplemented with 10% fetal bovine serum, penicillin, and streptomycin. HuH-7-derived OR6 and sOR cells were genome-length and subgenome HCV (O strain of genotype 1b) RNA harboring cells, respectively and cultured in the above medium supplemented with G418 (0.3 mg/ml; Geneticin, Invitrogen) [4]. HCVs replicating in OR6 and sOR cells contain *RL* and neomycin phosphotransferase (*NPT*) genes after 5′-untranslated region (UTR). HuH-7-derived RSc cells are cured cells, in which HCV RNA was eliminated by IFN-α; they are used for HCV JFH-1 infection [9]. RSc cells are also used for subgenomic JFH-1 RNA (JRN/35B) replication. JRN/35B contains *RL* and *NPT* genes after 5′-UTR.

2.3. RL assay

For the RL assay, 1.5×10^4 OR6 were plated onto 24-well plates in triplicate and cultured for 24 h. The cells were treated with each reagent for 72 h. Then the cells were harvested with *Renilla* lysis reagent (Promega, Madison, WI) and subjected to RL assay according to the manufacturer's protocol.

2.4. WST-1 cell proliferation assay

The cells (2×10^3 cells) were plated onto a 96-well plate in triplicate at 24 h before treatment with each reagent. At 72 h after treatment, the cells were subjected to a WST-1 cell proliferation assay (Takara Bio, Otsu, Japan) according to the manufacturer's protocol.

2.5. Western blot analysis

For Western blot analysis, 4×10^4 cells were plated onto 6-well plates, cultured for 24 h, and then treated with reagent(s) for 72 h and 120 h. Preparation of the cell lysates, sodium dodecyl sulfate–polyacrylamide gel electrophoresis, and immunoblotting were then performed as previously described [24]. Immunocomplexes on the membranes were detected by enhanced chemiluminescence assay (Renaissance; Perkin Elmer Life Science, Wellesley, MA).

2.6. HCV infection

RSc cells (1.5×10^4 cells) were plated onto a 24-well plate 24 h before infection. To evaluate the effect of the treatment prior to infection, the cells were first treated with raloxifene for 24 h, then inoculated with reporter JFH-1 (JR/C5B/BX-2) supernatant at a multiplicity of infection (MOI) of 0.2, cultured for 48 h, and subjected to RL assay as described previously [9]. The JR/C5B/BX-2 contains the *RL* gene in the first cistron following the encephalomyocarditis virus-internal ribosomal entry site (*EMCV-IRES*) gene and the open reading frame (ORF) of JFH-1 in the second cistron. To evaluate the effect of the treatment after infection, the cells were inoculated with reporter JFH-1 supernatant at MOI of 0.2, cultured for 72 h, and subjected to RL assay.

3. Results

3.1. Raloxifene inhibited HCV RNA replication

The HCV RNA that replicated in HuH-7-derived OR6 cells was a genome-length HCV with *RL*, *NPT*, and *EMCV-IRES* in the first cistron and the ORF of HCV (O strain of genotype 1b) in the second cistron [4]. OR6 cells could not produce infectious HCV. Therefore, we can monitor the replication step in the HCV life cycle using OR6 cells. Raloxifene inhibited HCV RNA replication in a dose-dependent manner, and its 50% effective concentration (EC_{50}) was 1 μM (Fig. 1A). Raloxifene did not exhibit cytotoxicity to OR6 cells until 2.5 μM (Fig. 1B). Raloxifene also inhibited intracellular Core and NS3 production in a dose- and time-dependent manner (Fig. 1C). The intensities of Core and NS3 in OR6 cells treated with 2.5 μM of raloxifene decreased to almost the level of cells treated with 10 IU/ml of IFN-α at 120 h after treatment. We also examined anti-HCV activity of raloxifene using subgenomic HCV replicon harboring sOR cells. Raloxifene exhibited weak anti HCV activity to sOR cells as compared with OR6 cells (Supplementary Figs. 1A and 1B). These results suggest that raloxifene exhibits anti-HCV activity and decreased the expression levels of HCV proteins more slowly compared to IFN-α.

3.2. Raloxifene enhanced anti-HCV activity of IFN-α

We investigated the anti-HCV activity of raloxifene in combination with a representative anti-HCV reagent, IFN-α. HCV RNA replication decreased in a dose-dependent manner after co-treatment with IFN-α and raloxifene (Fig. 2A). The results were almost similar to the expected effect of raloxifene in combination with IFN-α calculated from the anti-HCV activity of each reagent (Fig. 2B). These results indicate that the anti-HCV activity of raloxifene and IFN-α exhibited additive effect. We also examined the anti-HCV activity of previously reported SERM, tamoxifen. Tamoxifen also exhibited additive anti-HCV activity on HCV RNA replication in combination with IFN-α (Supplementary Figs. 2A–C). These results indicate that raloxifene as well as tamoxifen enhanced the anti-HCV activity of IFN-α. As both raloxifene and IFN-α are clinically used reagents, raloxifene seemed to be a candidate reagent as an add-on treatment to IFN-α in patients with CH–C.

3.3. Raloxifene antagonized anti-HCV activity of statin

We previously reported that statins exhibited anti-HCV activity using the OR6 assay system [14]. Statin is the first-choice reagent for dyslipidemia. As dyslipidemia and osteoporosis are major complications in postmenopausal women, we invested the effect of raloxifene on the anti-HCV activity of PTV. Raloxifene did not enhance the anti-HCV activity of PTV (Fig. 3A). Fig. 3B exhibits the expected anti-HCV activity of co-treatment with raloxifene and PTV calculated from the anti-HCV effect of either raloxifen or PTV alone. Raloxifene exhibited an antagonistic effect on PTV's anti-HCV activity. Raloxifene's antagonistic effect on PTV increased dose-dependently. The co-treatment with raloxifene (2.5 μM) and PTV (0.25, 0.5, and 1 μM) resulted in lower anti-HCV activity than did treatment with raloxifene alone (2.5 μM). These results suggest that we should be careful in the administration of statins with raloxifene to postmenopausal woman with CH–C.

3.4. Raloxifene inhibited infection of genotype 2a HCV

To further investigate the anti-HCV activity of raloxifene, we examined whether or not raloxifene could inhibit HCV infection. For this purpose, we used our recently developed JFH-1 reporter infection assay system [9]. HuH-7-derived RSc's are highly HCV-permissive cell lines. Raloxifene was pretreated at 24 h before HCV infection. The cells were inoculated with HCV JFH-1 virion with *RL* (JR/C5B/BX-2), and

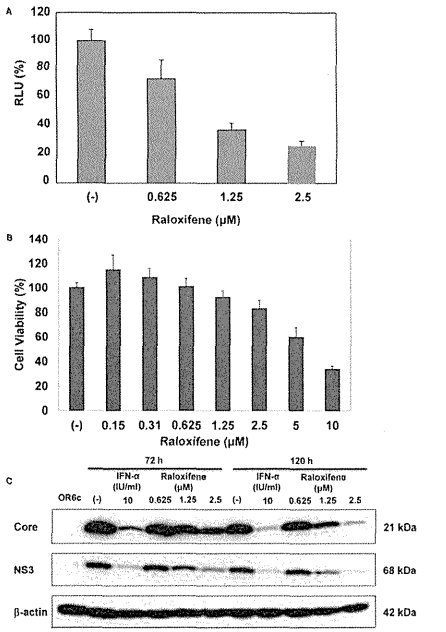

Fig. 1. Raloxifene inhibited HCV RNA replication. (A) Anti-HCV activity of raloxifene in OR6 cells. OR6 cells were treated with raloxifene (0, 0.625, 1.25, and 2.5 μM) for 72 h. Relative RL activity (relative light unit: RLU) for HCV RNA replication is expressed as a percentage of control. Each bar represents the average with standard deviations of triplicate data points. (B) Effect of raloxifene on OR6 cell viability. Cell viability at 72 h after raloxifene treatment (0.15, 0.31, 0.625, 1.25, 2.5, 5, and 10 μM) was determined using WST-1 cell proliferation assay and is expressed as a percentage of control. (C) Raloxifene inhibited HCV proteins. OR6 cells were treated with IFN-α (10 IU/ml) or raloxifene (0, 0.625, 1.25, and 2.5 μM). After 72 or 120 h treatment, the production of Core and that of NS3 were analyzed by immunoblotting using anti-Core and anti-NS3 antibodies, respectively. OR6c cells were cured cells in which HCV RNA was eliminated using IFN-α, and were used as a negative control. β-actin was used as a control for the amount of protein loaded per lane.

the infection was monitored with RL activity at 48 h after infection. As shown in Fig. 4A, raloxifene inhibited HCV infection in RSc cells in a dose-dependent manner. Next we examined the effect of raloxifene after HCV infection. RSc cells were inoculated with HCV JFH-1 virion with *RL*. After HCV infection, the cells were treated with raloxifene for 72 h and raloxifene's inhibitory effect on post-infection was assessed using the RL assay. Raloxifene inhibited HCV proliferation in a dose-dependent manner when it was added to the cells after infection in RSc cells, although inhibitory effect of raloxifene on JFH-1 HCV RNA replication seemed to be weak compared to the genotype 1b HCV-O RNA replication (Fig. 4B). Raloxifene did not exhibit cytotoxicity to RSc cells until 2.5 μM (Fig. 4C). We found that raloxifene could not inhibit subgenomic JFH-1 HCV (JRN/35B) RNA replication (Fig. 4D). We further examined the inhibitory action of raloxifene around infection step. RSc cells were treated for short time with raloxifene around infection step: for 1, 4, and 4 h before, during, and after inoculation, respectively (Fig. 4E). Raloxifene inhibited JFH-1 infection, when it was treated during inoculation but not just before or after inoculation. In case of genotype 2a JFH-1, raloxifene's anti-HCV activity is mainly due to the inhibition of infection. These results indicate that

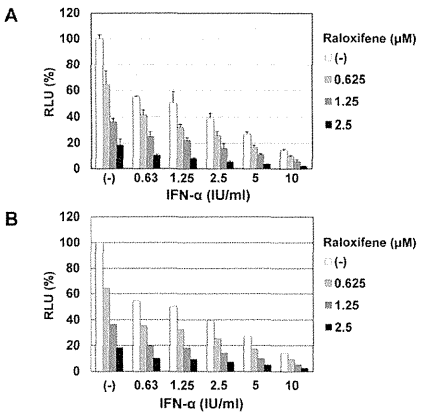

Fig. 2. Raloxifene enhanced the anti-HCV activity of IFN-α. (A) Anti-HCV activity of raloxifene in combination with IFN-α. OR6 cells were co-treated with raloxifene (0, 0.625, 1.25, and 2.5 μM) and IFN-α (0, 0.63, 1.25, 2.5, 5, 10 IU/ml). Relative RL activity is shown as a percentage of control. Each bar represents the average with standard deviations of triplicate data points. (B) Expected anti-HCV activity was calculated based on the results when the cells were treated with only raloxifene or IFN-α.

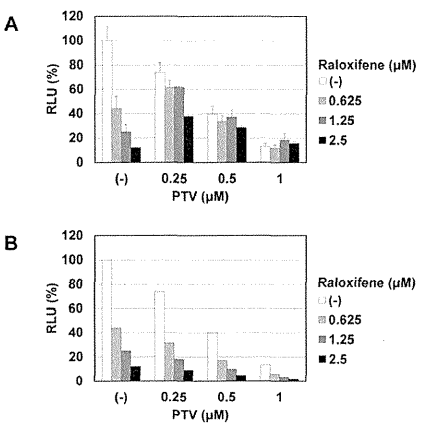

Fig. 3. Statin antagonized the anti-HCV activity of raloxifene. (A) OR6 cells were co-treated with raloxifene (0, 0.625, 1.25, and 2.5 μM) and PTV (0, 0.25, 0.5, and 1 μM). Relative RL activity was shown as a percentage of control. Each bar represents the average with standard deviations of triplicate data points. (B) Expected anti-HCV activity was calculated based on the results when the cells were treated with only raloxifene or PTV.

raloxifene inhibits JFH-1 infection but not its RNA replication.

4. Discussion

In this study, we demonstrated that raloxifene, an osteoporotic reagent, inhibited the replication of genotypes 1b HCV RNA replication and inhibited genotype 2a HCV JFH-1 infection. Raloxifene additively enhanced the anti-HCV activity of IFN-α. On the other hand, raloxifene exhibited an antagonistic effect on statins.

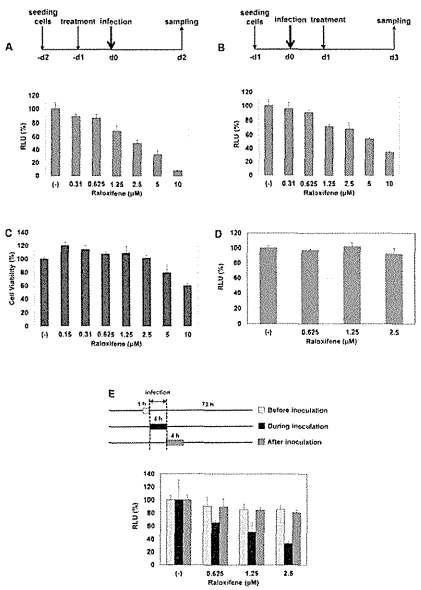

Fig. 4. Raloxifene inhibited genotype 2a HCV infection. (A) Raloxifene inhibited HCV *JFH-1 infection. RSc cells were treated with raloxifene (0, 0.31, 0.625, 1.25, 2.5, 5, and* 10 μM) 24 h before infection. HCV JFH-1 reporter virion was used as an inoculum after removal of raloxifene. The cells were then infected with reporter JFH-1 virion and cultured for 48 h. The inhibition of HCV infection was assessed by relative RL activity and expressed as a percentage of control. (B) Raloxifene inhibited HCV JFH-1 proliferation after infection. RSc cells were inoculated with HCV JFH-1 reporter virion *and cultured for 24 h. Then the cells were treated with raloxifene (0, 0.31, 0.625, 1.25,* 2.5, 5, and 10 μM) for 48 h. The inhibitory effect on HCV proliferation after infection was assessed by relative RL activity and expressed as a percentage of control. Each bar represents the average with standard deviations of triplicate data points. (C) Effect of raloxifene on RSc cells viability. Cell viability at 72 h after raloxifene treatment (0.15, 0.31, 0.625, 1.25, 2.5, 5, and 10 μM) was determined using WST-1 cell proliferation *assay and is expressed as a percentage of control. (D) Subgenomic JFH-1 RNA (JRN/35B)* replicating RSc cells were treated with raloxifene (0, 0.625, 1.25, and 2.5 μM) for 72 h. Relative RL activity for HCV RNA replication is expressed as a percentage of control. Each bar represents the average with standard deviations of triplicate data points. (E) Raloxifene (0, 0.625, 1.25, and 2.5 μM) was treated for 1, 4, and 4 h before, during, and after JFH-1 inoculation to RSc cells at MOI of 0.2, respectively. The cells were then *cultured for 72 h. The inhibition of HCV infection was assessed by relative RL activity* and expressed as a percentage of control.

PEG-IFN/RBV therapy led to a 40–50% SVR rate among patients with CH–C. Telaprevir with PEG-IFN/RBV increases the effect of PEG-IFN/RBV therapy by 10–20%. However, the major complication of anemia in PEG-IFN/RBV therapy increased when telaprevir was added. Considering that PEG-IFN/RBV-based therapy is less effective on postmenopausal women, an alternative therapy with minimal side effects is needed. Add-on therapy for postmenopausal women may be a candidate for improving the SVR in these patients. We focused on the reagents, which compensate for the lack of estrogen function. Dyslipidemia and osteoporosis are the major complications in postmenopausal women, and these complications are attributable to the decrease in estrogen. Statins are clinically used reagents for dyslipidemia; they inhibit HCV RNA replication in vivo as well as in vitro [13–17]. Therefore, we investigated whether or not raloxifene exhibits anti-HCV activity using genotype 1b HCV RNA replication and genotype 2a infection systems. In the HCV life cycle, raloxifene inhibited genotype 2a HCV infection and genotypes 1b HCV RNA replication. Raloxifene may be a potential reagent with different anti-HCV mechanisms in the HCV life cycle. Further study is needed to clarify these underlying mechanisms.

Recently it was reported that vitamin D3, an osteoporotic reagent, inhibited HCV production in cell culture systems [20,21]. Furthermore, it was reported that vitamin D3 was associated with the effect of therapy for patients with CH–C [18,19]. Statins inhibited HCV RNA replication by suppressing geranylgeranyl pyrophosphate (GGPP) production [14]. Another osteoporotic reagent, bisphosphonate, may possess anti-HCV activity, because it also inhibited the biosynthesis of GGPP in the mevalonate pathway by inhibiting farnesyl pyrophosphate synthetase. Taken together, these findings indicate it is likely that the HCV life cycle is associated with osteoporosis.

Raloxifene and tamoxifen are SERMs for osteoporosis and breast cancer, respectively. Tamoxifen is used for estrogen receptor-positive breast cancer, and it inhibits HCV RNA replication in cell culture [23]. Tamoxifen's anti-HCV activity is associated with ERα. In our study, raloxifene inhibited HCV infection as well as replication. To clarify the multi-potential effects of raloxifene, further study is needed. The incidence of side effects including uterine cancer is lower in raloxifene therapy than in tamoxifen therapy [25]. This is another advantage of raloxifene in clinical use for patients with CH–C.

As for the precise role of ERα or ERβ on the HCV life cycle, we could not reach a clear conclusion because microarray analysis revealed an absence of expression for both ERα and ERβ in OR6 cells (data not shown). Hayashida et al. [22] reported that the most potent physiological estrogen, 17-β-estradiol, inhibited infectious HCV production using HuH-7.5 cells, and that ERα-selective agonist inhibited infectious HCV production whereas ERβ-selective agonist did not. Watashi et al. [23] reported that RNA interference-mediated knockdown of ERα reduced HCV RNA replication. In our study, the anti-HCV activity of raloxifene in infection and replication did not seem attributable to ERα or ERβ. It is not clear why our HuH-7-derived OR6 cells did not express ERα or ERβ. HuH-7 cells were developed in 1982 at Okayama University and distributed worldwide [26]. Recently, Bensadoun et al. [27] reported that the genetic background of the IL28B genotype of HuH-7 cells differed among different laboratories. This may be a consequence of the polyploidal nature of hepatoma cells. A similar mechanism might cause the different expression levels of ERα and ERβ. Another ER, GPR30 [28], was expressed in OR6 cells (data not shown; from microarray analysis). GPR30 may be the responsible host factor for anti-HCV activity in OR6 cells. Further study is needed to clarify this issue.

In conclusion, we found that raloxifene inhibited HCV RNA replication in genotype 1b and infection in genotype 2a. Raloxifene additively enhanced the anti-HCV activity of IFN-α. The antagonistic effects of statins and raloxifene will yield information on the clinical use of these reagents. Our results, as well as the reports of vitamin D3's anti-HCV activity, will open new fields of treatment for both osteoporosis and HCV infection.

Acknowledgments

The authors would like to thank Masayo Takemoto for her technical assistance. This work was supported by a Grant-In-Aid for Research on Hepatitis from the Ministry of Health, Labor and Welfare of Japan.

Supplementary Material

Supplementary material associated with this article can be found, in the online version, at doi:10.1016/j.fob.2012.08.003.

References

[1] Kato N. (2001) Molecular virology of hepatitis C virus. Acta Med. Okayama. 55, 133–159.
[2] Kato N., Hijikata M., Ootsuyama Y., Nakagawa M., Ohkoshi S., Sugimura T. et al. (1990) Molecular cloning of the human hepatitis C virus genome from Japanese patients with non-A, non-B hepatitis. Proc. Natl. Acad. Sci. USA. 87, 9524–9528.
[3] Tanaka T., Kato N., Cho M.J., Sugiyama K., Shimotohno K. (1996) Structure of the 3' terminus of the hepatitis C virus genome. J. Virol. 70, 3307–3312.
[4] Ikeda M., Abe K., Dansako H., Nakamura T., Naka K., Kato N. (2005) Efficient replication of a full-length hepatitis C virus genome, strain O, in cell culture, and development of a luciferase reporter system. Biochem. Biophys. Res. Commun. 329, 1350–1359.
[5] Ikeda M., Yi M., Li K., Lemon S.M. (2002) Selectable subgenomic and genome-length dicistronic RNAs derived from an infectious molecular clone of the HCV-N strain of hepatitis C virus replicate efficiently in cultured Huh7 cells. J. Virol. 76, 2997–3006.
[6] Lohmann V., Korner F., Koch J., Herian U., Theilmann L., Bartenschlager R. (1999) Replication of subgenomic hepatitis C virus RNAs in a hepatoma cell line. Science. 285, 110–113.
[7] Pietschmann T., Lohmann V., Kaul A., Krieger N., Rinck G., Rutter G. et al. (2002) Persistent and transient replication of full-length hepatitis C virus genomes in cell culture. J. Virol. 76, 4008–4021.
[8] Wakita T. (2005) Production of infectious hepatitis C virus in tissue culture from a cloned viral genome. Nat. Med. 11, 791–796.
[9] Takeda M., Ikeda M., Ariumi Y., Wakita T., Kato N (2012) Development of hepatitis C virus production reporter assay systems using two different hepatoma cell lines. J. Gen. Virol. 93, 1422–1431.
[10] McHutchison J.G. (2009) Telaprevir with peginterferon and ribavirin for chronic HCV genotype 1 infection. N. Engl. J. Med. 360, 1827–1838.
[11] Hayashi J., Kishihara Y., Ueno K., Yamaji K., Kawakami Y., Furusyo N. et al. (1998) Age-related response to interferon alfa treatment in women vs men with chronic hepatitis C virus infection. Arch. Int. Med. 158, 177–181.
[12] Iwasaki Y. (2006) Limitation of combination therapy of interferon and ribavirin for older patients with chronic hepatitis C. Hepatology. 43, 54–63.
[13] Bader T., Fazili J., Madhoun M., Aston C., Hughes D., Rizvi S. et al. (2008) Fluvastatin inhibits hepatitis C replication in humans. Am. J. Gastroenterol. 103, 1383–1389.
[14] Ikeda M., Abe K., Yamada M., Dansako H., Naka K., Kato N. (2006) Different anti-HCV profiles of statins and their potential for combination therapy with interferon. Hepatology. 44, 117–125.
[15] Ikeda M., Kato N. (2007) Life style-related diseases of the digestive system: cell culture system for the screening of anti-hepatitis C virus (HCV) reagents: suppression of HCV replication by statins and synergistic action with interferon. J. Pharmacol. Sci. 105, 145–150.
[16] Rao G.A., Pandya P.K. (2011) Statin therapy improves sustained virologic response among diabetic patients with chronic hepatitis C. Gastroenterology. 140, 144–152.
[17] Sezaki H. (2009) An open pilot study exploring the efficacy of fluvastatin, pegylated interferon and ribavirin in patients with hepatitis C virus genotype 1b in high viral loads. Intervirology. 52, 43–48.
[18] Abu-Mouch S., Fireman Z., Jarchovsky J., Zeina A.R., Assy N. (2011) Vitamin D supplementation improves sustained virologic response in chronic hepatitis C (genotype 1)-naive patients. World J. Gastroenterol. 17, 5184–5190.
[19] Bitetto D. (2011) Vitamin D supplementation improves response to antiviral treatment for recurrent hepatitis C. Transpl. Int. 24, 43–50.
[20] Gal-Tanamy M., Bachmetov L., Ravid A., Koren R., Erman A., Tur-Kaspa R. et al. (2011) Vitamin D: an innate antiviral agent suppressing hepatitis C virus in human hepatocytes. Hepatology. 54, 1570–1579.
[21] Matsumura, T., Kato, T., Sugiyama, N., Tasaka-Fujita, M., Murayama, A., Masaki, T., Wakita, T., Imawari, M. 25-hydroxyvitamin D(3) suppresses hepatitis C virus production. Hepatology, in press.
[22] Hayashida K., Shoji I., Deng L., Jiang D.P., Ide Y.H., Hotta H. (2010) 17beta-estradiol inhibits the production of infectious particles of hepatitis C virus. Microbiol. Immunol. 54, 684–690.
[23] Watashi K., Inoue D., Hijikata M., Goto K., Aly H.H., Shimotohno K. (2007) Anti-hepatitis C virus activity of tamoxifen reveals the functional association of estrogen receptor with viral RNA polymerase NS5B. J. Biol. Chem. 282, 32765–32772.
[24] Kato N. (2003) Establishment of a hepatitis C virus subgenomic replicon derived from human hepatocytes infected in vitro. Biochem. Biophys. Res. Commun. 306, 756–766.
[25] Runowicz C.D., Costantino J.P., Wickerham D.L., Cecchini R.S., Cronin W.M., Ford L.G. et al. (2011) Gynecologic conditions in participants in the NSABP breast cancer prevention study of tamoxifen and raloxifene (STAR). Am. J. Obstet. Gynecol. 205, 535e1–535e5.
[26] Nakabayashi H., Taketa K., Miyano K., Yamane T., Sato J. (1982) Growth of human hepatoma cells lines with differentiated functions in chemically defined medium. Cancer Res. 42, 3858–3863.
[27] Bensadoun P., Rodriguez C., Soulier A., Higgs M., Chevaliez S., Pawlotsky J.M. (2011) Genetic background of hepatocyte cell lines: are in vitro hepatitis C virus research data reliable. Hepatology. 54, 748.
[28] Revankar C.M., Cimino D.F., Sklar L.A., Arterburn J.B., Prossnitz E.R. (2005) A transmembrane intracellular estrogen receptor mediates rapid cell signaling. Science. 307, 1625–1630.

AAC Journals.ASM.org

ENT1, a Ribavirin Transporter, Plays a Pivotal Role in Antiviral Efficacy of Ribavirin in a Hepatitis C Virus Replication Cell System

Minami Iikura,[a] Tomomi Furihata,[a] Misa Mizuguchi,[a] Miki Nagai,[a] Masanori Ikeda,[b] Nobuyuki Kato,[b] Akihito Tsubota,[c] and Kan Chiba[a]

Laboratory of Pharmacology and Toxicology, Graduate School of Pharmaceutical Sciences, Chiba University, Chiba, Japan[a]; Department of Tumor Virology, Okayama University Graduate School of Medicine, Dentistry, and Pharmaceutical Science, Okayama, Japan[b]; and Institute of Clinical Medicine and Research, Jikei University School of Medicine, Chiba, Japan[c]

We previously showed that equilibrative nucleoside transporter 1 (ENT1) is a primary ribavirin transporter in human hepatocytes. However, because the role of this transporter in the antiviral mechanism of the drug remains unclear, the present study aimed to elucidate the role of ENT1 in ribavirin antiviral action. OR6 cells, a hepatitis C virus (HCV) replication system, were used to evaluate both ribavirin uptake and efficacy. The ribavirin transporter in OR6 cells was identified by mRNA expression analyses and transport assays. Nitrobenzylmercaptopurine riboside (NBMPR) and micro-RNA targeted to ENT1 mRNA (miR-ENT1) were used to reduce the ribavirin uptake level in OR6 cells. Our results showed that ribavirin antiviral activity was associated with its accumulation in OR6 cells, which was also closely associated with the uptake of the drug. It was found that the primary ribavirin transporter in OR6 cells was ENT1 and that inhibition of ENT1-mediated ribavirin uptake by NBMPR significantly attenuated the antiviral activity of the drug as well as its accumulation in OR6 cells. The results also showed that even a small reduction in the ENT1-mediated ribavirin uptake, achieved in this case using miR-ENT1, caused a significant decrease in its antiviral activity, thus indicating that the ENT1-mediated ribavirin uptake level determined its antiviral activity level in OR6 cells. In conclusion, our results show that by facilitating its uptake and accumulation in OR6 cells, ENT1 plays a pivotal role in the antiviral effectiveness of ribavirin and therefore provides an important insight into the efficacy of the drug in anti-HCV therapy.

Chronic hepatitis C is a major cause of liver cirrhosis and hepatocellular carcinoma, and a combination of interferon-α (IFN-α) and ribavirin is a standard anti-hepatitis C virus (HCV) therapy. Since the addition of ribavirin to IFN-α significantly improves the rate of sustained virologic response (SVR) (40 to 60% in genotype 1 patients) (5), the drug plays a key role in current anti-HCV therapy.

Ribavirin, a purine nucleoside analog, is phosphorylated intracellularly to form mono-, di-, and tri-phosphates, which then accumulate within cells at high concentrations (4, 13). While the primary anti-HCV mechanisms of the drug are still under debate, it is considered likely that the important actions take place within the cells themselves, and several mechanisms have been proposed to explain what occurs there. These include inhibition of inosine monophosphate dehydrogenase (reviewed in references 4 and 7 and references therein). Additionally, a recent study revealed that ribavirin potentiates IFN-α action by augmenting IFN-stimulated induction of gene expression (16).

Taking into consideration the above-mentioned mechanisms, it is reasonable to assume that the uptake of ribavirin into hepatocytes is a prerequisite for its antiviral activity. Since ribavirin is a hydrophilic molecule, import of the drug into cells requires host nucleoside transporters, which are divided into two families: equilibrative nucleoside transporters (such as ENT1 to ENT4) and concentrative nucleoside transporters (such as CNT1 to CNT3) (9). ENTs are facilitated transporters, while CNTs are sodium-dependent active transporters. These transporters differ in tissue distribution, substrate preference, and inhibitor sensitivity. For example, sensitivities to inhibition by nitrobenzylmercaptopurine riboside (NBMPR) are different between ENT1 and ENT2 (20).

Our recent investigations into the ribavirin uptake system in human hepatocytes determined that ENT1 is a primary ribavirin uptake transporter (6). In addition, Morello et al. (12) reported the association of an intronic single nucleotide polymorphism (SNP) of the *SLC29A1* (ENT1) gene with rapid virologic response (RVR; defined as an undetectable serum HCV RNA level at week 4) of treatment of genotype-1 Caucasian patients. More recently, Tsubota and colleagues revealed that another intronic SNP in the *SLC29A1* gene is associated with SVR, as well as RVR, in genotype-1 Japanese patients (18). Based on these findings, it can be hypothesized that ENT1 plays an essential role in ribavirin anti-HCV activity.

In the present study, along with a detailed characterization of ribavirin uptake and its relationship to antiviral activity, we tested the above-mentioned hypothesis through the use of OR6 cells, which have been established as an efficient replication system for the HCV RNA genome. The HCV replication level was evaluated by monitoring the level of *Renilla* luciferase activity (8), which enabled us to simultaneously evaluate both ribavirin uptake and its antiviral activity.

MATERIALS AND METHODS

Cell culture. OR6 cells were cloned from ORN/C-5B/KE cells (derived from Huh-7 cells) supporting genome-length HCV RNA (strain O of

Received 20 September 2011 **Returned for modification** 24 October 2011
Accepted 27 December 2011
Published ahead of print 9 January 2012
Address correspondence to Tomomi Furihata, tomomif@faculty.chiba-u.jp.
Supplemental material for this article may be found at http://aac.asm.org/.

doi:10.1128/AAC.05762-11

genotype 1b) containing the *Renilla* luciferase reporter gene, and the cells were cultured as described previously (8). Huh-7 cells were obtained from the Institute of Development, Aging and Cancer, Tohoku University (Sendai, Japan). The Huh-7 cells were cultured at 37°C with 5% CO_2–95% air in RPMI 1640 medium (Invitrogen, Carlsbad, CA) with 10% fetal bovine serum, 50 U/ml penicillin, and 50 μg/ml streptomycin.

Luciferase reporter assay. OR6 cells were plated 1 day prior to the assay on 24-well plates at 1.5×10^4 to 2.5×10^4 cells/well, followed by treatment with ribavirin (Wako, Osaka, Japan) in the absence of G418 and at the indicated concentrations for 24, 48, and 72 h. The cells were then subjected to the luciferase assay using a dual-luciferase reporter assay system (Promega, Madison, WI) according to the manufacturer's protocol. For data normalization, the protein contents were determined with a Pierce 660-nm protein assay reagent (Thermo Fisher Scientific, Rockford, IL) according to the manufacturer's protocol. The relative luciferase activity value of the untreated or vehicle treated cells (dimethyl sulfoxide [DMSO] for NBMPR and sterile water for others) was set to 100%. NBMPR (Sigma, St. Louis, MO), hypoxanthine (MP Biomedicals, Solon, OH), and formycin B (Berry & Associates, Ann Arbor, MI) were included in inhibition analyses at various concentrations.

Western blot analysis. OR6 cells treated with ribavirin at various concentrations in the absence of G418 for 24, 48, and 72 h were harvested and homogenized. The homogenates (60 μg/well) were resolved in a sodium dodecyl sulfate (SDS)–15% polyacrylamide gel and then transferred onto a nitrocellulose membrane. The membrane was blocked with 5% skim milk and then incubated with either antibodies against the HCV core protein (2,000-fold dilution; Institute of immunology, Tokyo, Japan) or antibodies against β-actin (500-fold dilution; Sigma). Immunocomplexes were detected with enhanced chemiluminescence (ECL) Western blotting detection reagents (GE Healthcare, Giles, United Kingdom).

Accumulation assay. OR6 cells were plated 1 day prior to the assay on 24-well plates, after which the cells were incubated with 0.5 μCi/ml [^{3}H]ribavirin (Moravek Biochemicals, Brea, CA) and nonradiolabeled ribavirin at various concentrations. NBMPR was included in inhibition analyses at concentrations of 0.1, 1, 3, 10, 31, and 100 μM. After treatment for 9.6, 24, 48, or 72 h, the cells were washed twice with ice-cold Na^+-free Krebs-Henseleit buffer (KHB) and lysed with 0.2% SDS. Radioactivity was measured using a liquid scintillation counter (LSC 5100; Aloka, Tokyo, Japan). The protein contents were determined as described above. To completely inhibit ENT-mediated ribavirin uptake, 30 μM dipyridamole (Wako) was used in the same experimental sets (20). The data were calculated by subtracting the accumulation values obtained with dipyridamole from those without dipyridamole at the same ribavirin concentrations. All assays were performed at 37°C.

Transport assays. Transport assays were performed using the previously described centrifugal filtration method (6). OR6 cells were collected and resuspended in ice-cold Na^+-containing KHB or Na^+-free KHB at 1.4×10^6 cells/ml. NBMPR, troglitazone (Wako), hypoxanthine, and formycin B were included in the inhibition analyses. Since the rate of ribavirin uptake by OR6 cells was linear for at least 60 s in the preliminary assays, the incubation time was set to 30 s. The radioactivity and protein contents of the cells used in the assay were measured as described above. The same experiments were also performed at 4°C, and the data were obtained by subtracting the uptake levels at 4°C from those at 37°C at the same ribavirin concentrations.

Total RNA preparation, cDNA synthesis, reverse transcription-PCR (RT-PCR), and quantitative real-time PCR (qPCR). Total RNA preparation, cDNA synthesis, RT-PCR, and qPCR were performed using previously described procedures (6). Among the nucleoside transporters, ENT1, ENT2, CNT2, and CNT3 mRNAs were examined by RT-PCR because they have been identified as ribavirin transporters (21). The primers for RT-PCR and qPCR are listed in Table S1 in the supplemental material. The UPL universal probes used were no. 9 (ENT1), no. 48 (ENT2), and no. 60 (glyceraldehyde 3-phosphate dehydrogenase [GAPDH]).

Knockdown of ENT1 mRNA expression in OR6 cells. The BLOCK-iT Pol II miR RNAi expression vector kit (Invitrogen) was used to suppress ENT1 mRNA expression in OR6 cells. The oligonucleotide containing micro-RNA targeted to ENT1 mRNA (miR-ENT1) was cloned into the pcDNA6.2-GW/EmGFP-miR vector. The control plasmid pcDNA6.2-GW/EmGFP-miR-neg, carrying an insert that is not known to target any identified vertebrate genes (miR-Neg), was used as a negative control. The sequences of inserts are shown in Table S1 in the supplemental material. The plasmids were transfected into OR6 cells using Lipofectamine LTX (Invitrogen). Two days after transfection, the culture medium was replaced with fresh medium containing 4 μg/ml blasticidin to obtain cells stably expressing miR-ENT1 (OR6/miR-ENT1) and cells stably expressing miR-Neg (OR6/miR-Ng).

Data analysis. Statistical analysis was performed using Student's *t* test. The four-parameter logistic model was used to calculate the 50% effective concentration (EC_{50}).

RESULTS

Concentration- and time-dependent anti-HCV activity and accumulation of ribavirin in OR6 cells. The inhibitory effects of ribavirin (1 to 3,162 μM) on HCV replication in OR6 cells were analyzed by monitoring the luciferase activity and HCV core protein expression levels. It was found that the HCV replication activity and core protein levels decreased in a ribavirin concentration-dependent manner (Fig. 1A and B), while the level of ribavirin accumulation increased in a saturable manner (Fig. 1C). Next, the time course of anti-HCV activity of ribavirin at concentrations of 10, 100, and 1,000 μM was examined. The results of our examination showed that, similar to the concentration-dependent profile, the HCV replication activity and core protein amounts decreased over time at each of the ribavirin concentrations tested (Fig. 1D and E) and that the levels of ribavirin accumulation increased linearly or saturably over time (Fig. 1F). These results suggest that ribavirin exerts concentration- and time-dependent antiviral activity that could be associated with the concentration- and time-dependent intracellular accumulation of the drug.

Identification of the ribavirin uptake transporter in OR6 cells. To identify the ribavirin uptake transporter in OR6 cells, we characterized the uptake profile of the drug and the nucleoside transporters mRNA expression in the cells. The ribavirin (1 to 3,162 μM) uptake level in Na^+-plus KHB was found to increase linearly up to 3 mM (Fig. 2A), and the uptake activities of the drug (nmol/mg protein/30 s) at 10, 100 (data not shown), and 1,000 μM were recorded as 0.03 ± 0.01, 0.33 ± 0.02 and 3.2 ± 0.3, respectively (Fig. 2B). The removal of Na^+ from the transport medium did not affect the uptake activities at any of the ribavirin concentrations tested, indicating that all the uptake activities of the drug were sodium independent. These activities were mostly abolished by the addition of 100 μM NBMPR, an inhibitor of ENT1 and ENT2. Consistently, the results of RT-PCR showed that ENT1 and ENT2 mRNAs were abundantly expressed in OR6 cells, while hardly any CNT2 and CNT3 mRNAs were expressed (Fig. 2C). During the above-described experiments, we found that a low concentration of NBMPR (100 nM) failed to inhibit ribavirin uptake by OR6 cells (M. Iikura, unpublished data). Considering that ENT1-mediated nucleoside uptake is generally sensitive to NBMPR inhibition at 100 nM (20), it was hypothesized that ENT2 should have contributed to ribavirin uptake in OR6 cells. However, our previous results indicated that ENT2 cannot transport ribavirin (6). Therefore, to clearly distinguish between ENT1- and ENT2-mediated ribavirin uptake, inhibition analysis was performed using troglitazone (60 μM), hypoxanthine (5 mM), and formycin B (50 μM). Troglitazone has been reported to specifically inhibit ENT1 activity (10). Hypoxanthine and formycin B, at the indicated concentrations, were previously reported to preferentially inhibit ENT2 activity (3, 22), and we confirmed the inhibitory effects of these compounds on ENT2 activity by using HeLa cells (see Fig. S1 in the supplemental material). The results of the inhibition analysis showed that troglitazone completely inhibited the ribavirin uptake activity, while neither hypoxanthine nor formycin B inhibited uptake of the drug in OR6 cells (Fig. 2D). Taken together, the results indicated that, even though the affinity of ENT1 of OR6 cells for NBMPR was somehow reduced, ENT1 was exclusively responsible for the ribavirin uptake in OR6 cells.

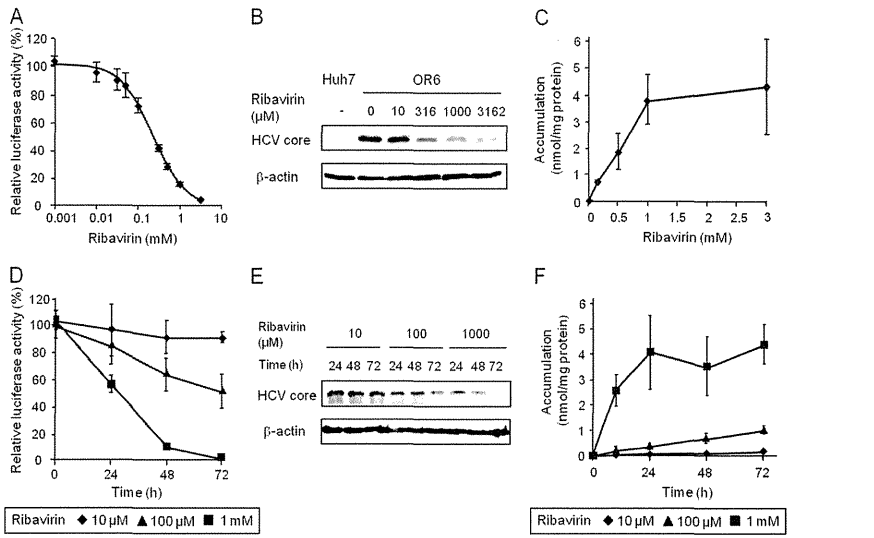

FIG 1 Concentration- and time-dependent profiles of anti-HCV activity and accumulation of ribavirin in OR6 cells. (A) OR6 cells were treated with ribavirin at concentrations of 0, 1, 10, 31, 50, 100, 316, 500, 1,000 and 3,162 μM for 48 h. The value of relative luciferase activity in the absence of ribavirin was set to 100%. (B) Expression levels of HCV core protein in OR6 cells treated with ribavirin for 48 h were examined by Western blot analysis. β-Actin was used as a loading control. Huh-7 cells were used as a negative control. (C) OR6 cells were treated with ribavirin at concentrations of 0.1, 0.5, 1, and 3 mM for 48 h, after which the radioactivity within the cells was determined. (D) OR6 cells were treated with ribavirin. The value of relative luciferase activity in the absence of ribavirin at each time point was set to 100%. (E) Expression levels of HCV core protein in OR6 cells treated with ribavirin were examined by Western blot analysis. (F) OR6 cells were treated with ribavirin, after which the radioactivity within the cells was determined. Values are means and standard deviations (SD) of the relative luciferase activity or the accumulation for three independent experiments. Each experiment was performed in duplicate. For Western blotting, the representative result for three independent assays was shown.

Effect of inhibition of ribavirin uptake on its anti-HCV activity. After it was determined that ENT1 was responsible for ribavirin uptake in OR6 cells, the role of ENT1 in the anti-HCV activity of the drug (100 μM and 1 mM) was examined by chemical inhibition of ENT1-mediated ribavirin uptake in OR6 cells. Since troglitazone itself somewhat repressed HCV replication in OR6 cells (Iikura, unpublished), NBMPR was used as an ENT1 inhibitor. As shown in Fig. 3A, NBMPR decreased the level of ribavirin uptake in a dose-dependent manner and, accordingly, decreased the accumulation level of the drug in a dose-dependent manner (Fig. 3B). In association with these decreases, it was determined that the ribavirin antiviral effect was weakened by NBMPR in a concentration-dependent manner (Fig. 3C). We confirmed that ENT1 protein expression was not changed in the cells treated with the highest ribavirin and NBMPR concentrations for 48 h (see Fig. S2 in the supplemental material). To further clarify the importance of ENT1-mediated ribavirin uptake in its antiviral effects, the concentration and time dependencies of the antiviral effects of the drug were examined in cells treated with NBMPR or its vehicle (0.1% DMSO). The concentration of NBMPR was set to 7 μM, which is near the EC_{50} against ENT1 activity calculated from the results of Fig. 3A, indicating that the ENT1 activity level of NBMPR-treated cells was approximately half that of the vehicle-treated cells. As shown in Fig. 3D, the EC_{50} of ribavirin in the NBMPR-treated cells was 399 ± 22 μM, which was significantly higher than that of the vehicle-treated cells (203 ± 47 μM, $P = 0.0005$) (The results of the individual experiments are shown in Fig. S3 in the supplemental material.) In addition, the response to ribavirin in the NBMPR-treated cells was significantly delayed in comparison to that in the vehicle-treated cells (Fig. 3E). We also examined the constraining effects of ENT2 inhibitors on ribavirin antiviral activity but found that hypoxanthine (5 mM) and formycin B (50 μM) had no effect (see Fig. S4 in the supplemental material). Furthermore, NBMPR, hypoxanthine and formycin B

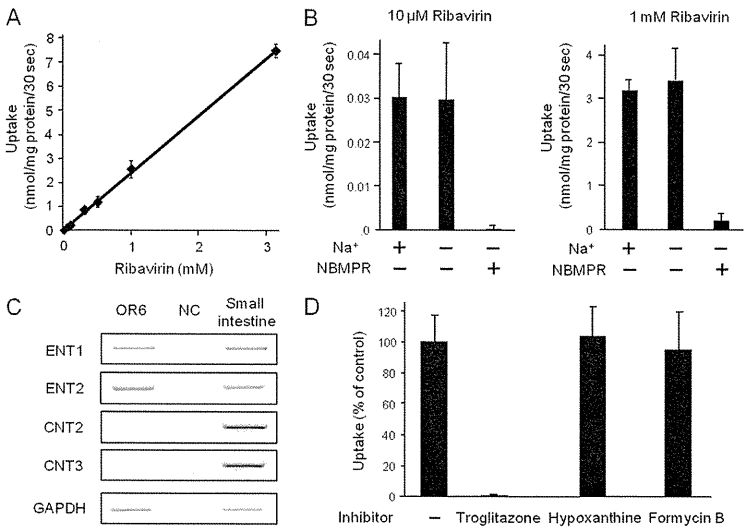

FIG 2 Identification of the ribavirin uptake transporter in OR6 cells. (A) The concentration dependence of ribavirin uptake (concentrations are given in the legend to Fig. 1A) by OR6 cells was analyzed in Na^+-containing KHB. (B) Ribavirin uptake by OR6 cells was analyzed in Na^+-containing KHB and Na^+-free KHB. In inhibition assays, the effect of 100 μM NBMPR on ribavirin uptake was analyzed in Na^+-free KHB. (C) ENT1, ENT2, CNT2, CNT3 and GAPDH mRNA expression was examined by RT-PCR. Small intestine cDNA was used as a PCR control. NC, nontemplate control. Representative results from one of three independent analyses are shown. (D) To clearly distinguish between ENT1- and ENT2-mediated ribavirin uptake, inhibition analysis of ribavirin (100 μM) uptake by OR6 cells was performed in Na^+-free KHB in the absence of inhibitor (−) or the presence of troglitazone (ENT1 inhibitor, 60 μM), hypoxanthine (ENT2 inhibitor, 5 mM), or formycin B (ENT2 inhibitor, 50 μM). The value of the transport activity of the control (no inhibitor) was set to 100%. In the above-described experiments, each value is the mean plus SD from three independent experiments, each performed in duplicate.

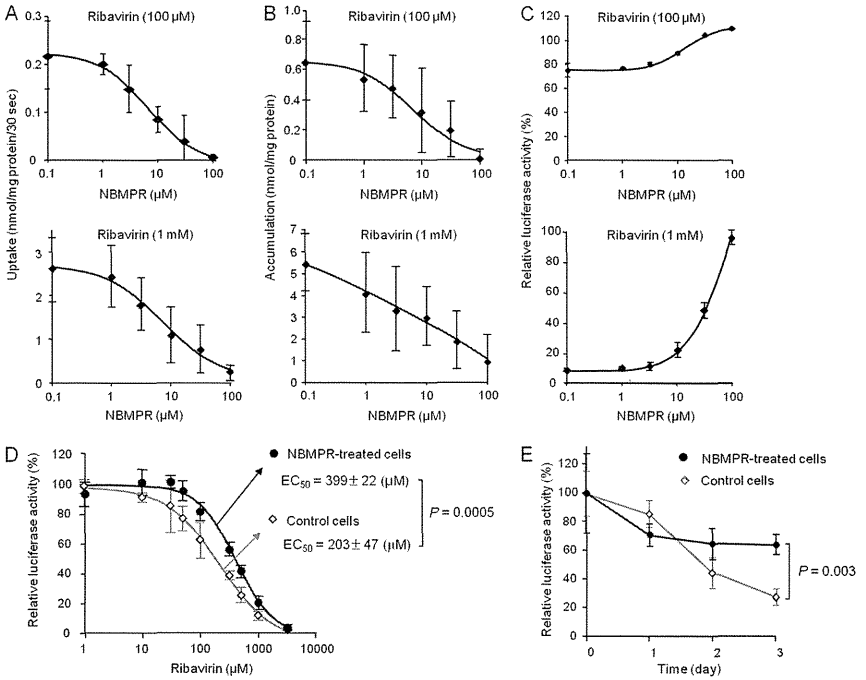

FIG 3 Inhibitory effect of NBMPR on ribavirin uptake, accumulation, and anti-HCV activity. The ribavirin concentration used in these experiments (A to C) was 100 μM or 1 mM, while the NBMPR concentrations used were 0.1, 1, 3, 10, 31, and 100 μM. (A) The effect of NBMPR on ribavirin uptake by OR6 cells was analyzed in Na^+-free KHB with NBMPR. Each value is the mean ± SD from five independent experiments, each performed in duplicate. (B) The effect of NBMPR on ribavirin accumulation in OR6 cells was analyzed by measuring the level of the drug within the cells, in the presence of NBMPR, for 48 h. Each value is the mean ± SD from three independent experiments, each performed in duplicate. (C) The effect of NBMPR on the anti-HCV activity of ribavirin in OR6 cells was analyzed by measuring the level of the luciferase activity, in the presence of NBMPR, for 48 h. The value of relative luciferase activity without ribavirin and NBMPR was set to 100%. Each value is the mean ± SD from three independent experiments, each performed in triplicate. (D) The concentration dependency of ribavirin antiviral action in the presence of NBMPR was examined. The ribavirin concentrations used are shown in the legend to Fig. 1A. The NBMPR concentration was set to 7 μM, which is near the EC_{50} of NBMPR calculated from the results in panel A. The value of relative luciferase activity in the absence of ribavirin was set to 100%. (E) The time dependency of ribavirin antiviral action in the presence of NBMPR was then examined. The ribavirin concentration was set to 150 μM, while the NBMPR concentration was still 7 μM. The value of relative luciferase activity in the absence of ribavirin at each time point was set to 100%.

were found to have no effect on HCV replication activity in the above-described experiments (see Fig. S4 in the supplemental material), and NBMPR (7 μM) failed to affect telaprevir antiviral activity (see Fig. S5 in the supplemental material).

These results clearly show that inhibition of ENT1-mediated ribavirin uptake significantly attenuates ribavirin antiviral effectiveness by reducing the accumulation level of the drug in the cells.

Effect of ENT1 mRNA knockdown on ribavirin anti-HCV activity. The above-mentioned results prompted us to investigate whether a small change in ENT1 activity would similarly affect ribavirin antiviral effectiveness. miRNA targeted to ENT1 mRNA was used in this examination. We found that when stably expressed in OR6 cells (OR6/miR-ENT1), miR-ENT1 reduced the ENT1 mRNA expression level to 72.5 ± 3.4% of that of the control cells (OR6/miR-Ng) without affecting the ENT2 mRNA expression level (Fig. 4A). Accordingly, the ribavirin uptake level in OR6/miR-ENT1 cells was about 66.7 ± 14.0% of that in OR6/miR-Ng cells (Fig. 4B). To determine the degree to which this ENT1 mRNA knockdown affected ribavirin antiviral action, concentration dependencies of ribavirin action in OR6/miR-ENT1 and OR6/miR-Ng cells were characterized. We found that the EC_{50} of ribavirin in OR6/miR-ENT1 cells was 212 ± 11 μM, which was significantly higher than the EC_{50} in OR6/miR-Ng cells (143 ± 33 μM; $P = 0.013$) (The results of the individual experiments are shown in Fig. S3 in the supplemental material.) These results showed that even a small reduction in the ENT1 mRNA expression level could decrease the ribavirin uptake level, thus causing a reduction in the antiviral efficacy of the drug.

Toxicological analyses. Concurrent with the above-described experiments, the cytotoxic effects of ribavirin and other reagents on OR6 cells were examined independently and/or simultaneously (see the supplemental methods in the supplemental material). As shown in Table S2 and Fig. S6 of the supplemental materials, the lactate dehydrogenase (LDH) release assay results showed that no severe cytotoxicity in OR6 cells occurred in any treatments (less than 10%). Microscopic observation also showed that the cells were viable upon treatment with ribavirin (3,162 μM) together with NBMPR (100 μM) for 48 h (see Fig. S2 in the supplemental material). We further performed the MTS assay, which can detect different types of toxicity, to confirm the results of the LDH assay. The results showed that even though marginal toxicity was observed at the highest ribavirin and NBMPR concentrations tested (at most 25%), most treatments did not display severe cytotoxicity for OR6 cells (less than 10%; see Table S2 in the supplemental material).

DISCUSSION

In this paper, we provide results supporting our hypothesis that ENT1 plays an essential role in the anti-HCV activity of ribavirin through detailed characterization of the antiviral activity of the drug and its association with ENT1-mediated uptake in OR6 cells.

Our results showed that the concentration and time dependency of ribavirin antiviral activity was closely associated with its accumulation in OR6 cells. This association is supported by several reports. For example, it has been reported that larger ribavirin accumulations were associated with significant decreases in the intracellular GTP pool (13) or with higher antiviral potency against the Hantaan virus (14). Therefore, it is considered likely that continuous ribavirin accumulation in hepatic cells at the higher levels, which are achieved by the sustained and higher ribavirin extracellular concentrations, is critical to the antiviral efficacy of the drug.

Due to its hydrophilicity, ribavirin requires a "gate" to penetrate the plasma membrane of cells prior to its accumulation. Our results clearly show that ENT1 provides this gate, thus facilitating the drug's import into and accumulation in OR6 cells. Since we recently showed that ENT1 is also exclusively involved in ribavirin uptake in human hepatocytes, which has a ribavirin uptake profile similar to that of OR6 cells (6), it is considered likely that this ENT1 role can probably be extended to human hepatocytes as well. The mode of ENT1-mediated ribavirin uptake in OR6 cells, as well as human hepatocytes, was represented by a linear increase in the uptake level along with an increase in extracellular ribavirin concentration (6; also this study). This uptake feature was the most probable reason why the higher extracellular ribavirin concentration resulted in a stronger antiviral effect in OR6 cells but might also explain why clinical findings show that a higher exposure to ribavirin leads to the better virologic response in HCV genotype-1 patients (11, 17). Therefore, our results, together with

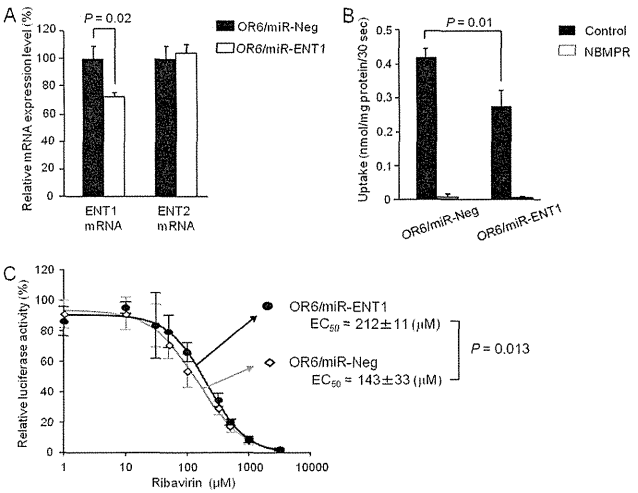

FIG 4 Effect of ENT1 mRNA knockdown on anti-HCV activity of ribavirin. (A) The expression levels of ENT1 and ENT2 mRNA were determined by real-time PCR. Abundance is shown relative to the level of ENT1 or ENT2 mRNA in OR6/miR-Ng cells. Each value is the mean plus SD from three independent experiments, each performed in duplicate. (B) Ribavirin (100 μM) uptake by OR6/miR-ENT1 and OR6/miR-Ng cells was analyzed in Na^+-free KHB in the absence (control) or presence of 100 μM NBMPR. Each value is the mean plus SD of transport activity from three independent experiments, each performed in duplicate. (C) The concentration dependency of ribavirin in OR6/miR-Ng and OR6/miR-ENT1 cells was then examined. The ribavirin concentrations used are shown in the legend to Fig. 1A. The relative luciferase activity value in the absence of ribavirin in each cell line was set to 100%. Each value is the mean ± SD of relative luciferase activity from four independent experiments, each performed in triplicate.

the other findings, indicate that ENT1 plays an indispensable role in ribavirin antiviral activity.

The importance of ENT1 in ribavirin antiviral activity was further underscored by the results of both the ENT1 knockdown and uptake inhibition experiments using NBMPR. It is noteworthy that even a small reduction of ENT1 activity significantly weakened ribavirin's antiviral potency. These results indicate that increasing or decreasing ENT1 activity level in the cells results in stronger or weaker ribavirin efficacy by increasing or reducing the uptake of the drug, even if extracellular ribavirin concentrations and exposure durations are constant. Therefore, it can be concluded that the ENT1-mediated ribavirin uptake level determines the level of ribavirin antiviral activity in OR6 cells and, presumably, in human hepatocytes.

The above-mentioned findings and suppositions prompt us to propose the following two possibilities (see Fig. S7 in the supplemental material). One is that patients with higher ENT1 activity levels in hepatocytes could more likely attain RVR (defined as a faster and stronger ribavirin antiviral effect in the early stage of the treatment) than those with lower ENT1 activity levels, when other factors affecting the treatment outcome are similar. The mechanisms underlying the interindividual difference in the hepatic ENT1 activity level remain unclear, but SNPs are promising candidates for the causal factors that result in the difference. Since two intronic SNPs have been revealed to be associated with RVR (and SVR) (12, 18), investigations should be conducted to determine whether these SNPs have a positive effect on the hepatic ENT1 expression level.

The other possibility is that the hepatic uptake of ribavirin by ENT1 could be hindered by coadministered chemicals, thus resulting in attenuation of the treatment response in some patients, as shown in Fig. 3. Although there have been no clinical reports supporting this possibility, preceding studies have been performed to determine whether hepatic uptake inhibition of pravastatin and metformin, which are hepatocyte-targeting drugs, reduces their effectiveness (1). These drugs are known substrates for hepatic organic ion transporters, and it has been shown that aberrations in these transporters significantly impair their *in vivo* functions (2, 15). Since, due to attendant complications or other chronic diseases, several drugs are often coprescribed along with ribavirin during treatment regimens, it may be worth considering whether interactions between ribavirin and other drugs at the point of ENT1-mediated uptake can affect the treatment response.

Exploration of these possibilities must await further studies aimed at clarification of the factors affecting the hepatic ENT1 activity level, including the above-described SNP studies and ribavirin-drug interaction studies. The results obtained from such studies could contribute not only to a better understanding of the mode of action of ENT1 on ribavirin antiviral activity but also to identification of the associated markers for RVR or null responses in clinical settings.

It should be noted that, unexpectedly, ENT1 activity was found to be insensitive to inhibition by NBMPR in the nanomolar range in OR6 cells. This was not due to nucleotide alterations in ENT1 cDNA of OR6 cells (Iikura, unpublished). Since OR6 cells were derived from Huh-7 cells, we examined the sensitivity of ENT1 to inhibition of NBMPR using Huh-7 cells and obtained results similar to those obtained with OR6 cells (Iikura, unpublished). Therefore, the lower sensitivity of ENT1 to NBMPR in OR6 cells was thought to have originated from the Huh-7 cells. Although the reason for the altered sensitivity of ENT1 to NBMPR remains unknown at this time, it is believed that the cell-specific posttranslational modification might be involved. It has been reported that defective glycosylation of ENT1 leads to decreased affinity for NBMPR (19). Therefore, it can be speculated that the type or structure of glycochain and/or other modifications could be responsible for decreased affinity of ENT1 of OR6/Huh-7 cells for NBMPR. Further studies aimed at ascertaining the reason might provide novel insights into the biology of ENT1.

Finally, we briefly discuss the static cytotoxic effects of ribavirin and NBMPR on OR6 cells. According to the results of toxicological analyses, these reagents (at most concentrations tested) did not cause severe toxicity in OR6 cells (less than 10%), and only marginal toxicity was found in treatment of the reagents at the highest concentrations tested in an MTS assay. In contrast, blasticidin S treatment (20 ng/ml) significantly damaged the cells (>50% in the MTS assay [Iikura, unpublished]). Therefore, it is assumed that OR6 cells possess inherent resistance to ribavirin and NBMPR, and this factor might be related to the relatively high EC_{50} of ribavirin. Although we do not know the reason for the behavior of the cells, it is unlikely that the limited toxicity would give rise to a question regarding the present results. In actuality, 100 μM NBMPR treatment, which caused marginal toxicity, did not affect HCV replication activity (see Fig. S4 in the supplemental material).

In conclusion, we have clearly demonstrated that ENT1 plays an indispensable role in ribavirin antiviral activity by facilitating the uptake and accumulation of the drug in OR6 cells, thereby indicating that ENT1 provides a gate that is essential to the success of ribavirin's mission. Our study limitations include an *in vitro* HCV model system using hepatoma cells and no *in vivo* evidence of association between hepatic ENT1 activity and ribavirin efficacy. Nevertheless, our results, together with the literature, strongly suggest that ENT1 also plays the determinant role in the antiviral efficacy of ribavirin in the human liver during the course of anti-HCV therapy. Accordingly, it is believed that our results, as well as the ideas described in this paper, will encourage further studies aimed at the clarification of the clinical importance of ENT1 in anti-HCV therapy.

ACKNOWLEDGMENTS

This work was supported by a grant (20790128) from the Ministry of Education, Sciences, Sports and Culture of Japan and partially supported by a Special Funds for Education and Research (Development of SPECT Probes for Pharmaceutical Innovation) from the Ministry of Education, Culture, Sports, Science and Technology, Japan, and a research grant from the Nakatomi Foundation (Tokyo, Japan).

REFERENCES

1. Bachmakov I, Glaeser H, Fromm MF, König J. 2008. Interaction of oral antidiabetic drugs with hepatic uptake transporters: Focus on organic anion transporting polypeptides and organic cation transporter 1. Diabetes 57:1463–1469.
2. Becker ML, et al. 2009. Genetic variation in the organic cation transporter 1 is associated with metformin response in patients with diabetes mellitus. Pharmacogenomics J. 9:242–247.
3. Burke T, Lee S, Ferguson PJ, Hammond JR. 1998. Interaction of 2′,2′-difluorodeoxycytidine (gemcitabine) and formycin B with the Na^+-dependent and -independent nucleoside transporters of Ehrlich ascites tumor cells. J. Pharmacol. Exp. Ther. 286:1333–1340.
4. Dixit NM, Perelson AS. 2006. The metabolism, pharmacokinetics and mechanisms of antiviral activity of ribavirin against hepatitis C virus. Cell. Mol. Life Sci. 63:832–842.
5. Fried MW, et al. 2002. Peginterferon alfa-2a plus ribavirin for chronic hepatitis C virus infection. N. Engl. J. Med. 347:975–982.
6. Fukuchi Y, Furihata T, Hashizume M, Iikura M, Chiba K. 2010. Characterization of ribavirin uptake systems in human hepatocytes. J. Hepatol. 52:486–492.
7. Hofmann WP, Herrmann E, Sarrazin C, Zeuzem S. 2008. Ribavirin mode of action in chronic hepatitis C: from clinical use back to molecular mechanisms. Liver Int. 28:1332–1343.
8. Ikeda M, et al. 2005. Efficient replication of a full-length hepatitis C virus genome, strain O, in cell culture, and development of a luciferase reporter system. Biochem. Biophys. Res. Commun. 329:1350–1359.
9. Kong W, Engel K, Wang J. 2004. Mammalian nucleoside transporters. Curr. Drug Metab. 5:63–84.
10. Leung GP, Man RY, Tse CM. 2005. Effect of thiazolidinediones on equilibrative nucleoside transporter-1 in human aortic smooth muscle cells. Biochem. Pharmacol. 70:355–362.
11. Lindahl K, Stahle L, Bruchfeld A, Schvarcz R. 2005. High-dose ribavirin in combination with standard dose peginterferon for treatment of patients with chronic hepatitis C. Hepatology 41:275–279.
12. Morello J, et al. 2010. Influence of a single nucleotide polymorphism at the main ribavirin transporter gene on the rapid virological response to pegylated interferon-ribavirin therapy in patients with chronic hepatitis C virus infection. J. Infect. Dis. 202:1185–1191.
13. Smee DF, Matthews TR. 1986. Metabolism of ribavirin in respiratory syncytial virus-infected and uninfected cells. Antimicrob. Agents Chemother. 30:117–121.
14. Sun Y, Chung DH, Chu YK, Jonsson CB, Parker WB. 2007. Activity of ribavirin against Hantaan virus correlates with production of ribavirin-5′-triphosphate, not with inhibition of IMP dehydrogenase. Antimicrob. Agents Chemother. 51:84–88.
15. Tachibana-Iimori R, et al. 2004. Effect of genetic polymorphism of OATP-C (SLCO1B1) on lipid-lowering response to HMG-CoA reductase inhibitors. Drug Metab. Pharmacokinet. 19:375–380.
16. Thomas E, et al. 2011. Ribavirin potentiates interferon action by augmenting interferon-stimulated gene induction in hepatitis C virus cell culture models. Hepatology 53:32–41.
17. Tsubota A, Hirose Y, Izumi N, Kumada H. 2003. Pharmacokinetics of ribavirin in combined interferon-alpha 2b and ribavirin therapy for chronic hepatitis C virus infection. Br. J. Clin. Pharmacol. 55:360–367.
18. Tsubota A, et al. 2011. Contribution of ribavirin transporter gene polymorphism to treatment response in peginterferon plus ribavirin therapy for HCV genotype 1b patients. Liver Int. [Epub ahead of print.10.1111/j.1478–3231.2011.02727.x.
19. Vickers MF, et al. 1999. Functional production and reconstitution of the human equilibrative nucleoside transporter (hENT1) in Saccharomyces cerevisiae. Interaction of inhibitors of nucleoside transport with recombinant hENT1 and a glycosylation-defective derivative (hENT1/N48Q). Biochem. J. 339:21–32.
20. Ward JL, Sherali A, Mo ZP, Tse CM. 2000. Kinetic and pharmacological properties of cloned human equilibrative nucleoside transporters, ENT1 and ENT2, stably expressed in nucleoside transporter-deficient PK15 cells. J. Biol. Chem. 275:8375–8381.
21. Yamamoto T, et al. 2007. Ribavirin uptake by cultured human choriocarcinoma (BeWo) cells and Xenopus laevis oocytes expressing recombinant plasma membrane human nucleoside transporters. Eur. J. Pharmacol. 557:1–8.
22. Yao SY, et al. 2002. Functional and molecular characterization of nucleobase transport by recombinant human and rat equilibrative nucleoside transporters 1 and 2. J. Biol. Chem. 277:24938–24948.

Inhibition of Both Protease and Helicase Activities of Hepatitis C Virus NS3 by an Ethyl Acetate Extract of Marine Sponge *Amphimedon* sp.

Yuusuke Fujimoto[1], Kazi Abdus Salam[2,9], Atsushi Furuta[3,4,9], Yasuyoshi Matsuda[3,4], Osamu Fujita[3,4], Hidenori Tani[5], Masanori Ikeda[6], Nobuyuki Kato[6], Naoya Sakamoto[7], Shinya Maekawa[8], Nobuyuki Enomoto[8], Nicole J. de Voogd[9], Masamichi Nakakoshi[10], Masayoshi Tsubuki[10], Yuji Sekiguchi[3], Satoshi Tsuneda[4], Nobuyoshi Akimitsu[2], Naohiro Noda[3,4], Atsuya Yamashita[1]*, Junichi Tanaka[11]*, Kohji Moriishi[1]*

1 Department of Microbiology, Division of Medicine, Graduate School of Medicine and Engineering, University of Yamanashi, Yamanashi, Japan, **2** Radioisotope Center, The University of Tokyo, Tokyo, Japan, **3** Biomedical Research Institute, National Institute of Advanced Industrial Science and Technology, Ibaraki, Japan, **4** Department of Life Science and Medical Bioscience, Waseda University, Tokyo, Japan, **5** Research Institute for Environmental Management Technology, National Institute of Advanced Industrial Science and Technology, Ibaraki, Japan, **6** Department of Tumor Virology, Okayama University Graduate School of Medicine, Dentistry, and Pharmaceutical Sciences, Okayama, Japan, **7** Department of Gastroenterology and Hepatology, Hokkaido University Graduate School of Medicine, Sapporo, Japan, **8** First Department of Internal Medicine, Faculty of Medicine, University of Yamanashi, Yamanashi, Japan, **9** Netherlands Centre for Biodiversity Naturalis, Leiden, The Netherlands, **10** Institute of Medical Chemistry, Hoshi University, Tokyo, Japan, **11** Department of Chemistry, Biology and Marine Science, University of the Ryukyus, Okinawa, Japan

Abstract

Combination therapy with ribavirin, interferon, and viral protease inhibitors could be expected to elicit a high level of sustained virologic response in patients infected with hepatitis C virus (HCV). However, several severe side effects of this combination therapy have been encountered in clinical trials. In order to develop more effective and safer anti-HCV compounds, we employed the replicon systems derived from several strains of HCV to screen 84 extracts from 54 organisms that were gathered from the sea surrounding Okinawa Prefecture, Japan. The ethyl acetate-soluble extract that was prepared from marine sponge *Amphimedon* sp. showed the highest inhibitory effect on viral replication, with EC_{50} values of 1.5 and 24.9 μg/ml in sub-genomic replicon cell lines derived from genotypes 1b and 2a, respectively. But the extract had no effect on interferon-inducing signaling or cytotoxicity. Treatment with the extract inhibited virus production by 30% relative to the control in the JFH1-Huh7 cell culture system. The *in vitro* enzymological assays revealed that treatment with the extract suppressed both helicase and protease activities of NS3 with IC_{50} values of 18.9 and 10.9 μg/ml, respectively. Treatment with the extract of *Amphimedon* sp. inhibited RNA-binding ability but not ATPase activity. These results suggest that the novel compound(s) included in *Amphimedon* sp. can target the protease and helicase activities of HCV NS3.

Citation: Fujimoto Y, Salam KA, Furuta A, Matsuda Y, Fujita O, et al. (2012) Inhibition of Both Protease and Helicase Activities of Hepatitis C Virus NS3 by an Ethyl Acetate Extract of Marine Sponge *Amphimedon* sp.. PLoS ONE 7(11): e48685. doi:10.1371/journal.pone.0048685

Editor: Tetsuo Takehara, Osaka University Graduate School of Medicine, Japan

Received June 16, 2012; **Accepted** October 1, 2012; **Published** November 7, 2012

Funding: This work was supported in part by grants-in-aid from the Ministry of Health, Labor, and Welfare (http://www.mhlw.go.jp/) and from the Ministry of Education, Culture, Sports, Science, and Technology of Japan (http://www.mext.go.jp/). The funders had no role in study design, data collection and analysis, decision to publish, or preparation of the manuscript.

Competing Interests: The authors have declared that no competing interests exist.

* E-mail: atsuyay@yamanashi.ac.jp (AY); jtanaka@sci.u-ryukyu.ac.jp (JT); kmoriishi@yamanashi.ac.jp (KM)

These authors contributed equally to this work.

Introduction

Hepatitis C virus (HCV) is an enveloped RNA virus of the genus *Hepacivirus* of the *Flaviviridae* family. More than 170 million patients persistently infected with HCV have been reported worldwide, leading to liver diseases including steatosis, cirrhosis, and hepatocellular carcinoma [1,2]. The genome of HCV is characterized as a single positive-strand RNA with a nucleotide length of 9.6 kb, flanked by 5′ and 3′-untranslated regions (UTRs). The genomic RNA encodes a large polyprotein consisting of approximately 3,000 amino acids [3], which is translated under the control of an internal ribosome entry site (IRES) located within the 5′-UTR of the genomic RNA [4]. The translated polyprotein is cleaved by host and viral proteases, resulting in 10 mature viral proteins [3]. The structural proteins, consisting of core, E1, and E2, are located in the N-terminal quarter of the polyprotein, followed by viroporin p7, which has not yet been classified into a structural or nonstructural protein. Further cleavage of the remaining portion by viral proteases produces six nonstructural proteins–NS2, NS3, NS4A, NS4B, NS5A, and NS5B–which form a viral replication complex with various host factors. The viral protease NS2 cleaves its own C-terminal between NS2 and NS3. After that, NS3 cleaves the C-terminal ends of NS3 and NS4A and then forms a complex with NS4A. The NS3/4A complex becomes a fully active form to cleave the C-terminal parts of the polyprotein, including nonstructural proteins. NS3 also possesses RNA helicase activity to unwind the double-stranded RNA during the synthesis of genomic RNA [5,6].

Although the previous standard therapy, combining pegylated interferon with ribavirin, was effective in only about half of patients infected with genotype 1, the most common genotype worldwide [7–9], recent biotechnological advances have led to the development of a novel therapy using anti-HCV agents that directly target HCV proteins or host factors required for HCV replication and have improved the sustained virologic response (SVR) [10–12]. Telaprevir and boceprevir, which are categorized as advanced NS3/4A protease inhibitors, were recently approved for the treatment of chronic hepatitis C patients infected with genotype 1 [13,14]. The triple combination therapy with pegylated interferon, ribavirin, and telaprevir improved SVR by 77% in patients infected with genotype 1 [15]. However, this therapy exhibits side effects including rash, severe cutaneous eruption, influenza-like symptoms, cytopenias, depression, and anemia [7,16,17]. Furthermore, the possibility of the emergence of drug-resistant viruses is a serious problem with therapies that use antiviral compounds [18,19].

Recent technical advances in the determination of molecular structures and the synthesis of chemical compounds have led to the development of various drugs based on natural products, especially drugs identified from terrestrial plants and microbes [20–22]. Marine organisms, including plants and animals, were recently established as representative of a natural resource library for drug development. Potent biological activity is often found in products isolated from marine organisms because of their novel molecular structures [23,24]. Trabectedin (Yondelis), cytarabine (Ara-C), and eribulin (Halaven), which are known as antitumor drugs, were developed from compounds found in marine organisms [25].

In this study, we screened 84 extracts prepared from 54 marine organisms by using replicon cell lines derived from HCV genotype 1b and attempted to identify the extract that inhibits HCV RNA replication. A marine organism may produce anti-HCV agent(s) that could inhibit the protease and helicase activities of NS3.

Results

Effect of the Extract from Marine Sponge and Tunicate on HCV Replication

We prepared methanol (MeOH)- and ethyl acetate (EtOAc)-soluble extracts from 54 marine organisms in order to test which of these extracts could best suppress HCV replication. Each extract was added at 25 μg/ml to the culture supernatant of HCV replicon cell lines derived from O and Con1 strains of genotype 1b, which produce the luciferase/neomycin hybrid protein depending on RNA replication. Luciferase activity and cell viability were measured 72 h after treatment with the extracts (Table 1). The extracts exhibiting more than 85% cell viability and lower than 15% luciferase activity were selected as arbitrary candidates for the extract including anti-HCV compounds. The EtOAc-extract prepared from sample C-29 (C-29EA) was selected as a candidate in both cell lines. Thus, the anti-HCV activity of extract C-29EA was tested.

The EtOAc-soluble extract C-29EA was prepared from the marine sponge *Amphimedon* sp. (Fig. 1A), which inhabits the sea surrounding Okinawa Prefecture, Japan. HCV replication was inhibited in a dose-dependent manner but did not exhibit cytotoxicity when replicon cells were treated with C-29EA (Fig. 1 B). The extract C-29EA exhibited EC_{50} values of 1.5 μg/ml (Table 2). Furthermore, treatment with C-29EA suppressed the HCV replication derived from the genotype 2a strain JFH1 with an EC_{50} of 24.9 μg/ml, irrespective of cell viability (Fig. 2A and Table 2). Extract C-29EA also inhibited the production of infectious viral particles, viral RNA, and core protein from JFH1-infected cells in the supernatant (Fig. 2B and C). These results suggest that the marine sponge *Amphimedon* sp. possesses anti-HCV agents.

Effect of Extract C-29EA on IRES-dependent Translation

Extract C-29EA had the most potent inhibitory activity against HCV replication. The viral replication (Fig. 1 B and 2 A) and viral proteins (Fig. 3 A and B) in replicon cell lines derived from genotype 1b strain Con1 and 2a strain JFH1 were decreased 72 h after treatment in a dose-dependent manner. HCV protein has been translated based on the positive-sense viral RNA in an IRES-dependent manner. The replicon RNA of HCV is composed of the 5′-UTR of HCV, indicator genes (a luciferase-fused drug-resistant gene), encephalomyocarditis virus (EMCV) IRES, the viral genes encoding complete or nonstructural proteins, and the 3′-UTR of HCV, in that order [26]. The replicon RNA replicated autonomously in several HCV replication-permissive cell lines derived from several hepatoma cell lines. Nonstructural proteins in replicon cells were polycistronically translated through EMCV IRES. The cap-dependent translated mRNA, including *Renilla* luciferase, EMCV IRES, and the firefly luciferase/neomycin-resistant gene, in that order, was constructed to examine the effect of the extract on EMCV-IRES-dependent translation (Fig. 3C). When the mRNA expression was transcribed by an EF promoter of the transfected plasmid in the presence of C-29EA, the ratio of firefly luciferase activity to *Renilla* luciferase activity was not changed (Fig. 3C). This suggested that treatment with C-29EA exhibited no effect on EMCV-IRES-dependent translation. Furthermore, treatment with C-29EA did not significantly affect the activity of HCV IRES that was used instead of EMCV IRES in the system described above (Fig. 3D). Thus, these results suggest that treatment with C-29EA exhibits no effect on EMCV- or HCV-IRES-dependent translation.

Effect of C-29EA on the Interferon Signaling Pathway

It has been well known that HCV replication in cultured cells is potently inhibited by interferon [27,28]. We examined whether or not treatment with C-29EA elicits an interferon-inducible gene from replicon cells. The replicon cells were treated with various concentrations of interferon-alpha 2b or 15 μg of C-29EA per milliliter. The treated cells were harvested at 72 h post-treatment. The interferon-inducible gene 2′, 5′-OAS, was induced with IFN-alpha 2b but not with a 10-times EC_{50} concentration of C-29EA (Fig. 4). These results suggest that the inhibitory effect of C-29EA on the replication of the HCV replicon is independent of the IFN signaling pathway.

Effect of C-29EA on the NS3 Helicase Activity

We previously established an assay system for unwinding HCV activity based on photoinduced electron transfer (PET) [29,30]. The fluorescent dye (BODIPY FL) is attached to the cytosine at the 5′-end of the fluorescent strand and quenched by the guanine base at the 3′-end of the complementary strand via PET. When helicase unwinds the double-strand RNA substrate, the fluorescence of the dye emits a bright light upon the release of the dye from the guanine base. The capture strand, which is complementary to the complementary strand, prevents the reannealing of the unwound duplex. Treatment with C-29EA inhibited the helicase activity in a dose-dependent manner, with an IC_{50} value of 18.9 μg/ml (Fig. 5A). We confirmed the effect of C-29EA on NS3 helicase unwinding activity by the RNA helicase assay using ^{32}P-labeled double-stranded RNA (dsRNA) as a substrate. Treatment

Table 1. Effect of marine organism extracts on HCV replication and cell viability.

No.	Sample	Luciferase activity (% of control)		Cell viability (% of control)		Phylum	Specimen	Extract	Site
		O	Con1	O	Con1				
1	A-1	10	111	105	104	Sponge	*Unidentified*	MeOH	A
2	A-2	82	209	91	132	Soft coral	*Briareum*	MeOH	A
3	A-3	87	177	54	110	Tunicate	*unidentified*	MeOH	A
4	A-4	82	186	84	100	Sponge	*Liosina*	MeOH	A
5	B-5	110	165	86	110	Sponge	*unidentified*	MeOH	B
6	B-6	70	149	103	119	Sponge	*Xestospongia*	MeOH	B
7	B-7	89	191	111	144	Sponge	*Epipolasis*	MeOH	B
8	B-8	89	182	115	132	Sponge	*unidentified*	MeOH	B
9	B-9	57	72	92	124	Sponge	*Strongylophora*	MeOH	B
10	B-10	106	182	73	96	Sponge	*Stylotella aurantium*	MeOH	B
11	C-12	96	162	114	98	Sponge	*Epipolasis*	MeOH	B
12	C-13	123	141	91	103	Sponge	*unidentified*	MeOH	B
13	C-14	89	175	77	100	Sponge	*Hippospongia*	MeOH	B
14	C-16	80	177	108	88	Sponge	*unidentified*	MeOH	B
15	C-18	119	170	93	94	Sponge	*unidentified*	MeOH	B
16	C-19	0	0	0	4	Sponge	*unidentified*	MeOH	B
17	C-20	101	158	61	106	Sponge	*Xestospongia testudinaria*	MeOH	B
18	C-21	85	161	83	102	Sponge	*unidentified*	MeOH	B
19	C-22	109	88	38	89	Sponge	*unidentified*	MeOH	B
20	C-23	94	156	32	90	Sponge	*unidentified*	MeOH	B
21	C-24	118	86	42	94	Sponge	*Theonella*	MeOH	B
22	C-25	82	111	91	106	Sponge	*unidentified*	MeOH	B
23	C-27	0	0	15	2	Sponge	*unidentified*	MeOH	B
24	C-28	90	166	30	90	Sponge	*Petrosia*	MeOH	B
25	C-29	65	151	29	101	Sponge	*Amphimedon*	MeOH	B
26	D-31	81	127	55	91	Tunicate	*unidentified*	MeOH	C
27	D-32	80	141	47	93	Sponge	*unidentified*	MeOH	C
28	D-33	88	153	72	90	Gorgonian	*Junceella fragilis*	MeOH	C
29	E-35	114	156	40	118	Sponge	*Phyllospongia sp.*	MeOH	C
30	E-36	80	125	69	116	Tunicate	*Didemnum molle*	MeOH	C
31	E-37	88	129	54	108	Sponge	*Xestospongia sp.*	MeOH	C
32	E-38	70	153	35	112	Sponge	*unidentified*	MeOH	C
33	F-40	119	170	38	104	Sponge	*unidentified*	MeOH	C
34	F-41	88	166	48	101	Soft coral	*unidentified*	MeOH	C
35	G-42	113	157	31	126	Sponge	*unidentified*	MeOH	D
36	H-43	83	0	39	5	Sponge	*unidentified*	MeOH	D
37	J-44	62	183	27	105	Sponge	*Cinachyra*	MeOH	D
38	J-45	96	140	47	103	Sponge	*Liosina*	MeOH	D
39	J-46	83	149	77	102	Sponge	*unidentified*	MeOH	D
40	J-47	94	37	40	111	Sponge	*unidentified*	MeOH	D
41	J-48	24	16	53	70	Sponge	*Stylotella*	MeOH	D
42	J-49	78	123	55	105	Sponge	*unidentified*	MeOH	D
43	J-50	93	138	51	108	Sponge	*unidentified*	MeOH	D
44	J-51	103	73	41	115	Sponge	*unidentified*	MeOH	D
45	J-52	162	237	113	131	Sponge	*unidentified*	MeOH	D
46	J-53	51	90	93	122	Tunicate	*Didemnum*	MeOH	D
47	J-54	42	90	113	124	Sponge	*unidentified*	MeOH	D

Table 1. Cont.

No.	Sample	Luciferase activity (% of control)		Cell viability (% of control)		Phylum	Specimen	Extract	Site
		O	Con1	O	Con1				
48	J-55	88	133	131	110	Jellyfish	*unidentified*	MeOH	D
49	J-56	28	51	113	103	Sponge	*unidentified*	MeOH	D
50	J-57	8	63	94	85	Tunicate	*Pseudodistoma kanoko*	MeOH	D
51	J-58	0	2	48	65	Sponge	*unidentified*	MeOH	D
52	J-59	0	2	45	71	Sponge	*unidentified*	MeOH	D
53	J-60	98	134	122	95	Annelid	*unidentified*	MeOH	D
54	A-2	0	1	6	15	Soft coral	*Briareum*	EtOAc	A
55	A-3	0	0	6	9	Tunicate	*unidentified*	EtOAc	A
56	A-4	22	36	74	76	Sponge	*Liosina*	EtOAc	A
57	B-5	33	107	69	93	Sponge	*unidentified*	EtOAc	B
58	B-6	0	0	5	8	Sponge	*Xestospongia*	EtOAc	B
59	B-7	0	0	5	9	Sponge	*Epipolasis*	EtOAc	B
60	B-8	0	0	2	46	Sponge	*unidentified*	EtOAc	B
61	B-9	0	0	8	14	Sponge	*Strongylophora*	EtOAc	B
62	B-10	0	0	3	8	Sponge	*Stylotella aurantium*	EtOAc	B
63	C-12	0	0	4	14	Sponge	*Epipolasis*	EtOAc	B
64	C-13	0	0	4	5	Sponge	*unidentified*	EtOAc	B
65	C-14	48	119	82	102	Sponge	*Hippospongia*	EtOAc	B
66	C-15	0	0	8	11	Sponge	*unidentified*	EtOAc	B
67	C-18	0	0	4	3	Sponge	*unidentified*	EtOAc	B
68	C-19	23	76	63	109	Sponge	*unidentified*	EtOAc	B
69	C-20	34	32	63	112	Sponge	*Xestospongia testudinaria*	EtOAc	B
70	C-21	1	0	52	12	Sponge	*unidentified*	EtOAc	B
71	C-22	76	34	74	110	Sponge	*unidentified*	EtOAc	B
72	C-24	0	0	20	7	Sponge	*Theonella*	EtOAc	B
73	C-26	41	43	80	110	Sponge	*unidentified*	EtOAc	B
74	C-27	1	0	35	40	Sponge	*unidentified*	EtOAc	B
75	C-28	68	62	82	115	Sponge	*Petrosia*	EtOAc	B
76	C-29	10	11	93	88	Sponge	*Amphimedon*	EtOAc	B
77	D-31	20	71	85	120	Tunicate	*Eudistoma*	EtOAc	C
78	D-33	0	0	5	7	Gorgonian	*Junceella fragilis*	EtOAc	C
79	E-35	0	0	4	5	Sponge	*Phyllospongia sp.*	EtOAc	C
80	E-36	71	83	75	100	Tunicate	*Didemnum molle*	EtOAc	C
81	F-40	72	110	87	130	Sponge	*unidentified*	EtOAc	C
82	F-41	8	33	73	104	Soft coral	*unidentified*	EtOAc	C
83	H-43	0	197	4	119	Sponge	*unidentified*	EtOAc	D
84	J-46	113	58	103	126	Sponge	*unidentified*	EtOAc	D

There are a total of 54 marine organisms, while 84 extracts were prepared from them with ethyl acetate and/or methanol. Aragusuku, Iriomote, Kohama, and Ishigaki islands are indicated by A, B, C, and D, respectively, in the collection-site column?(right end). EtOAc: Ethyl acetate; MeOH: Methanol.

doi:10.1371/journal.pone.0048685.t001

with C-29EA inhibited dsRNA dissociation at a concentration of 16 μg/ml and above (Fig. 5B).

The unwinding ability of HCV helicase depends on ATP binding, ATP hydrolysis, and RNA binding [30,31]. We examined the effect of C-29EA on the ATPase activity of NS3. The ratio of free phosphate (^{32}P-Pi) to ATP (^{32}P-ATP) was determined in the presence of C-29EA. The reaction was carried out between 16 and 250 μg of C-29EA per milliliter. The ATPase activity of NS3 helicase was not inhibited (Fig. 6A), although the helicase activity was decreased to less than 20% in the presence of 50 μg of C-29EA per milliliter (Fig. 5A). Next, we examined the effect of C-29EA on the binding of NS3 helicase to single-strand RNA (ssRNA). A gel-mobility shift assay was employed to estimate the binding activity of NS3 to the 21-mer of ssRNA. The binding of NS3 to ssRNA was inhibited by C-29EA in a dose-dependent manner (Fig. 6 B and C). These results suggest that treatment with C-29EA inhibits the helicase activity of NS3 by suppressing RNA binding.

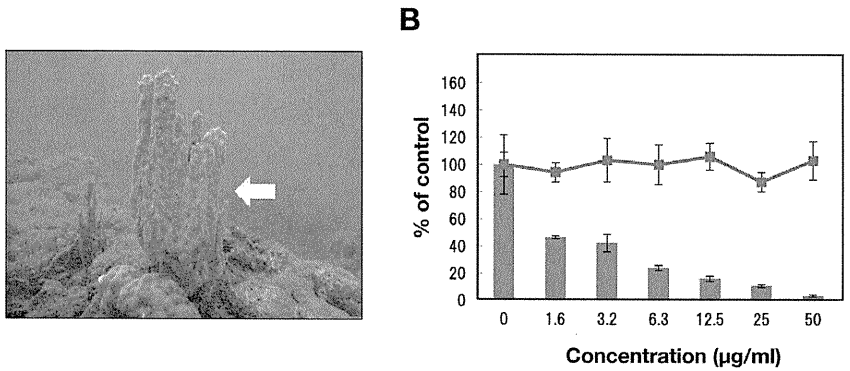

Figure 1. Effect of the extract prepared from a marine sponge on viral replication in the replicon cell line derived from viral genotype 1b. (A) *Amphimedon* sp. belongs to a marine sponge. The ethyl acetate fraction prepared from the marine organism was designated C-29EA in this study. (B) The Huh7 cell line, including the subgenomic replicon RNA of genotype 1b strain Con1, was incubated in medium containing various concentrations of C-29EA or DMSO (0). Luciferase and cytotoxicity assays were carried out as described in Materials and Methods. Error bars indicate standard deviation. The data represent three independent experiments.
doi:10.1371/journal.pone.0048685.g001

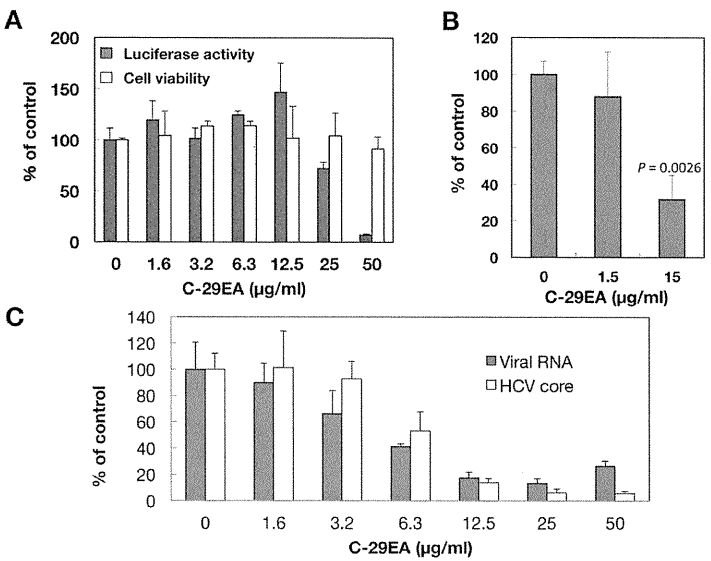

Figure 2. Effect of C-29EA extract on viral replication in the replicon cell line derived from viral genotype 2a. (A) The Huh7 cell line, including the subgenomic replicon RNA of genotype 2a strain JFH1, was incubated in medium containing various concentrations of C-29EA or DMSO (0). Luciferase and cytotoxicity assays were carried out as described in Materials and Methods. (B) The Huh7 OK1 cell line infected with HCVcc JFH1 was incubated with various concentrations of C-29EA or DMSO (0). The virus titers were determined by a focus-forming assay. The significance of differences in the means was determined by Student's *t*-test. (C) Amounts of viral RNA and core protein were estimated by qRT-PCR and ELISA, respectively. Error bars indicate standard deviation. The data represent three independent experiments. Treatment with DMSO corresponds to '0'.
doi:10.1371/journal.pone.0048685.g002

Table 2. Effect of C29EA on HCV replication.

HCV strain (genotype)	EC_{50} (μg/ml)[a]	CC_{50} (μg/ml)[b]	SI[c]
Con 1 (1b)	1.5	>50	>33.3
JFH1 (2a)	24.9	>50	>2.3

[a]: Fifty percent effective concentration based on the inhibition of HCV replication.
[b]: Fifty percent cytotoxicity concentration based on the reduction of cell viability.
[c]: SI, selectivity index (CC_{50}/EC_{50}).
doi:10.1371/journal.pone.0048685.t002

Effect of C-29EA on NS3 Protease Activity

Serine protease and helicase domains are respectively located on the N-terminal and C-terminal portions of NS3 [32]. Thus, we examined the effect of C-29EA on NS3 protease activity by using an NS3 protease assay based on FRET. NS3/4A serine protease was mixed with various concentrations of C-29EA. The initial velocity at each concentration of C-29EA was calculated during a 120 min reaction. The initial velocity in the absence of C-29EA represented 100% of relative protease activity. C-29EA decreased the serine protease activity in a dose-dependent manner (Fig. 7). The IC_{50} of C-29EA was 10.9 μg/ml, which is similar to the value estimated by helicase assay. These results suggest that C-29EA includes the compound(s) inhibiting the protease activity of NS3 in addition to the helicase activity.

Combination Antiviral Activity of C-29EA and Interferon-alpha

Treatment with C-29EA may potentiate inhibitory action of interferon-alpha, since it inhibited the protease and helicase activities of NS3 but not induce the interferon response as described above. Then, we examined effect of treatment using both interferon and C-29EA on HCV replication. The replication

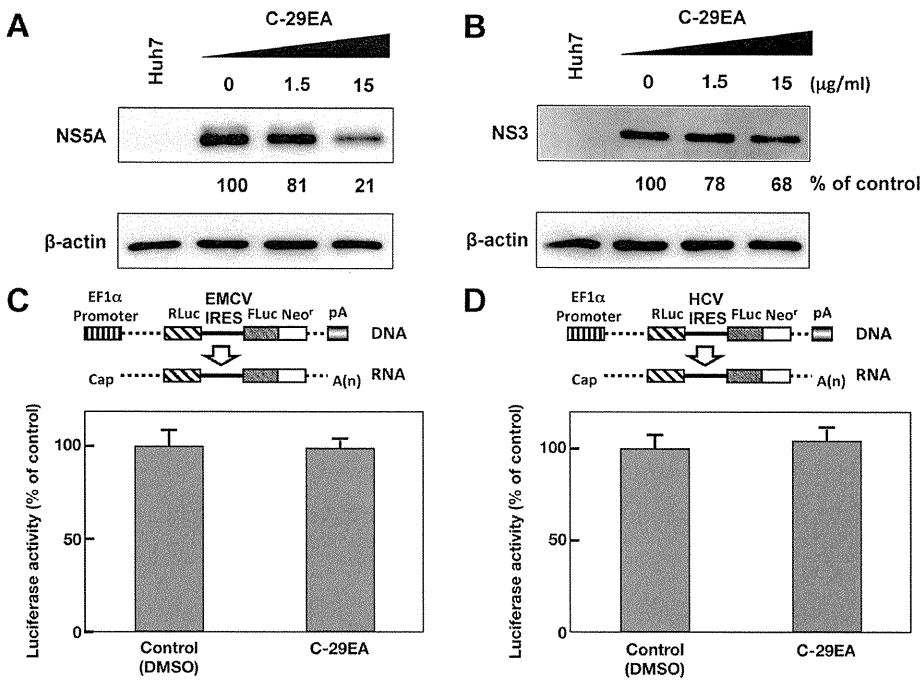

Figure 3. Effect of C-29EA on expression of viral proteins in replicon cell lines. The Huh7 replicon cell lines derived from genotype 1b (A) and 2a (B) were incubated with C-29EA at 37°C for 72 h. The treated cells were harvested and then subjected to Western blotting. Treatment with DMSO corresponds to '0'. The bicistronic gene is transcribed under the control of the elongation factor 1α (EF1α) promoter. The upstream cistron encoding *Renilla* luciferase (RLuc) is translated by a cap-dependent mechanism. The downstream cistron encodes the fusion protein (Feo), which consists of the firefly luciferase (Fluc) and neomycin phosphotransferase (Neo^r), and is translated under the control of the EMCV IRES (C) or HCV IRES (D). The Huh7 cell line transfected with the plasmid (each above the panel in C and D) was established in the presence of G418. The cells were incubated for 72 h without (control) and with 15 μg/ml of C-29EA. Firefly or *Renilla* luciferase activity was measured by the method described in Materials and Methods and was normalized by the protein concentration. F/R: relative ratio of firefly luciferase activity to *Renilla* luciferase activity. F/R is presented as a percentage of the control condition. Error bars indicate standard deviation. The data represent three independent experiments.
doi:10.1371/journal.pone.0048685.g003

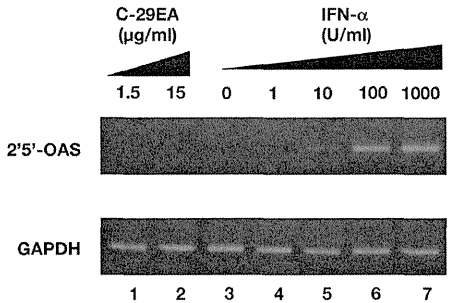

Figure 4. Effect of C-29EA on interferon signaling pathway. The Huh7 replicon cell line of genotype 1b was treated without (lane 3) or with 1, 10, 100, or 1000 U/mL interferon-alpha 2b (lanes 4–7), and 1.5 or 15 μg/ml C-29EA (lanes 1–2) for 48 h. Treatment with DMSO corresponds to '0'. The mRNAs of 2′, 5′-OAS, and GAPDH as an internal control were detected by RT-PCR. Error bars indicate standard deviation. The data represent three independent experiments.
doi:10.1371/journal.pone.0048685.g004

of replicon was decreased in the presence of C-29EA or interferon-alpha and further decreased by combination treatment using interferon-alpha and C-29EA (Fig. 8A). Furthermore, we employed the isobologram method [33] to determine whether antiviral effect of the combination treatment exhibits additive or synergistic. EC_{90} values of interferon-alpha and C-29EA were estimated at 10.7 U/ml and 26.4 μg/ml, respectively, in the absence of each other. EC_{90} values of C-29EA in the presence of 0, 2.5 and 5 U/ml interferon-alpha were plotted to generate an isobole. Figure 8B shows that the isobole exhibits concave curvilinear, representing synergy but not additivity. These results suggest that combination treatment of interferon-alpha and C-29EA exhibits synergistic inhibition of HCV replication.

Discussion

Several natural products have been reported as anti-viral agents against HCV replication. Silbinin, epigallocatechin 3-gallate, and proanthocyanidins, which were prepared from milk thistle, green tea, and blueberry leaves, respectively, have exhibited inhibitory activity against HCV replication in cultured cells [34–37]. In our previous report, we identified manoalide as an anti-HCV agent from a marine sponge extract by high-throughput screening targeting NS3 helicase activity [38]. Manoalide inhibited ATPase, RNA binding, and NS3 helicase activity in enzymological assays. The EtOAc extract of the marine feather star also suppressed HCV replication in HCV replicon cell lines derived from genotype 1b, and it inhibited the RNA-binding activity but not the ATPase activity of NS3 helicase [30]. In this study, we screened 84 extracts of marine organisms for their ability to inhibit HCV replication in replicon cell lines and HCV cell culture system. Among these extracts, C-29EA, which was extracted from *Amphimedon* sp., most strongly inhibited HCV replication regardless of cytotoxicity. We previously reported that the EtOAc extract (SG1-23-1) of the feather star *Alloeocomatella polycladia* inhibited HCV replication with an EC_{50} of 22.9 to 44.2 μg/ml in HCV replicon cells derived from genotype 1b [30]. Treatment with C-29EA potently inhibited HCV replication with an EC_{50} of 1.5 μg/ml and with an SI of more than 33.3 in the replicon cell line derived from genotype 1b, regardless of cytotoxicity (Fig. 1B and Table 2). However, C-29EA exhibited an EC_{50} of 24.9 μg/ml in a replicon cell line derived from genotype 2a at a weaker level than in the replicon cell line derived from genotype 1b (Figs. 1 and 2), suggesting that the ability of C-29EA to suppress HCV replication is dependent on the viral genotype or strain.

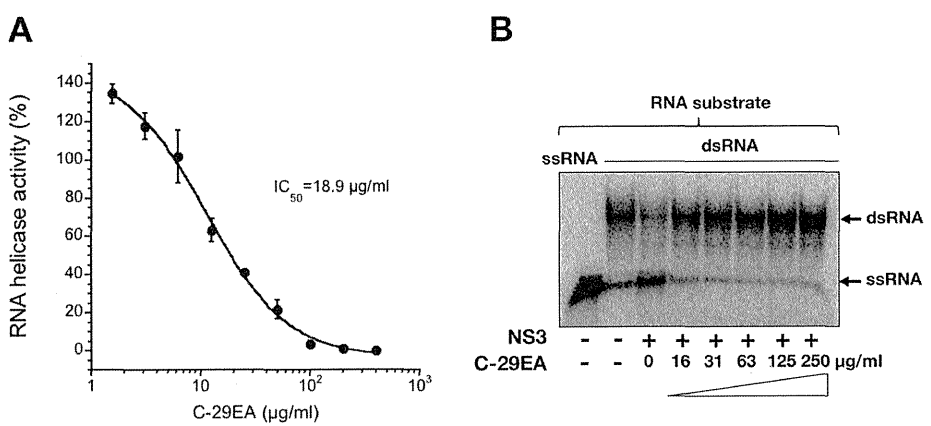

Figure 5. Effect of C-29EA on unwinding activity of NS3 helicase. (A) NS3 helicase activity was measured by PET assay. The reactions were carried out in the absence or presence of C-29EA. Helicase activity in the absence of C-29EA was defined as 100% helicase activity. Treatment with DMSO corresponds to '0'. The data are presented as the mean ± standard deviation for three replicates. (B) The unwinding activity of NS3 helicase was measured by an RNA unwinding assay using radioisotope-labeled RNA. The heat-denatured single-strand RNA (26-mer) and the partial duplex RNA substrate were applied to lanes 1 and 2, respectively. The duplex RNA was reacted with NS3 (300 nM) in the presence of C-29EA (lanes 4–9, 16–250 μg/ml). The resulting samples were subjected to native polyacrylamide gel electrophoresis. Treatment with DMSO corresponds to '0'.
doi:10.1371/journal.pone.0048685.g005

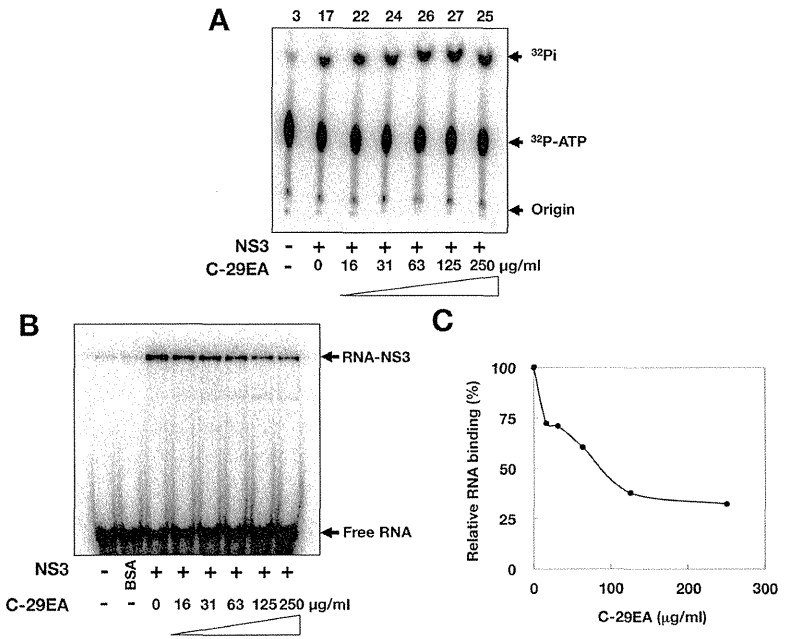

Figure 6. Effect of C-29EA on ATPase and RNA-binding activities of NS3 helicase. (A) The reaction mixtures were incubated with [γ-^{32}P] ATP as described in Materials and Methods. The reaction mixtures were subjected to thin-layer chromatography. The start positions and migrated positions of ATP and free phosphoric acid are indicated as 'Origin', '^{32}P-ATP', and '^{32}P-Pi', respectively, on the right side of the figure. The data represent three independent experiments. Treatment with DMSO corresponds to '0'. (B) Gel mobility shift assay for RNA-binding activity of NS3 helicase. The reaction was carried out with 0.5 nM labeled ssRNA at the indicated concentrations of C-29EA or DMSO. The reaction mixture was subjected to gel mobility shift assay. (C) The relative RNA-binding ability was calculated with band densities in each lane and presented as a percentage of RNA-NS3 in the total density. The data represent three independent experiments. Treatment with DMSO corresponds to '0'.
doi:10.1371/journal.pone.0048685.g006

HCV NS3 is well known to play a crucial role in viral replication through helicase and protease activities [5,39]. The N-terminal third of NS3 is responsible for serine protease activity in order to process the C-terminal portion of polyprotein containing viral nonstructural proteins [32]. The remaining portion of NS3 exhibits ATPase and RNA-binding activities responsible for helicase activity, which is involved in unwinding double-stranded RNA during replication of genomic viral RNA [40–42]. A negative-strand RNA is synthesized based on a viral genome (positive strand) after viral particles in the infected cells are uncoated, and is then used itself as a template to synthesize a positive-stranded RNA, which is translated or packaged into viral particles. Thus, both helicase and protease activities of NS3 are critical for HCV replication and could be targeted for the development of antiviral agents against HCV.

NS3 helicase activity was inhibited by treatment with C-29EA in a dose-dependent manner with an IC_{50} of 18.9 μg/ml (Fig. 5A). RNA-binding activity, but not ATPase activity, was inhibited by treatment with C-29EA (Fig. 6). Treatment with C-29EA did not significantly affect the HCV-IRES activity and did not induce interferon-stimulated gene 2′,5′-OAS (Figs. 3 and 4). Furthermore, the serine protease activity of NS3 was inhibited by using C-29EA with an IC_{50} of 10.9 μg/ml (Fig. 7). These results suggest that *Amphimedon* sp. includes the unknown compound(s) that could suppress NS3 enzymatic activity to inhibit HCV replication. Although the mechanism by which treatment with C-29EA could inhibit HCV replication has not yet been revealed, the unknown compound(s) may be associated with the inhibition of NS3 protease and helicase, leading to the suppression of HCV replication. However, other effects of extract C-29EA on HCV replication could not be excluded in this study.

The compound 1-N, 4-N-bis [4-(1H-benzimidazol-2-yl)phenyl] benzene-1,4-dicarboxamide, which is designated as $(BIP)_2B$, was reported to be a potent and selective inhibitor of HCV NS3 helicase [43]. This compound competitively decreases the binding ability of HCV NS3 helicase to nucleic acids. The compound $(BIP)_2B$ inhibited RNA-induced stimulation of ATPase, although it did not directly affect the ATP hydrolysis activity of NS3 helicase. Thus, $(BIP)_2B$ could not affect ATPase activity without RNA or with a high concentration of RNA. Treatment with C-29EA inhibited helicase activity and viral replication but not ATPase activity (Figs. 1B, 2, 5, and 6). This extract suppressed the binding of RNA to helicase but exhibited no suppression of ATPase by NS3 helicase. Thus, the inhibitory action of extract C-29EA seems

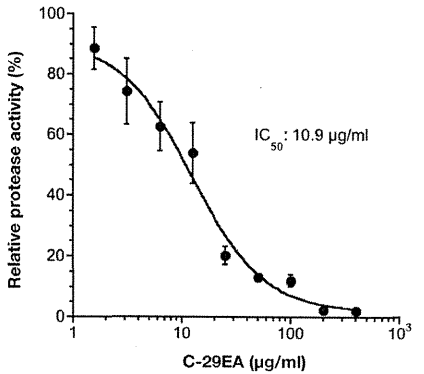

Figure 7. Effect of C-29EA on the activity of NS3 serine protease. NS3/4A serine protease was mixed with various concentrations of C-29EA or DMSO (0) in the reaction mixture and then incubated at 37°C for 120 min. The initial velocity at each concentration of C-29EA was calculated during 120 min reaction. The initial velocity in the absence of C-29EA was defined as 100% of relative protease activity. The data are presented as the mean ± standard deviation for three replicates.
doi:10.1371/journal.pone.0048685.g007

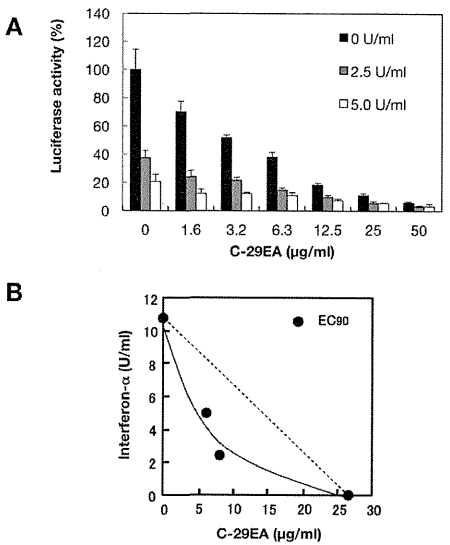

Figure 8. Effect of C-29EA on the antiviral activity of interferon-alpha. (A) The Huh7 cell line, including the subgenomic replicon RNA of genotype 1b strain Con1, was incubated in medium containing various concentrations of C-29EA or DMSO (0) in the presence or the absence of interferon-alpha. Luciferase assay were carried out as described in Materials and Methods. Error bars indicate standard deviation. The data represent three independent experiments. (B) Isobole plots of 90% inhibition of HCV replication. The broken line indicates the additive effect in the isobologram.
doi:10.1371/journal.pone.0048685.g008

different from that of $(BIP)_2B$. The quinolone derivative QU663 was reported to inhibit the unwinding activity of NS3 helicase by binding to an RNA-binding groove irrespective of its own ATPase activity [44]. The compound QU663 may competitively bind the RNA-binding site of NS3 but not affect ATPase activity, resulting in the inhibition of unwinding activity. In this study, treatment with C-29EA inhibited the RNA-binding activities of NS3 helicase but did not affect ATPase activity (Fig. 6). Furthermore, treatment with C-29EA suppressed the viral replication of HCV in an HCV cell culture system derived from several virus strains (Figs. 1 and 2, Table 2). The mechanism of C-29EA on the inhibition of NS3 helicase may be similar to that of compound QU663.

It is unknown whether one or several molecules included in C-29EA are critical for the inhibition of protease and helicase activities. The serine protease NS3/4A is one of the viral factors targeted for development into antiviral agents. Improvements in HCV therapy over the past several years have resulted in FDA approval of telaprevir (VX-950) [15,45] and boceprevir (SCH503034) [46,47]. Several studies suggest that the activities of NS3/4A protease and helicase in the full-length molecule enhance each other [48,49]. The NS3/4A protease has formed a complex with macrocyclic acylsulfonamide inhibitors [50,51]. Schiering et al. recently reported the structure of full-length NS3/4A in complex with a macrocyclic acylsulfonamide protease inhibitor [52], although the structure of full-length HCV NS3/4A in complex with a protease inhibitor has not been reported. The inhibitor binds to the active site of the protease, while the P4-capping and P2 moieties of the inhibitor are exposed toward the helicase interface and interact with both protease and helicase residues [52]. An unknown compound included in C-29EA might interact with both protease and helicase domains of NS3 to inhibit their activities. However, our data in this study have not excluded the possibility that several compounds included in C-29EA are related to the inhibition of protease and helicase of NS3/4A.

In conclusion, we showed that the EtOAc extract from *Amphimedon* sp. significantly inhibits HCV replication by suppressing viral helicase and protease activities. The purification of an inhibitory compound from the extract of *Amphimedon* sp. will be necessary in order to improve its efficacy by chemical modification.

Materials and Methods

Preparation of Extracts from Marine Organisms

All marine organisms used in this study were hand-collected by scuba diving off islands in Okinawa Prefecture, Japan. No specific permits were required for the described field studies. We do not have to obtain a local government permit to collect invertebrates except for stony corals and marine organisms for fisheries, which we did not collect in this study. The areas where we collected are not privately-owned or protected in any way. We did not collect any invertebrates listed in the red data book issued by Ministry of Environment, Japan. The sponges, tunicates, and soft corals used in this study are not listed at all. Hence, no specific permits are required for this collection in the same way as the previous report of Aratake et al. [53].

The sponge from which C-29EA was extracted was identified as *Amphimedon* sp. and deposited at Naturalis under the code RMNH POR 6100. Each specimen was soaked in acetone. The acetone-extract fraction prepared from each specimen was concentrated. The resulting material was fractionated as an EtOAc- and water-soluble fraction. The water-soluble fraction was dried up and solubilized in MeOH. The EtOAc- and the MeOH-soluble fractions were used for screening. All samples were dried and then solubilized in dimethyl sulfoxide (DMSO) before testing.

Cell Lines and Virus

The following Huh-7-derived cell lines used in this study were maintained in Dulbecco's modified Eagle's medium containing 10% fetal calf serum and 0.5 mg/ml G418. The Lunet/Con1 LUN Sb #26 cell line, which harbors the subgenomic replicon RNA of the Con1 strain (genotype 1b), was kindly provided by Ralf Bartenschlager [26]. Huh7/ORN3-5B #24 cell line, which harbors the subgenomic replicon RNA of the O strain (genotype 1b) was reported previously [54] and used for screening in this study (Table 1). HCV replicon cell line derived from genotype 2a strain JFH1 was described previously [55]. The surviving cells were infected with the JFH-1 virus at a multiplicity of infection (moi) of 0.05. The viral RNA derived from the plasmid pJFH1 was transcribed and introduced into Huh7OK1 cells according to the method of Wakita et al. [56]. The infectivity of the JFH1 strain was determined by a focus-forming assay [56].

Quantitative Reverse-transcription PCR (qRT-PCR) and Estimation of Core Protein

The estimation of viral RNA genome was carried out by the method described previously [57] with slight modification. Total RNAs were prepared from cells and culture supernatants by using an RNeasy mini kit (QIAGEN, Tokyo, Japan) and QIAamp Viral RNA mini kit (QIAGEN), respectively. First-strand cDNA was synthesized by using a high capacity cDNA reverse transcription kit (Applied Biosystems, Carlsbad, CA, USA) with random primers. Each cDNA was estimated by using Platinum SYBR Green qPCR SuperMix UDG (Invitrogen, Carlsbad, CA, USA) according to the manufacturer's protocol. Fluorescent signals of SYBR Green were analyzed by using an ABI PRISM 7000 (Applied Biosystems). The HCV internal ribosomal entry site (IRES) region was amplified using the primer pair 5′-GAGTGTCGTGCAGCCTCCA -3′ and 5′- CACTCGCAAG-CACCCTATCA -3′. Expression of HCV core protein was determined by an enzyme-linked immunosorbent assay (ELISA) as described previously [57].

Determination of Luciferase Activity and Cytotoxicity in HCV Replicon Cells

HCV replicon cells were seeded at 2×10^4 cells per well in a 48-well plate 24 h before treatment. C-29EA was added to the culture medium at various concentrations. The treated cells were harvested 72 h post-treatment and lysed in cell culture lysis reagent (Promega, Madison, WI, USA) or *Renilla* luciferase assay lysis buffer (Promega). Luciferase activity in the harvested cells was estimated with a luciferase assay system (Promega) or a *Renilla* luciferase assay system (Promega). The resulting luminescence was detected by the Luminescencer-JNR AB-2100 (ATTO, Tokyo, Japan) and corresponded to the expression level of the HCV replicon. Cell viability was measured by a dimethylthiazol carboxymethoxy-phenylsulfophenyl tetrazolium (MTS) assay using a CellTiter 96 aqueous one-solution cell proliferation assay kit (Promega).

Effects on Activities of Internal Ribosome Entry Site (IRES)

Huh7 cells were transfected with pEF.Rluc.HCV.IRES.Feo or pEF.Rluc.EMCV.IRES.Feo and then were established in medium containing 0.25 mg/ml G418, as described previously [58]. These cell lines were seeded at 2×10^4 cells per well in a 48-well plate 24 h before treatment, treated with 15 μg/ml extract C-29EA, and then harvested at 72 h post-treatment. The firefly luciferase activities were measured with a luciferase assay system (Promega). The total protein concentration was measured using the BCA Protein Assay Reagent Kit (Thermo Scientific, Rockford, IL, USA) to normalize luciferase activity.

Western Blotting and Reverse-transcription Polymerase Chain Reaction (RT-PCR)

Western blotting was carried out by a method described previously [30]. The antibodies to NS3 (clone 8G-2, mouse monoclonal, Abcam, Cambridge, UK), NS5A (clone 256-A, mouse monoclonal, ViroGen, Watertown, MA, USA), and beta-actin were purchased from Cell Signaling Technology (rabbit polyclonal, Danvers, MA, USA) and were used as the primary antibodies in this study. RT-PCR was carried out by a method described previously [30,58].

Assays for RNA Helicase, ATPase, and RNA-binding Activities

A continuous fluorescence assay based on photoinduced electron transfer (PET) was described previously [29] and was slightly modified with regard to the reaction mixture [30]. The NS3 RNA unwinding assay was carried out by the method of Gallinari et al. [59] with slight modifications [30]. NS3 ATPase activity was determined by the method of Gallinari et al. [59] with slight modifications [30]. RNA binding to NS3 helicase was analyzed by a gel mobility shift assay [30,31]. The gene encoding NS3 helicase was amplified from the viral genome of genotype 1b and was introduced into a plasmid for the expression of a recombinant protein [38,60]. The radioactive band was visualized with the Image Reader FLA-9000 and quantified by Multi Gauge V 3.11 software.

NS3 Protease Assay

The fluorescence NS3 serine protease assay based on fluorescence resonance energy transfer (FRET) was carried out by the modified method using the SensoLyte^{TM} 520 HCV protease assay kit (AnaSpec, Fremont, CA, USA). In brief, NS3 protein with a two-fold excess of NS4A cofactor peptide (Pep4AK) was prepared in 1× assay buffer provided with the kit. HCV NS3/4A protease was mixed with increasing concentrations of C-29EA and incubated at 37°C for 15 min. The reaction was started by adding the 5-FAM/QXL 520 substrate to the reaction mixture containing 180 nM HCV NS3/4A protease and various concentrations (0–400 μg/ml) of C-29EA. The resulting mixture (20 μl) was incubated at 37°C for 120 min using a LightCycler 1.5 (Roche Diagnostics, Basel, Switzerland). The fluorescence intensity was recorded every minute for 120 min. The NS3 serine protease activity was calculated as the initial reaction velocity and presented as a percentage of relative activity to that of the control examined with DMSO solvent but not C-29EA, in the same way as described in the fluorescence helicase assay [29].

Analysis of Drug-drug Interaction

The effects of drug combinations were evaluated using the isobologram method [33]. Various doses of C-29EA and interferon-alpha on 90% inhibition of HCV replication were combined to generate an isoeffect curve (isobole) to determine drug–drug interaction. Concave, linear, and convex curves exhibit synergy, additivity, and antagonism, respectively.